AD-A270 058

MENTATION PAGE

Form Approved
OMB No. 0704-0188

2. REPORT DATE	3. REPORT TYPE AND DATES COVERED
Aug 93	THESIS/DISSERTATION

4. TITLE AND SUBTITLE
Flight Test Techniques ofr Aircraft Parameter Estimation in Ground Effect

5. FUNDING NUMBERS

6. AUTHOR(S)
James M. Clark

7. PERFORMING ORGANIZATION NAME(S) AND ADDRESS(ES)
AFIT Student Attending: Texas A&M Univ

8. PERFORMING ORGANIZATION REPORT NUMBER
AFIT/CI/CIA- 93-145

9. SPONSORING/MONITORING AGENCY NAME(S) AND ADDRESS(ES)
DEPARTMENT OF THE AIR FORCE
AFIT/CI
2950 P STREET
WRIGHT-PATTERSON AFB OH 45433-7765

10. SPONSORING/MONITORING AGENCY REPORT NUMBER

11. SUPPLEMENTARY NOTES

12a. DISTRIBUTION/AVAILABILITY STATEMENT
Approved for Public Release IAW 190-1
Distribution Unlimited
MICHAEL M. BRICKER, SMSgt, USAF
Chief Administration

12b. DISTRIBUTION CODE

13. ABSTRACT (Maximum 200 words)

140PT

14. SUBJECT TERMS

15. NUMBER OF PAGES
145

16. PRICE CODE

17. SECURITY CLASSIFICATION OF REPORT	18. SECURITY CLASSIFICATION OF THIS PAGE	19. SECURITY CLASSIFICATION OF ABSTRACT	20. LIMITATION OF ABSTRACT

FLIGHT TEST TECHNIQUES FOR AIRCRAFT PARAMETER ESTIMATION IN GROUND EFFECT

A Thesis

by

JAMES MATTHEW CLARK

Submitted to the Office of Graduate Studies of
Texas A&M University
in partial fulfillment of the requirements for the degree of

MASTER OF SCIENCE

December 1993

Major Subject: Aerospace Engineering

FLIGHT TEST TECHNIQUES FOR AIRCRAFT PARAMETER ESTIMATION IN GROUND EFFECT

A Thesis

by

JAMES MATTHEW CLARK

Submitted to Texas A&M University
in partial fulfillment of the requirements
for the degree of

MASTER OF SCIENCE

Approved as to style and content by:

Donald T. Ward
(Chair of Committee)

Costas Georghiades
(Member)

Andrew J. Kurdila
(Member)

Walter E. Haisler
(Head of Department)

December 1993

Major Subject: Aerospace Engineering

ABSTRACT

Flight Test Techniques for Aircraft Parameter Estimation
in Ground Effect. (December 1993)
James Matthew Clark, B.S., United States Air Force Academy
Chair of Advisory Committee: Dr. Donald T. Ward

The effect of ground proximity on the performance and handling of an aircraft has received extensive study, particularly in the wind tunnel. Previous research, however, provides few consistent quantitative conclusions regarding ground effect, and flight test methods for directly measuring ground effect are needed. This effort identifies flight test maneuvers suitable for measuring aircraft stability and control parameters in ground effect, using simulated response data and pEst, a parameter estimation program developed at NASA-Dryden. This study also considers the effects of instrument precision, system sampling rate, instrument bias, and response noise.

Five simple longitudinal and eleven lateral-directional maneuvers that allow accurate parameter estimation, keep the aircraft in ground effect, and do not result in responses that are unsafe in ground proximity are identified. The longitudinal maneuvers provide accurate lift and moment parameters, and the lateral-directional analysis estimates all fifteen lateral-directional derivatives of interest within ten percent of their simulated values.

Adequate instrument precision levels are recommended for longitudinal and lateral-directional maneuvers. The system sampling rate has no significant effect on parameter estimates for noise-free data, as long as the sampling frequency is at least

twice that of the input and the transient responses. Instrument bias is harmful to the estimation, and using pEst's bias estimators provides mixed results. The noise analysis specifies levels of random noise acceptable in the data. The effects of precision, bias and noise are combined to realistically simulate flight test data. In this combined analysis, useful parameter estimates result from both longitudinal and lateral-directional test maneuvers.

ACKNOWLEDGMENTS

The author gratefully acknowledges the support of the Air Force Institute of Technology (AFIT) for making this effort possible. He also acknowledges the invaluable guidance and advice of Dr. Donald T. Ward, his Graduate Committee Chairman. In addition, the author thanks Dr. Costas Georghiades and Dr. Andrew Kurdila for their cooperation and assistance.

Dr. Richard Maine, at NASA's Dryden Flight Research Facility, provided valuable help in obtaining the parameter estimation software and installing it at Texas A&M.

The author finally acknowledges the faculty of the Department of Aeronautical Engineering, U.S. Air Force Academy, for inspiring him to further study, and thanks his parents, H. Fletcher and Betty J. Clark, for their steadfast encouragement during this project.

TABLE OF CONTENTS

LIST OF TABLES

LIST OF FIGURES

Page

Page

Page

NOMENCLATURE

Symbol	Definition	Units
a_n	Normal acceleration	g or ft/sec^2
a_x	Longitudinal acceleration	g or ft/sec^2
a_y	Lateral acceleration	g or ft/sec^2
b	Wing span width	ft
$\bar{c}$	Mean aerodynamic chord	ft
C-R	Cramer-Rao (uncertainty bound)	
C_{D0}	Drag coefficient at zero angle of attack	
C_{Du}	Variation of drag with airspeed	
C_{Dq}	Variation of drag with pitch rate	
$C_{D\alpha}$	Variation of drag with angle of attack	/rad or /deg
$C_{D\delta e}$	Variation of drag with elevator deflection	/rad or /deg
C_{L0}	Lift coefficient at zero angle of attack	
C_{Lu}	Variation of lift with airspeed	
C_{Lq}	Variation of lift with pitch rate	
$C_{L\alpha}$	Variation of lift with angle of attack	/rad or /deg
$C_{L\delta e}$	Variation of lift with elevator deflection	/rad or /deg
C_{lp}	Variation of rolling moment with roll rate	
C_{lr}	Variation of rolling moment with yaw rate	
$C_{l\beta}$	Variation of rolling moment with sideslip angle	/rad or /deg

Symbol	Definition	Units
$C_{l_{\delta_a}}$	Variation of rolling moment with aileron deflection	/rad or /deg
$C_{l_{\delta_r}}$	Variation of rolling moment with rudder deflection	/rad or /deg
C_{m0}	Pitch moment coefficient at zero angle of attack	
C_{m_u}	Variation of pitch with airspeed	
C_{mq}	Variation of pitch with pitch rate	
$C_{m\alpha}$	Variation of pitch with angle of attack	/rad or /deg
$C_{m_{\delta_e}}$	Variation of pitch with elevator deflection	/rad or /deg
C_{np}	Variation of yawing moment with roll rate	
C_{nr}	Variation of yawing moment with yaw rate	
$C_{n\beta}$	Variation of yawing moment with sideslip angle	/rad or /deg
$C_{n_{\delta_a}}$	Variation of yawing moment with aileron deflection	/rad or /deg
$C_{n_{\delta_r}}$	Variation of yawing moment with rudder deflection	/rad or /deg
C_{yp}	Variation of side-force with roll rate	
C_{yr}	Variation of side-force with yaw rate	
$C_{y\beta}$	Variation of side-force with sideslip angle	/rad or /deg
$C_{y_{\delta_a}}$	Variation of side-force with aileron deflection	/rad or /deg
$C_{y_{\delta_r}}$	Variation of side-force with rudder deflection	/rad or /deg
E	Least-squares response residual	
f	Least-squares parameter increment vector	

Symbol	Definition	Units
g	Gravitational acceleration constant	ft/sec^2
h	Height	ft
Hz	Hertz	cycles/sec
I	Identity matrix	
I_{xx}	Moment of inertia about x-axis	slug ft^2
I_{yy}	Moment of inertia about y-axis	slug ft^2
I_{zz}	Moment of inertia about z-axis	slug ft^2
I_{xz}	Product of inertia about x- and z-axes	slug ft^2
J	pEst cost function	
L	Dimensional variation of rolling moment	/sec or /sec^2
M	Dimensional variation of pitching moment	/sec or /sec^2 or rad / ft sec
m	Mass	slugs
N	Dimensional variation of yawing moment	/sec or /sec^2
n_t	Number of time points	
n_z	Number of response variables	
p	Perturbed roll rate	deg/sec or rad/sec
Q	Dynamic pressure	lbs/ft^2
q	Perturbed pitch rate	deg/sec or rad sec
r	Perturbed yaw rate	deg/sec or rad/sec

Symbol	Definition	Units
S	Wing surface area	ft^2
Std Dev	Statistical standard deviation	
T	Transpose operator	
t	Time	sec
u	Perturbed longitudinal velocity	ft/sec
u_0	Steady state longitudinal velocity	ft/sec
V	Least-squares cost function	
v	Perturbed lateral velocity	ft/sec
W	Response weighting matrix	
w	Perturbed normal velocity	ft/sec
X	Dimensional variation of longitudinal force	/sec or ft / sec^2 rad
Y	Dimensional variation of lateral force	ft / sec rad or ft / sec^2 rad
Z	Dimensional variation of normal force	/sec or ft / sec rad or ft / sec^2 rad
z	pEst measured response vector	
$\tilde{z}$	pEst computed response vector	
α	Angle of attack	deg or rad
β	Sideslip angle	deg or rad
Δ	Perturbation quantity	various
δ_a	Aileron deflection	deg or rad

Symbol	Definition	Units
δ_e	Elevator deflection	deg or rad
δ_r	Rudder deflection	deg or rad
ε	Parameter vector	
ϕ	Bank angle	deg or rad
θ	Pitch angle	deg or rad
θ_0	Steady-state pitch angle	deg or rad
ψ	Least-squares state prediction gradient	

INTRODUCTION

BACKGROUND

When an aircraft is close to the ground, it encounters a phenomenon known as ground effect. This effect is caused by vortices at the wing tips, which are a by-product of lift, striking the ground below and altering the airflow about the aircraft. As early as the 1920's, researchers and designers noted a distinct change in the behavior of airplanes as they descended within about a wingspan of the ground. In general, they observed that an airplane created more lift and less drag when near the ground.

In the years that followed, ground effect was investigated further, primarily through wind tunnel testing. Qualitative conclusions about the effects of ground proximity resulted, but little verification through flight testing was performed. Ground effect is the result of an aircraft moving in relatively stationary air over a stationary surface (the runway). In a wind tunnel test, the aircraft model and ground surface are generally stationary, and the air moves past at some velocity. Difficulties arise reproducing ground effect in the wind tunnel, primarily because of the boundary layer that forms as moving air passes stationary objects. Attempts have been made to correct for the influence of this boundary layer, but the quantitative results of ground effect wind tunnel testing remain uncertain.

As the performance of aircraft improves, takeoff and landing characteristics are increasingly important since runway length is limited. Automated takeoff and landing systems, now in use in large aircraft, would benefit from a better understanding of ground effect. Safety concerns also demand a better under-

---

This thesis follows the format and style of the *AIAA Journal of Aircraft*.

standing of the effect of the ground on the handling of aircraft. Finally, as high-fidelity flight simulators become more important in the training of pilots, better simulation of the takeoff and landing phases would improve their effectiveness. For all these reasons, verification of wind tunnel results and further study of ground effect through flight testing are of practical importance.

Stability and control parameters are numbers which quantify the flight characteristics of a given aircraft at a specified flight condition. These parameters give the response of the aircraft to a change in its state or any deflection of its control surfaces. A military fighter obviously flies quite differently than a large commercial transport; the stability and control parameters of the respective aircraft quantify this difference in part. Likewise, if an aircraft handles differently when it is very close to the ground than when it is at higher altitude, a distinct difference will be evident in these parameters.

Measurement of aircraft stability and control parameters through flight testing has been given a great deal of attention and is now done with reasonable accuracy, particularly in the low angle of attack flight regime. Typically, these parameters are estimated by measuring aircraft states during test maneuvers and applying a numerical system identification algorithm to the measured data. Figure 1 illustrates the iterative concept of aircraft parameter estimation.

PRESENT STATUS OF GROUND EFFECT RESEARCH

Previous ground effect research includes numerous wind tunnel tests, a number of flight test investigations, and some theoretical models. Because of the difficulties involved in collecting data when flying an aircraft close to the ground, most work regarding ground effect has been done in the wind tunnel. East presents

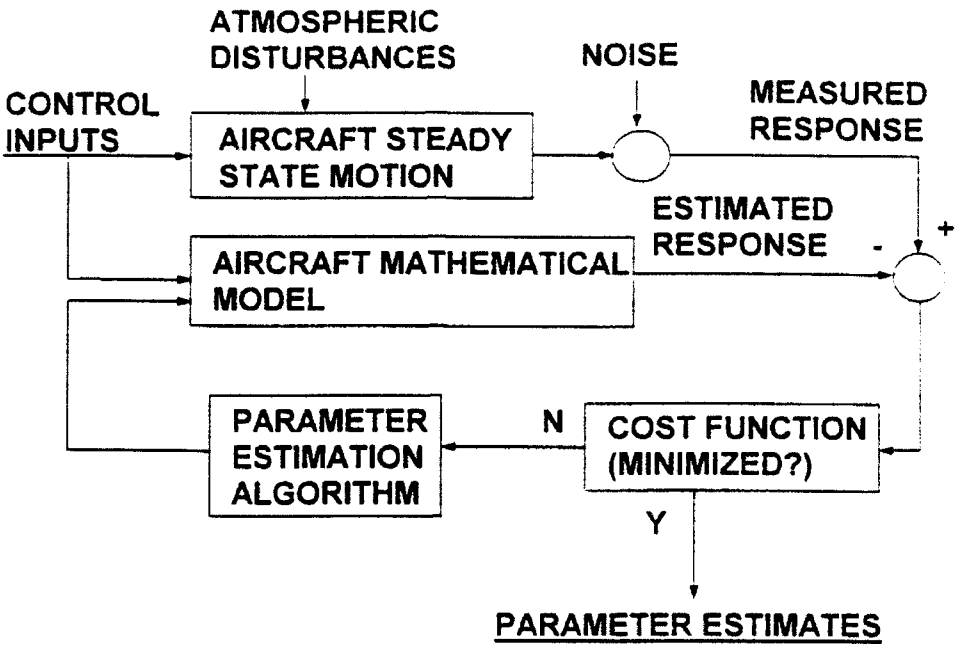

Figure 1 Parameter Estimation Concept

the three primary methods used to simulate ground proximity in the wind tunnel[1].

The first and perhaps most obvious method is the fixed ground board. Its chief advantage is simplicity; however, a stationary board in a moving flow inevitably creates a boundary layer. Reducing the upstream extent of the board helps reduce the boundary layer, or suction may be used to remove the layer, but how much this suction disrupts the wing tip vortex motion is uncertain. Another method uses a moving belt to simulate the ground. This approach removes the surface boundary problem, but requires a complex rig and is limited to lower flow speeds. Additionally, the size of the apparatus may make uniform flow in the test section impossible, and the suction required to keep the belt flat at higher rotation speed may again disrupt the vortex flow near the surface. The third method uses two nearly identical models mounted symmetrically about a plane between them.

The stream surface along this axis of symmetry represents the ground. Difficulties arise in using this method because no vortex-ground boundary layer forms, interaction between the vortices coming off separate models may corrupt the results, and complexity necessitates the use of small models.

Although each wind tunnel method has its drawbacks, attempts are generally made to correct the data, and results tend to agree, at least qualitatively. In an early study, Recant[2] concludes that ground proximity increases the lift coefficient in the same manner as a higher aspect ratio does, as well as decreasing drag coefficient. He bases his results on tests of three-dimensional wing sections over relatively large ground boards. The ratios of quarter-chord height to chord length in the test, ranging from 3 to 0.5, keep the wing itself out of the ground board's boundary layer. The layer's effect on the tip vortices, however, cannot be negated. Qualitatively, Recant observes that the slope of the lift curve progressively increases and the drag coefficient progressively decreases as the wing gets nearer to the ground. Recant also concludes that the maximum lift coefficient of a wing is unaffected by ground proximity.

East[1] uses a stationary ground board as well, and attempts to correct for the boundary layer by taking measurements both with and without wing section models. He notes a fifty percent increase in lift for low aspect ratio wings, and a five percent increase for those with high aspect ratios. He also detects a significant ground board error, and develops a linear interpolation approach for estimating its order of magnitude. He cautions that this approach contains various simplifying assumptions, and that it should not be relied on quantitatively. East recognizes that boundary layers induced by the tip vortices of a passing aircraft exist, but remains uncertain of

their effect. Finally, East concludes that the ground board boundary layer error is greatest in tests with low aspect ratio wings, but identifies no critical aspect ratio.

Acknowledging that there is no universally accepted method of predicting ground effect from wind tunnel data, Chambliss and Millikan[3] employ a moving ground belt, with suction used both to pull the belt flat and to remove the boundary layer. While adding no specifics, they suggest that the ground effect has influence to about one wingspan above the ground, and that it adds to the lift coefficient at a constant angle of attack, alters the moment coefficient, and changes the control effectiveness. Chambliss and Millikan also postulate that low aspect ratio configurations are more sensitive because they fly at a higher incidence angle for a given lift coefficient.

In a detailed investigation of ground effect on a highly swept configuration, Coe and Thomas[4] use a moving ground belt to estimate ground effect at 0.1 to 1.0 span widths above the ground, and develop a theoretical approach for simulating ground effect. They make no mention of belt suction corrections, but do correct for tunnel wall and sting effects. With their low aspect ratio model, they find that ground effect increases lift and horizontal tail downwash, decreases induced drag, and improves longitudinal stability. These tests, unlike Recant's investigation and flight tests, indicate that the lift curve slope is unchanged by ground effect - only the intercept at zero angle of attack is altered. Coe and Thomas find that the moment coefficient at zero angle of attack is independent of height, and that this parameter's slope is changed. The two also reference a vortex-lattice computational method that predicts their experimental results rather well. In this case, the lattice consists of a dual image of the model, symmetric with respect to the ground plane. At the ground plane, zero flow normal to the ground is enforced as a boundary condition.

The symmetric layout of the grid results in a "ground induced upwash" from the image which is inversely proportional to distance and serves to simulate ground effect. The computed solutions agree reasonably with the wind tunnel results, but the code is only referenced and is not readily available.

Stewart and Kemmerly[5] investigate ground effect by removing the effects of vertical thrust from a short takeoff, powered lift wind tunnel model. Using a fixed ground board and suction to remove the boundary layer, they encounter difficulties isolating the "thrust removed" forces, in essence the aerodynamic ground effect. They conclude that ground effect flight test data are needed to correlate with wind tunnel data, particularly for powered lift or short takeoff configurations. While this is a highly specialized application, it clearly demonstrates the need for ground effect flight test data to verify wind tunnel and computational investigations.

Many of the shortcomings of the wind tunnel methods, such as ground board boundary layers and complex models, could be negated through flight test measurements, but the difficulty in obtaining suitable flight data near the ground has prevented a great deal of investigation in this area. Flight profiles in past ground effect studies are the approach and flare and the constant altitude flyby. Both techniques require either an on-board data acquisition system or some other means of accurately tracking aircraft states such as altitude and airspeed.

Rolls and Koenig[6] equip a modified Douglas F5D Skyray with a data acquisition system and perform a series of constant altitude passes at various heights above a runway. Their flight data show an eighteen percent increase in lift and an increased lift curve slope, as well as an increase in the nose down pitching moment requiring an additional four degrees of up elevon to compensate. For comparison, they also perform three separate wind tunnel tests, one with the actual aircraft

mounted above the tunnel floor, and two with scale models above fixed ground boards and moving belts. Considering all four sets of data, they conclude that lift and pitching moment data agree fairly well, but note differences in drag coefficient among the tests, which they attribute to an erroneous thrust model in flight and sealed engine inlets on the tunnel models. Their wind tunnel tests also indicate a twenty percent change in elevon effectiveness in proximity to the ground.

Schweikhard[7] utilizes precise external tracking of two test aircraft, a Lockheed F-104 and a North American XB-70, during the approach phase to measure changes in the aircraft states as it approaches the ground. The cinetheodolite system at the U.S. Air Force Flight Test Center tracks the test aircraft through a constant angle of attack, constant power approach, flare, and level off. From the tracking data, a time history is developed, from which lift, drag, and other data are calculated. For the F-104, with an aspect ratio of 2.5, Schweikhard notes ground effects at heights up to three span widths, well above the widely accepted limit of one span width. He also notes a high lift increment of up to forty percent, and little pitching moment change. The XB-70, with an aspect ratio of 1.75, exhibits more conventional characteristics, with ground effects beginning at about one span width above the ground and more moderate lift increments between five and sixteen percent. Schweikhard attributes the unique nature of the F-104 results to its very small span and its high-mounted tail. While noting that the cinetheodolite method results in less erratic data when test conditions are gusty or turbulent, Schweikhard recommends direct measurement of aircraft accelerations as more accurate than his camera data. In general, Schweikhard's conclusions are similar to East's wind tunnel results, but it should be noted that East considers wing sections only.

O'Leary[8] uses a technique similar to that used by Schweikhard to measure ground effect on a Comet 3 airliner. In addition to using tracking cameras, he measures aircraft data with on-board recorders during an approach and flare maneuver. By adjusting the autopilot variable flare height control, O'Leary collects data for a number of altitudes between ten and forty percent of the span width. He notes an increase in lift coefficient and, with the dubious assumption that ground effect does not change elevator power, a positive increase in the pitching moment coefficient. This result contradicts Rolls and Koenig's conclusion regarding the pitching moment in ground effect. Using wind tunnel models similar to the test configuration, O'Leary conducts a wind tunnel investigation that is in reasonable agreement with the flight test data, although only corrections for model discrepancies are noted. A limitation of this technique is that it is best suited to aircraft with a radar altimeter and an autopilot. An advantage is that it allows data collection at various heights above the runway.

OBJECTIVES

From the previous discussion, it is evident that researchers do not agree on a standard technique for measuring ground effect data, particularly in the wind tunnel. While qualitative conclusions tend to support one another, a consistent database from flight test is needed. Furthermore, virtually all investigations to date measure only lift, drag, and moment coefficients, and the effect of ground proximity on other aircraft parameters is unexplored.

The overall purpose of this research is to investigate flight test techniques for estimating stability and control parameters in close proximity to the ground. Isolating useful test maneuvers and adequate acquisition system characteristics are the primary goals. Specific objectives are:

1. Identification of flight test maneuvers which, when using a modern data acquisition system to measure aircraft responses and control deflections, provide parameter estimates within ten percent of the simulated values.

2. Of those maneuvers suitable for parameter estimation, determining maneuvers that do not violate established safety criteria or result in the aircraft flying out of ground effect.

3. For a more realistic appraisal, isolating levels of measurement precision, sampling rate, bias, and noise that are acceptable for the parameter identification.

This study proposes to identify flight test maneuvers suitable for measuring the ground effect on a general set of aircraft stability and control parameters, rather than just the total lift, drag, and moment coefficients. In addition, this effort aims to isolate levels of uncertainty (noise, bias, etc.) that do not excessively corrupt the measured data, and permit estimates within ten percent. The measure of merit for each estimate is its value in percent of the simulated value - one hundred percent is therefore the best possible estimate. Past research indicates that ground effect's influence on lift, drag, and moment parameters is between ten and forty percent and that parameter estimates within ten percent are achievable; therefore, ten percent is established as a quantitative success goal for each parameter. Estimates substantially less than ten percent off are desired, because a ten percent error in estimating a parameter may cancel a ten percent ground effect correction. In the following analyses, estimates significantly less than ten percent result in many cases.

While accurate estimation of all parameters may not be realistic, the study isolates maneuvers and uncertainty levels that identify as many stability parameters as possible.

MANEUVER ANALYSIS OVERVIEW

The maneuver analysis involves three primary tasks: (1) simulating the aircraft's transient response to control inputs; (2) estimating parameters from the simulated data; and (3) studying the effects of precision, sampling rate, bias, and noise. Since the Texas A&M University Flight Mechanics Laboratory is currently installing a data acquisition system in a twin-engine light piston aircraft (Grumman GA-7 Cougar), the maneuver analysis procedure simulates a Beech B99 commuter airliner, which is similar in configuration but larger in size and weight.

Simulating the aircraft's *dynamic* response in ground effect has not yet been precisely done - the model required for such a simulation is likely nonlinear and would require substantial and accurate knowledge of ground effect. The model specifics and ground effect characteristics are simply not well enough understood, based on previous research, to precisely simulate ground effect in a mathematical model.

Therefore, two linear state-space systems are developed from the linearized small perturbation aircraft equations of motion. These systems simulate the aircraft responses during longitudinal and lateral-directional maneuvers, without a ground effect correction. Given an input and an initial set of perturbations, the responses are obtained using a fourth-order Runge-Kutta numerical integration scheme in MATLAB, a commercial engineering mathematics software package[9]. This solution is a time history of the perturbations - the time histories of the states result from simply adding the steady-state values of each state variable. Additional variables of

interest for the parameter estimation are computed using these state histories. Using this simulation procedure, simulating the response of the aircraft to any control input is possible.

System identification, broadly defined, is the process of building mathematical models of dynamical systems based on observed responses of the systems[10]. Since an aircraft may be represented as a system of differential equations, identification techniques may be applied to an aircraft to determine its characteristics. When identification is performed to determine aircraft stability and control parameters, the process is called parameter estimation.

Numerous identification techniques exist for linear and nonlinear systems analysis. Two requirements all techniques share are a time history of observed data and some knowledge of the system to be modeled. In a flight test program, measurements of pertinent aircraft states provide the observations. In this study, simulated time history data replace actual flight test data, allowing flight test maneuvers to be analyzed more efficiently and safely. In addition, the model is known exactly, removing a significant source of uncertainty.

With the simulated maneuver time histories, stability and control parameters are estimated using pEst, a FORTRAN 77 parameter identification program developed for flight test work at the NASA Dryden Flight Research Facility[11]. This program is selected because it is readily available public-domain software and is the primary estimation package used at Dryden for flight test work. PEst automates the mathematics of parameter estimation, using a prediction error method to minimize a quadratic cost function[12]. The program, in effect, performs a nonlinear least-squares fit to the selected maneuver history by incrementing its "guess" at the parameter vector. It permits the user to specify initial parameter values and the

relative weights of the responses in the cost function. In addition, pEst allows the user complete flexibility in selecting the active parameters and responses in the estimation, and provides a selection of gradient and Newtonian minimization algorithms. Installation files included with the pEst software recommend the Levenberg-Marquardt algorithm, a regularized Newton method, as the most robust for numerical derivative extraction.

Therefore, given a set of aircraft state histories, the pEst program identifies a set of parameters to model the dynamic responses recorded. To estimate parameters accurately, numerical identification techniques, such as pEst, require that the data contain sufficient excitation of the system modes of motion and an adequate signal-to-noise ratio. If the data are not of sufficient quantity and quality, the parameter estimation is poor.

The excitation and signal-to-noise requirements for the data are largely unexplored for flight testing in close proximity to the ground. In addition, these requirements are directly at odds with safety concerns, which dictate that aircraft control inputs and motions be small. It is thus the objective of this analysis to determine flight test maneuvers which excite aircraft motions sufficiently for accurate parameter estimation, and yet do not violate reasonable safety constraints. Any maneuver suitable for studying ground effect through flight test must satisfy these conflicting requirements. A set of safety criteria is used to ensure the aircraft motions are not dangerous. An additional constraint is that, during the maneuver, the aircraft must remain within one span width of the ground, which is generally accepted as the upper limit of ground effect.

As noted earlier, the ground effect on each parameter is unknown, and no attempt is made to incorporate ground effect corrections into the simulation.

Rather, maneuvers are simulated using the free-flight (away from the ground) parameters, which are known from previous flight test work or geometric analysis, or are assumed. This study assumes that the free-flight simulation of the maneuver is a good approximation of the actual flight path in ground effect, from a safety standpoint. Thus, the changes in aircraft response due to ground effect are assumed large enough to be measured in flight data, yet not so great that they make the maneuvers unsafe. Previous studies do indicate that test pilots seldom have difficulty compensating for the ground's effect on an aircraft's handling, if allowed to intervene. Nevertheless, this assumption is untested and, if erroneous, potentially fatal; therefore, validating it in flight prior to using the suggested maneuvers is extremely important.

Past research indicates that ground effect is a progressive phenomenon; it becomes more pronounced as aircraft height decreases. Because of the excitations required for parameter estimation, however, test maneuvers contain altitude changes and analysis at constant height is impossible. This study, therefore, assumes that ground effect has some "average" value within its region of influence. In practice, an aircraft is seldom at a constant height during takeoff or landing; therefore, determining maneuvers for measuring this "average" ground effect is useful.

Additional considerations in the maneuver analysis concern bias and noise. These quantities are almost always present in the flight data and are caused by such factors as imperfect sensors, wind gusts, and vibrations in the aircraft structure. In parameter estimation, these factors reduce the accuracy of the results by introducing uncertainty in the data. Since perfect test conditions and measurement devices are not realistically attainable, the effects of bias and noise are considered. Furthermore,

the effects of various levels of instrument precision and of acquisition system sampling rate are also studied.

When all the aforementioned assumptions and concerns are considered, the maneuver analysis is an iterative application of the following procedure: (1) develop sets of maneuvers that allow accurate parameter estimation using pEst, (2) within these sets, determine which maneuvers satisfy the ground proximity and safety requirements, and (3) with these maneuvers, determine whether realistic levels of uncertainty are acceptable in the parameter estimation. This procedure is presented in Figure 2. Similar analysis is performed for both longitudinal and lateral-directional maneuvers. These maneuver analyses identify flight test techniques that meet all the criteria, and thus are suitable for aircraft parameter estimation in ground effect.

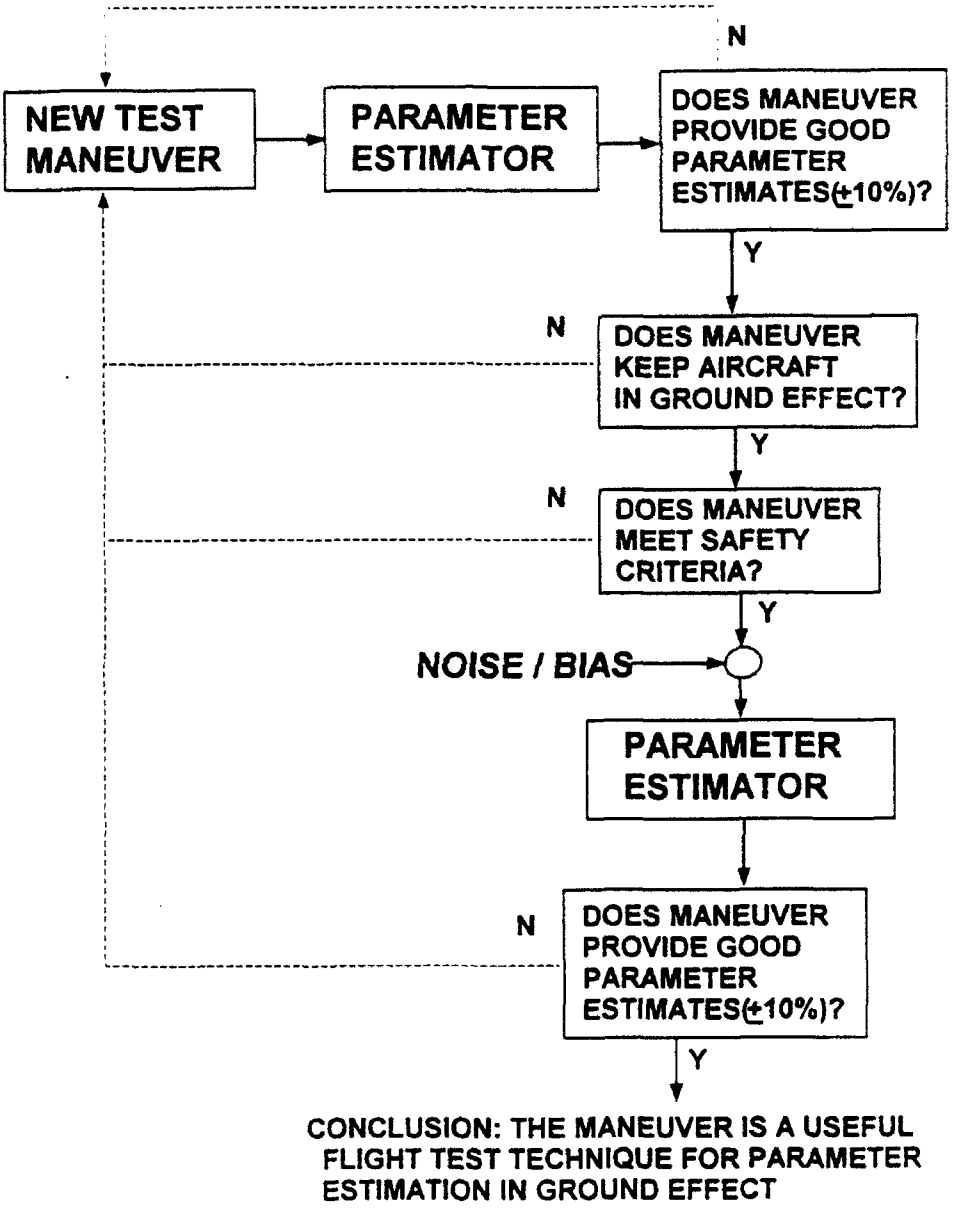

Figure 2 Maneuver Analysis Procedure

MANEUVER ANALYSIS METHOD

SIMULATION OF AIRCRAFT RESPONSE

The first requirement for aircraft parameter estimation is a set of time history data representing the aircraft's dynamic motion. For flight tests, these data are measured as each test maneuver is flown. This study simulates the states numerically rather than measuring them in flight, and therefore requires an accurate and repeatable means of simulating aircraft maneuvers.

An aircraft in flight is a dynamical system whose behavior can be modeled using a system of ordinary differential equations. Assuming the aircraft is a rigid body, the constant-thrust, linearized small perturbation equations of motion are:

$$\begin{aligned}
&\left(d/dt - X_u\right)\Delta u - X_w \Delta w + (g\cos\theta_0)\Delta\theta = X_{\delta e}\Delta\delta_e \\
&-Z_u \Delta u + \left((1 - Z_{\dot{w}})d/dt - Z_w\right)\Delta w - \left(\left(u_0 + Z_q\right)d/dt - g\sin\theta_0\right)\Delta\theta = Z_{\delta e}\Delta\delta_e \\
&-M_u \Delta u - \left(M_{\dot{w}}\, d/dt + M_w\right)\Delta w + \left(d^2/dt^2 - M_q\, d/dt\right)\Delta\theta = M_{\delta e}\Delta\delta_e \qquad (1)
\end{aligned}$$

$$\begin{aligned}
&\left(d/dt - Y_v\right)\Delta v + (u_0 - Y_r)\Delta r - (g\cos\theta_0)\Delta\phi = Y_{\delta r}\Delta\delta_r \\
&-L_v \Delta v + \left(d/dt - L_p\right)\Delta p - \left(I_{xz}/I_{xx}\, d/dt + L_r\right)\Delta r = L_{\delta a}\Delta\delta_a + L_{\delta r}\Delta\delta_r \\
&-N_v \Delta v - \left(I_{xz}/I_{zz}\, d/dt + N_p\right)\Delta p + \left(d/dt - N_r\right)\Delta r = N_{\delta a}\Delta\delta_a + N_{\delta r}\Delta\delta_r \qquad (2)
\end{aligned}$$

Aircraft motion can be divided into two separate modes, the longitudinal (Equation (1)) and the lateral-directional (Equation (2)), which are independent for most maneuvers and can be treated separately. In these equations, the *X, Y, Z, L, M,*

and N terms are constant dimensional force and moment derivatives, and are thus functions of the stability and control parameters of interest. Although these linear equations remain valid only for small changes in the aircraft states, they are adequate for most maneuvers, and will be accurate for those that are acceptable near the ground. Additional terms may be added to account for engine thrust, if appropriate control derivatives are available, but these terms are not modeled. Without a thrust model, this model assumes thrust and drag are effectively equal. Nelson[13] develops these equations of motion in some detail.

Longitudinal Mode Simulation

For the longitudinal case, $\Delta\dot{\theta} = \Delta q$, and assume $\theta_0 \approx 0$ and $Z_{\dot{w}} = 0$ (this assumes the parameter $C_{L_{\dot{\alpha}}} = 0$). The first set of equations becomes:

$$\Delta\dot{u} = X_u \Delta u + X_w \Delta w - g\Delta\theta + X_{\delta_e} \Delta\delta_e$$

$$\Delta\dot{w} = Z_u \Delta u + Z_w \Delta w + (u_0 + Z_q)\Delta q + Z_{\delta_e} \Delta\delta_e$$

$$\begin{aligned}\Delta\dot{q} = (M_u + M_{\dot{w}} Z_u)\Delta u + (M_w + M_{\dot{w}} Z_w)\Delta w + \left(M_q + M_{\dot{w}}(u_0 + Z_q)\right)\Delta q \\ + (M_{\delta_e} + M_{\dot{w}} Z_{\delta_e})\Delta\delta_e \end{aligned} \quad (3)$$

The system above models a general aircraft's dynamic response to any elevator input and any small perturbation about its flight path. Each term is a function of the aircraft's flight condition, its physical dimensions, and its stability and control parameters. Table 1 summarizes the relations for the longitudinal terms.

This system is easily arranged in state-space form:

$$\begin{bmatrix} \Delta\dot{u} \\ \Delta\dot{w} \\ \Delta\dot{q} \\ \Delta\dot{\theta} \end{bmatrix} = \begin{bmatrix} X_u & X_w & 0 & -g \\ Z_u & Z_w & u_0 + Z_q & 0 \\ M_u + M_{\dot{w}} Z_u & M_w + M_{\dot{w}} Z_w & M_q + M_{\dot{w}}(u_0 + Z_q) & 0 \\ 0 & 0 & 1 & 0 \end{bmatrix} \begin{bmatrix} \Delta u \\ \Delta w \\ \Delta q \\ \Delta\theta \end{bmatrix}$$

$$+ \begin{bmatrix} X_{\delta_e} \\ Z_{\delta_e} \\ M_{\delta_e} + M_{\dot{w}} Z_{\delta_e} \\ 0 \end{bmatrix} [\Delta\delta_e] \qquad (4)$$

Table 1 Longitudinal Dimensional Parameter Definitions

$X_u = -(C_{D_u} + 2C_{D_0})QS/mu_0$	$Z_{\delta_e} = -C_{L_{\delta_e}} QS/m$
$X_w = -(C_{D_\alpha} - C_{L_0})QS/mu_0$	$M_u = C_{m_u} QS\bar{c}/u_0 I_{yy}$
$X_{\delta_e} = -C_{D_{\delta_e}} QS/m$	$M_{\dot{w}} = C_{m_{\dot{\alpha}}} QS\bar{c}^2/2I_{yy}u_0^2$
$Z_u = -(C_{L_u} + 2C_{L_0})QS/mu_0$	$M_w = C_{m_\alpha} QS\bar{c}/u_o I_{yy}$
$Z_w = -(C_{L_\alpha} + C_{D_0})QS/mu_0$	$M_q = C_{m_q} QS\bar{c}^2/2u_0 I_{yy}$
$Z_q = -C_{L_q} QS\bar{c}/2mu_0$	$M_{\delta_e} = C_{m_{\delta_e}} QS\bar{c}/I_{yy}$

To specify the system for a particular aircraft and flight condition, the appropriate values, determined from flight testing, wind tunnel testing, or geometric analysis, are used in the relations in Table 1. For this project, the aircraft of interest is of the light twin class, and the flight condition of interest for ground effect analysis is a final approach with landing gear and flaps extended. The numerical quantities for a Beech B99, a representative twin engine aircraft, are provided in Appendix A. Table 2 also summarizes the stability and control parameters for the Beech B99. To simplify the parameter estimation, the small parameters C_{L_u} and $C_{M_{\dot{\alpha}}}$ are assumed zero.

Table 2 Beech B99 Longitudinal Stability and Control Parameters

$C_{L_0} = 1.1500$	$C_{D_0} = 0.1620$	$C_{m_0} = 0.0000$
$C_{L_u} = 0.0000$	$C_{D_u} = 0.0000$	$C_{m_u} = 0.0000$
$C_{L_\alpha} = 6.2400$	$C_{D_\alpha} = 0.9330$	$C_{m_\alpha} = -2.0800$
$C_{L_q} = 8.1000$	$C_{D_q} = 0.0000$	$C_{m_q} = -34.0000$
$C_{L_{\delta_e}} = 0.5800$	$C_{D_{\delta_e}} = 0.0000$	$C_{m_{\delta_e}} = -1.9000$

Note: Angular parameters are per radian.

With the parameters and other values for the approach flight condition substituted into Equation 4, the longitudinal linear system becomes:

$$\begin{bmatrix} \Delta\dot{u} \\ \Delta\dot{w} \\ \Delta\dot{q} \\ \Delta\dot{\theta} \end{bmatrix} = \begin{bmatrix} -0.0536 & 0.0359 & 0 & -32.1741 \\ -0.3807 & -1.0598 & 165.6422 & 0 \\ 0 & -0.0378 & -2.0074 & 0 \\ 0 & 0 & 1 & 0 \end{bmatrix} \begin{bmatrix} \Delta u \\ \Delta w \\ \Delta q \\ \Delta\theta \end{bmatrix}$$

$$+ \begin{bmatrix} 0 \\ -16.3222 \\ -5.8679 \\ 0 \end{bmatrix} [\Delta\delta_e] \tag{5}$$

Appendix B includes the program LONGDERV.C, which automates calculating the elements of the above system.

With the system in numerical form, the solution for any desired elevator input is straightforward. MATLAB is used for the maneuver simulation. Once the state-space matrices are entered, MATLAB requires a time vector, the input time history and an initial state vector to simulate the aircraft's response. The file LONGSTUP.M, which may be used to set up the matrices and initial conditions, is also in Appendix B. The time histories for the four states in the system are calculated using MATLAB's *lsim* command, which integrates the system equations in a fourth-order Runge-Kutta numerical scheme. The time increment for the integration is specified by the input time vector. From these state histories, additional quantities of interest are determined using the following relations:

$$\Delta\alpha = \Delta w / u_0 \tag{6}$$

$$\Delta h = (u\sin\theta - w\cos\theta)\Delta t \tag{7}$$

$$a_{n_k} = -\left(\left(\Delta w_{k+1} - \Delta w_k\right)/\Delta t + \left(\Delta w_k - \Delta w_{k-1}\right)/\Delta t\right)/2 \tag{8}$$

$$a_{x_k} = \left(\left(\Delta u_{k+1} - \Delta u_k\right)/\Delta t + \left(\Delta u_k - \Delta u_{k-1}\right)/\Delta t\right)/2 \tag{9}$$

$$\dot{q}_k = \left(\left(\Delta q_{k+1} - \Delta q_k\right)/\Delta t + \left(\Delta q_k - \Delta q_{k-1}\right)/\Delta t\right)/2 \tag{10}$$

The file LONGSIM.M, included in Appendix B, automates the noise-free simulation procedure. In addition, this file arranges all pertinent time histories into a single matrix, called MEASURED, that the user may save for later use in pEst. MATLAB also permits the user to plot the time histories, which helps determine the suitability of each maneuver for use in ground effect. All maneuvers are simulated for ten seconds, with the input(s) beginning at the one second point. For longitudinal maneuvers, most responses damp out within ten seconds. In the lateral-directional case, excitation sometimes persists longer than ten seconds, but good estimates are obtained with just ten seconds of simulated data.

Figure 3 presents the time histories for a three degree up-down elevator doublet. The maneuver begins with the aircraft in level, unaccelerated flight at twenty-five feet above the runway and 170 ft/s (100 knots). The maximum altitude is 30 feet, well within ground effect, and the minimum is 23 feet. Airspeed changes only slightly. Pitch angle and pitch rate vary moderately, as does angle of attack. In view of these considerations, this maneuver is acceptable for use in ground effect, if it provides useful parameter estimates.

Lateral-Directional Mode Simulation

For the lateral-directional case, assume $\Delta\dot{\phi} = \Delta p$, $\theta_0 \approx 0$, and let:

$$\Delta\beta \approx \tan^{-1}\left(\Delta v / u_0\right) = \Delta v / u_0 \tag{11}$$

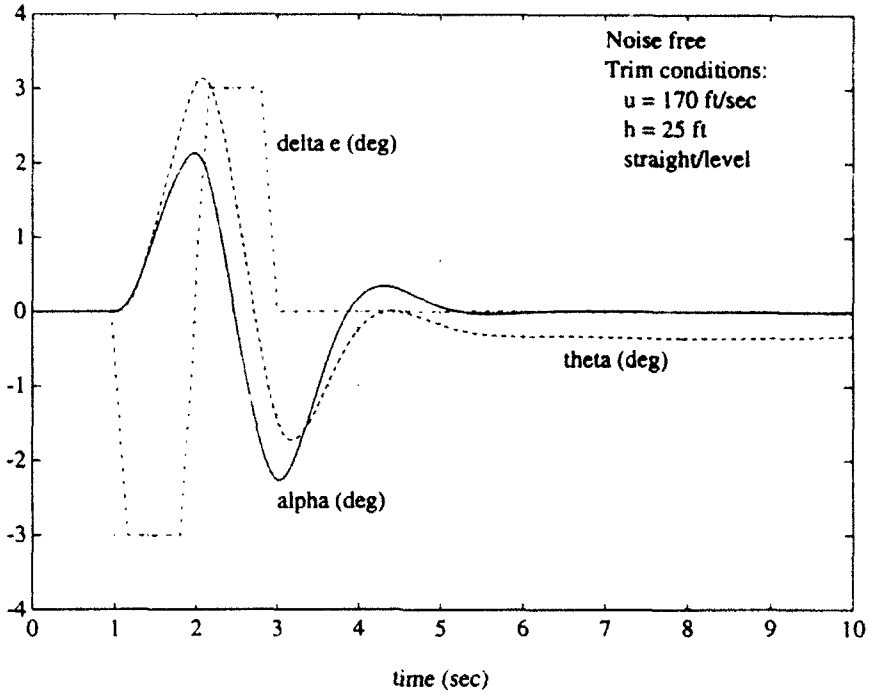

Figure 3a Beech B99 Response to a Three Degree Elevator Doublet

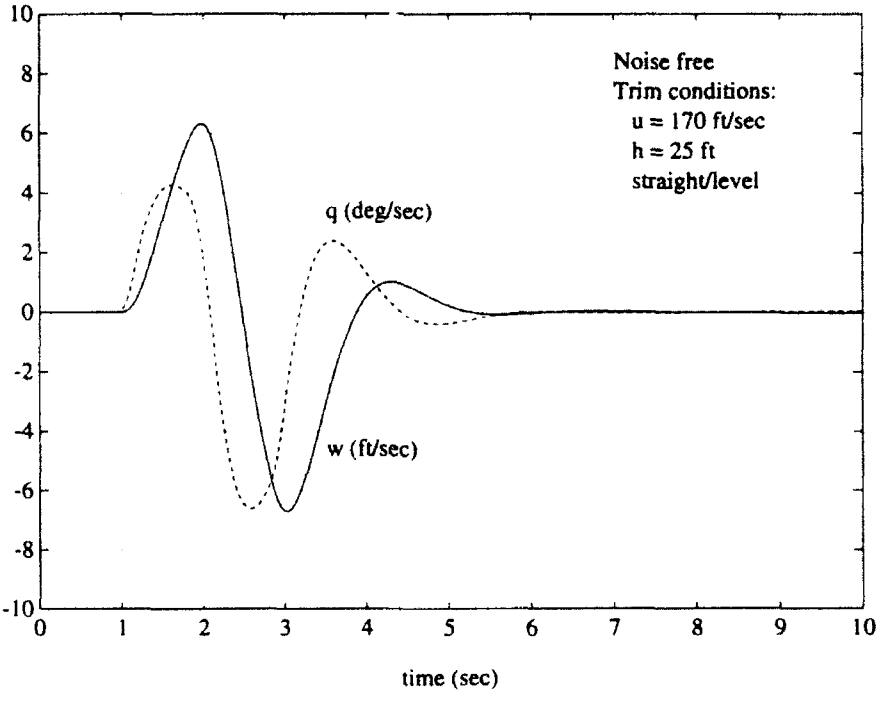

Figure 3b Beech B99 Response to a Three Degree Elevator Doublet

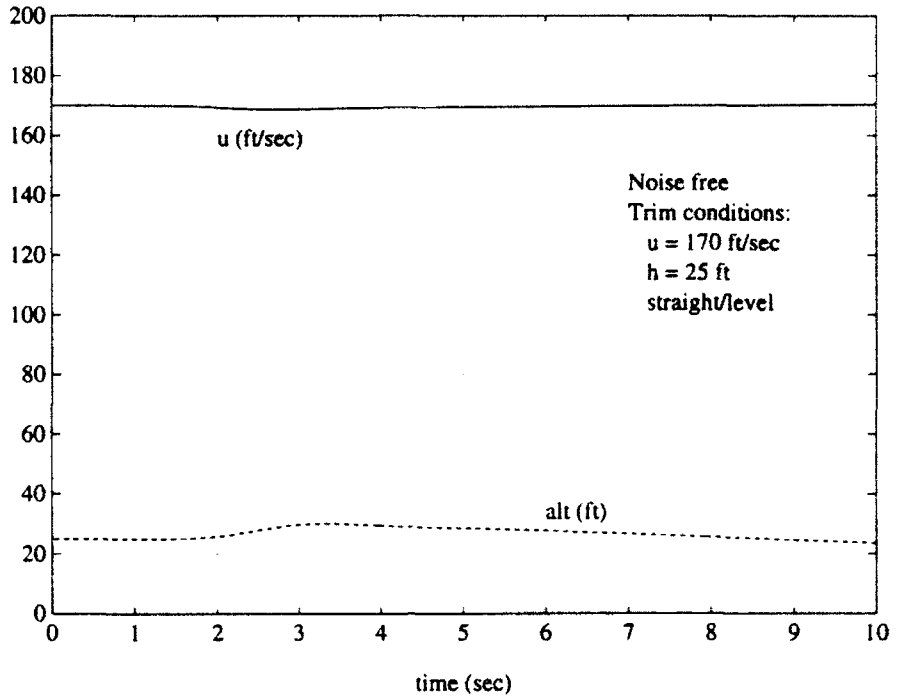

Figure 3c Beech B99 Response to a Three Degree Elevator Doublet

For the simulation, assume I_{xz} is small (this assumption may be more valid for some aircraft and configurations than others). With these assumptions, Equation (2) reduces to:

$$\Delta\dot{\beta} = {}^{Y_\beta}\!/_{u_0}\,\Delta\beta + {}^{Y_p}\!/_{u_0}\,\Delta p - \left(1 - {}^{Y_r}\!/_{u_0}\right)\Delta r + {}^{g}\!/_{u_0}\,\Delta\phi + {}^{Y_{\delta_r}}\!/_{u_0}\,\Delta\delta_r$$

$$\Delta\dot{p} = L_v\Delta v + L_p\Delta p + L_r\Delta r + L_{\delta_a}\Delta\delta_a + L_{\delta_r}\Delta\delta_r$$

$$\Delta\dot{r} = N_\beta\Delta\beta + N_p\Delta p + N_r\Delta r + N_{\delta_a}\Delta\delta_a + N_{\delta_r}\Delta\delta_r \qquad (12)$$

In state-space form, the system is:

$$\begin{bmatrix} \Delta\dot{\beta} \\ \Delta\dot{p} \\ \Delta\dot{r} \\ \Delta\dot{\phi} \end{bmatrix} = \begin{bmatrix} Y_\beta/_{u0} & Y_p/_{u0} & -\left(1 - Y_r/_{u0}\right) & g/_{u0} \\ L_\beta & L_p & L_r & 0 \\ N_\beta & N_p & N_r & 0 \\ 0 & 1 & 0 & 0 \end{bmatrix} \begin{bmatrix} \Delta\beta \\ \Delta p \\ \Delta r \\ \Delta\phi \end{bmatrix}$$

$$+ \begin{bmatrix} 0 & Y_{\delta_r}/_{u0} \\ L_{\delta a} & L_{\delta_r} \\ N_{\delta a} & N_{\delta_r} \\ 0 & 0 \end{bmatrix} \begin{bmatrix} \Delta\delta_a \\ \Delta\delta_r \end{bmatrix} \tag{13}$$

With the numerical values for the B99, the system becomes:

$$\begin{bmatrix} \Delta\dot{\beta} \\ \Delta\dot{p} \\ \Delta\dot{r} \\ \Delta\dot{\phi} \end{bmatrix} = \begin{bmatrix} -0.0977 & -0.0047 & -0.9913 & 0.1893 \\ -3.7880 & -1.9711 & 0.2365 & 0 \\ 1.5556 & -0.0088 & -0.3578 & 0 \\ 0 & 1 & 0 & 0 \end{bmatrix} \begin{bmatrix} \Delta\beta \\ \Delta p \\ \Delta r \\ \Delta\phi \end{bmatrix}$$

$$+ \begin{bmatrix} 0 & 0.0238 \\ 4.5456 & 0.2535 \\ -0.0156 & -0.9891 \\ 0 & 0 \end{bmatrix} \begin{bmatrix} \Delta\delta_a \\ \Delta\delta_r \end{bmatrix} \tag{14}$$

Similar to the longitudinal system developed earlier, the system above models the Beech B99's response to any aileron or rudder inputs. The numerical relations for the terms in the system are in presented Table 3. Table 4 summarizes the lateral-directional parameters for the Beech B99, as used in Equation (14).

Table 3 Lateral-Directional Dimensional Parameter Definitions

$Y_\beta = C_{y_\beta} QS / m$	$L_{\delta_a} = C_{l_{\delta_a}} QSb / I_{xx}$
$Y_p = C_{y_p} QSb / 2mu_0$	$L_{\delta_r} = C_{l_{\delta_r}} QSb / I_{xx}$
$Y_r = C_{y_r} QSb / 2mu_0$	$N_\beta = C_{n_\beta} QSb / I_{zz}$
$Y_{\delta_r} = C_{y_{\delta_r}} QS / m$	$N_p = C_{n_p} QSb^2 / 2I_{zz}u_0$
$L_\beta = C_{l_\beta} QSb / I_{xx}$	$N_r = C_{n_r} QSb^2 / 2I_{zz}u_0$
$L_p = C_{l_p} QSb^2 / 2I_{xx}u_0$	$N_{\delta_a} = C_{n_{\delta_a}} QSb / I_{zz}$
$L_r = C_{l_r} QSb^2 / 2I_{xx}u_0$	$N_{\delta_r} = C_{n_{\delta_r}} QSb / I_{zz}$

Table 4 Beech B99 Lateral-Directional Stability and Control Parameters

C_{y_β} = -0.5900	C_{l_β} = -0.1300	C_{n_β} = 0.1200
C_{y_p} = -0.2100	C_{l_p} = -0.5000	C_{n_p} = -0.0050
C_{y_r} = 0.3900	C_{l_r} = 0.0600	C_{n_r} = -0.2040
$C_{y_{\delta_a}}$ = 0.0000	$C_{l_{\delta_a}}$ = 0.1560	$C_{n_{\delta_a}}$ = -0.0012
$C_{y_{\delta_r}}$ = 0.1440	$C_{l_{\delta_r}}$ = 0.0087	$C_{n_{\delta_r}}$ = -0.0763

Note: Angular parameters are per radian.

An automated routine for calculating the terms in Equation (13), called LATDERV.C, is provided in Appendix B.

As in the longitudinal case, MATLAB simulates the aircraft response to any aileron or rudder inputs. Now, the input time history is a two-dimensional vector which specifies both aileron and rudder movements. Two files, LATSTUP.M and LATSIM.M, are used in MATLAB for the maneuver simulation. In LATSIM.M, rate term estimates use the following relations:

$$v_y = v_0 \tan\beta \tag{15}$$

$$a_{y_k} = -\left(\left(\Delta v_{y_{k+1}} - \Delta v_{y_k}\right)/\Delta t + \left(\Delta v_{y_k} - \Delta v_{y_{k-1}}\right)/\Delta t\right)/2 \tag{16}$$

$$\dot{p}_k = \left(\left(\Delta p_{k+1} - \Delta p_k\right)/\Delta t + \left(\Delta p_k - \Delta p_{k-1}\right)/\Delta t\right)/2 \tag{17}$$

$$\dot{r}_k = \left(\left(\Delta r_{k+1} - \Delta r_k\right)/\Delta t + \left(\Delta r_k - \Delta r_{k-1}\right)/\Delta t\right)/2 \tag{18}$$

The pertinent time histories are again arranged in a variable named MEASURED. Appendix B includes both LATSTUP.M and LATSIM.M. As noted earlier, lateral-directional maneuvers are simulated for ten seconds, with the input sequence beginning at the one-second mark. Maneuvers 5c and 6b are examples of maneuvers which exhibit sizable transient behavior beyond ten seconds. Simulating these maneuvers for twenty seconds provides no significant differences in the parameter estimates; therefore, ten seconds of response is adequate for the estimation. These results are available for comparison in Appendix E.

Figure 4 illustrates the response history for a combined aileron doublet - rudder doublet maneuver for level, unaccelerated flight at 170 ft/s. This maneuver merely serves as an example, but will prove to provide excellent parameter estimates

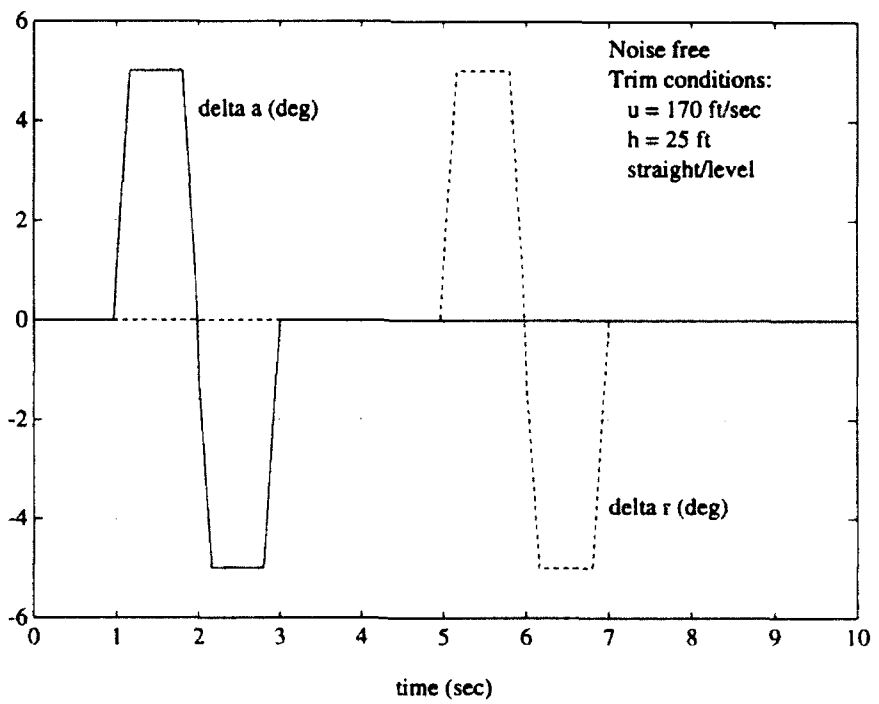

Figure 4a Beech B99 Response to Aileron and Rudder Doublets

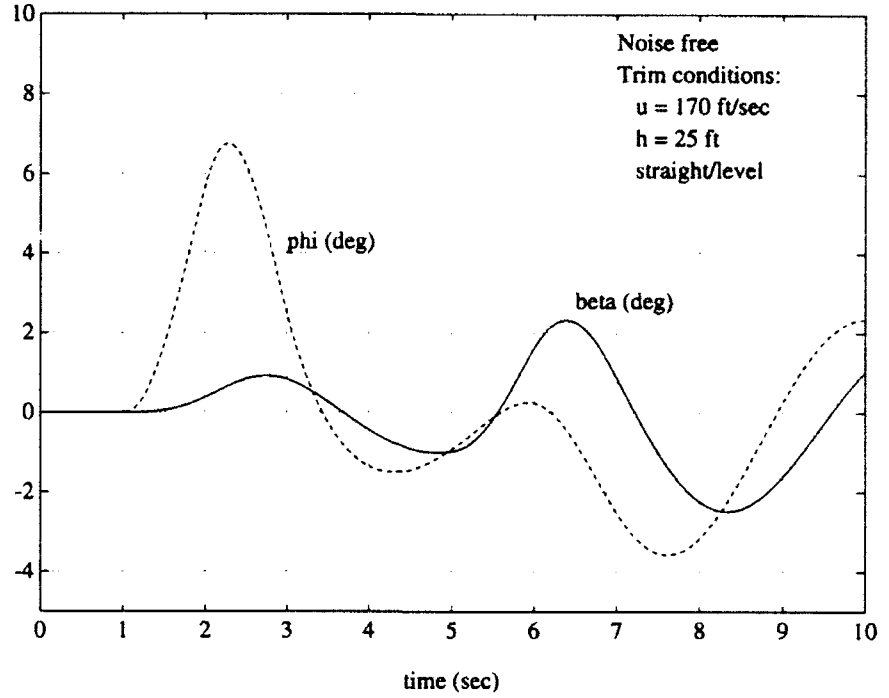

Figure 4b Beech B99 Response to Aileron and Rudder Doublets

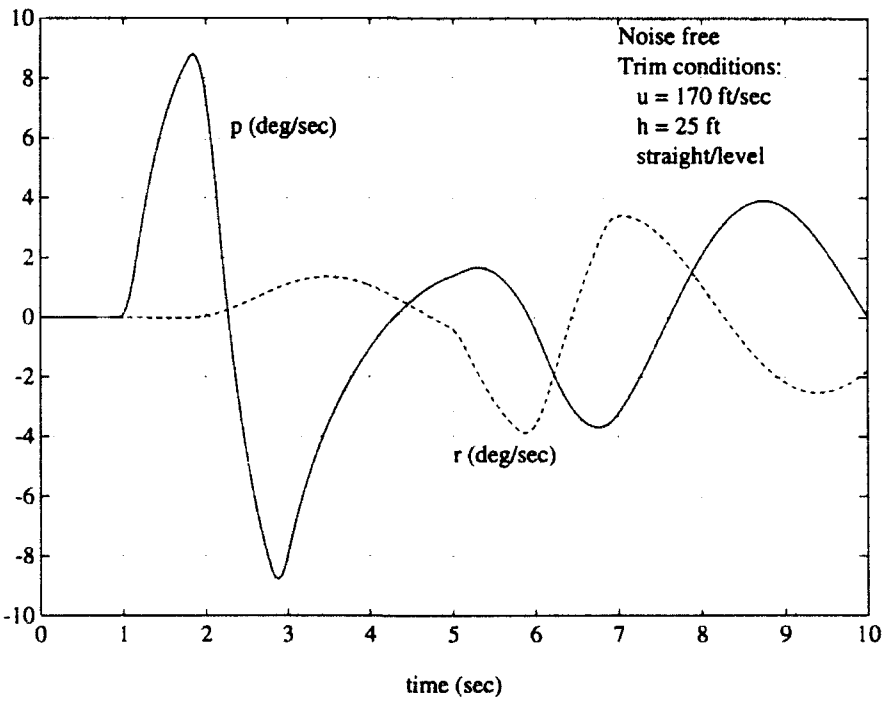

Figure 4c Beech B99 Response to Aileron and Rudder Doublets

later. Since the lateral-directional and longitudinal modes are assumed uncoupled, altitude loss or gain during moderate lateral-directional maneuvers is assumed negligible. This study does not verify this idealization with six degree-of-freedom simulations.

AIRCRAFT PARAMETER ESTIMATION

The maneuver time histories, here simulated in MATLAB, are analyzed in a system identification routine to estimate the stability and control parameters. The purpose of the parameter estimation is to return the parameter values used in the simulation. Thus, the study identifies maneuvers that provide accurate parameter estimation from simulated data. In the future, using these flight test techniques in ground effect should result in direct measurement of these parameters, and thus the effect of ground proximity on them.

The parameter estimation is performed using pEst, a program written by James E. Murray and Richard E. Maine at NASA's Dryden Flight Research Facility[11]. This software is used extensively at Dryden for experimental parameter estimation in both linear and non-linear flight regimes.

To estimate stability and control parameters, pEst requires mass and geometric quantities specific to the aircraft in question and time histories of the aircraft's dynamic responses. Given the constant quantities above and the control input, pEst performs its own integration of the equations of motion with an initial "guess" at the parameter vector. The program begins an iterative search for a "best" parameter vector by the prediction-error (or output-error) approach, which optimizes agreement between the measured response and its computed response. The prediction-error approach, described below, differs from other estimation

methods, such as ARMAX and Box-Jenkins, in that it deals only with the error between the computed and measured responses[9]. Some methods, such as the two mentioned above, model the properties of the error terms. The prediction-error approach, on the other hand, does not attempt to characterize or predict the error as it increments the estimated parameter vector; therefore, it is more appropriate in cases where the sources of error are numerous, random, or unknown. PEst optimizes by minimizing the scalar cost function

$$J(\varepsilon) = \left(\frac{1}{2 n_z n_t}\right) \sum_{i=1}^{n_t} [z(t_i) - \tilde{z}(t_i)]^T W [z(t_i) - \tilde{z}(t_i)] \tag{19}$$

where z is the measured response, $\tilde{z}$ is the computed response, n_t and n_z are the numbers of time points and response variables respectively, W is a response weighting matrix, ε is the parameter vector, and ^{T} denotes transpose.

In pEst, the user may tailor the cost function by changing the weights of each response in W; the program also permits complete flexibility in the active parameters and responses, convergence criteria, and initial parameter values. In fact, this study only begins to utilize pEst's estimation capability - for consistency, the default values given in Appendix A are used for response weights, convergence bounds, and initial parameter guesses. The default values allow acceptable parameter estimation for longitudinal and lateral-directional maneuvers; optimizing the above terms is beyond the scope of this study, but may improve estimates and should be attempted.

The prediction-error approach used in pEst is described in detail in Ljung's book[9]. The approach estimates parameters by minimizing the cost function

$$V_N(\varepsilon) = \frac{1}{N} \sum_{t=1}^{N} \frac{1}{2} E^2(t, \varepsilon) \tag{20}$$

where ε is the parameter vector, N the number of time points, and E the error (or residual) between the measured and computed responses. The similarities between this form and Equation (19) are obvious - pEst simply adds a weighting factor to the basic nonlinear least-squares minimization.

A number of methods may be used to increment the parameter estimate; Ljung describes the method recommended by Murray for pEst, the Levenberg-Marquardt algorithm. In prediction-error methods, the parameter vector is incremented using the relation:

$$\hat{\varepsilon}^{(i+1)} = \hat{\varepsilon}^{(i)} + \mu f^{(i)} \tag{21}$$

Here, $f^{(i)}$ is the "search direction," based on the cost function at the i^{th} iteration, μ is a positive constant chosen such that cost always decreases, and ^ denotes an estimate. Newton minimization methods use V' and V'' (the Hessian) in determining $f^{(i)}$, so

$$f^{(i)} = -\left[V''(\hat{\varepsilon}^{(i)})\right]^{-1} V'(\hat{\varepsilon}^{(i)}) \tag{22}$$

which is termed the "Newton direction."

The terms in Equation (22) are

$$V'_N(\varepsilon) = -\frac{1}{N}\sum_{t=1}^{N} \psi(t,\varepsilon)E(t,\varepsilon) \tag{23}$$

and

$$V''_N(\varepsilon) = \frac{1}{N}\sum_{t=1}^{N} \psi(t,\varepsilon)\psi^T(t,\varepsilon) + \frac{1}{N}\sum_{t=1}^{N} \psi'(t,\varepsilon)E(t,\varepsilon) = H_N(\varepsilon) \tag{24}$$

where ψ is the gradient matrix of the state prediction and ψ' is the Hessian of the error E. The ψ' term is often costly to compute, so it is left out, and an approximation of H_N is used in determining the search direction. This omission is

acceptable because a good estimate of the Hessian is required only near the solution, and near the solution the error, and consequently the omitted term, is small. Thus,

$$V''_N(\varepsilon) \approx \frac{1}{N}\sum_{t=1}^{N}\psi(t,\varepsilon)\psi^T(t,\varepsilon) = H_N(\hat{\varepsilon}) \tag{25}$$

This estimate has the advantage of being positive semidefinite, which guarantees convergence. This Newtonian technique is called the Gauss-Newton method or (in pEst) the modified Newton-Raphson method.

When this modified Newton-Raphson method is used, the Hessian sometimes becomes singular or close to singular. The Levenberg-Marquardt procedure implements a solution to this weakness, where

$$V''_N(\varepsilon) \approx \frac{1}{N}\sum_{t=1}^{N}\psi(t,\varepsilon)\psi^T(t,\varepsilon) + \eta I \tag{26}$$

is used in this event, and η is some small positive scalar. In pEst, this algorithm is available and is recommended by the programmers as the most efficient and robust.

Several other variations of the prediction-error approach are available in pEst: among them are the Gauss-Newton method, the steepest descent (or gradient) method, and the Davidson-Fletcher-Powell algorithm. These methods differ mainly in their search direction calculations. All are more prone to converging away from the solution than the Levenberg-Marquardt method, particularly the steepest descent approach. The main advantage these methods have over Levenberg-Marquardt is in computer workload. According to the authors of pEst, the Levenberg-Marquardt method is clearly superior to these alternative methods in estimate accuracy.

Before data from the simulation may be used in pEst, they must be arranged in a format acceptable to the program. All time history data are saved into an ASCII data file while in MATLAB, but the format is not recognized by pEst or

getData[14], a file manipulation program designed for use with pEst. The getData manual provides an example of an acceptable data format.

Two programs, LONGFRMT.C and LATFRMT.C, edit the data file from MATLAB and configure the file for input into getData or pEst. In addition to adjusting the numerical format, these programs add the appropriate heading to the file, indicating to pEst the name of each time history. Appendix C includes both programs.

Once the simulation data are modified by one of these programs, they may be entered into getData or pEst. If a segment of the data is deemed unusable, getData may be used to remove the unwanted time points or signals. Although removing time points is usually unnecessary for the data in this study, getData can also compress the data. All data files used in pEst for this research are compressed by getData to save memory space and to allow faster file manipulation. It should be noted that compressed data result in negligibly different parameter estimates, presumably due to subtle changes inherent in the compression.

After the data file is read into pEst, program specifics must be set before the parameter estimation may begin. The program requires physical dimensions, weight, and inertias of the test aircraft, and the parameters of interest must be activated. In addition, the user must specify the desired state and response equations. This procedure may be done using an input file, or the required information may be specified on-line after entering pEst. Example longitudinal and lateral-directional input files are included in Appendix C. After this information is entered, pEst can save an initial status file to provide startup points for elevator, aileron, rudder, and combined aileron-rudder maneuvers, or the input files may be used each time pEst is initialized.

This research uses the default options for other program settings, based on the recommendations of the pEst manual; among these are integration method (fourth-order Runge-Kutta), minimization method (Levenberg-Marquardt), and gradient method (single-sided). The Runge-Kutta integration uses the time points in the measured data file - there is no requirement for constant step size. All the states are activated, and the cost function contains four responses for each case. In the longitudinal case, angle of attack, pitch angle, pitch rate, and velocity are the active responses. For lateral-directional maneuvers, the responses are sideslip angle, bank angle, roll rate, and yaw rate.

In addition to returning estimates of the active parameters, pEst calculates a Cramer-Rao bound for each parameter, which provides a relative measure of the regression's confidence in the estimate. The Cramer-Rao bounds are based on the estimated Fisher information matrix and probability density function at the final iteration. and approximate the variance of each parameter's estimates about the converged value[9].

FLIGHT TEST MANEUVER EVALUATION

The objective of this research, as stated previously, is to identify flight test techniques suitable for estimating stability and control parameters in ground effect. Some evaluation of flight test maneuvers is therefore necessary. The first segment of this section presents the procedure for simulating longitudinal and lateral-directional maneuvers numerically. A description of the parameter estimation program pEst and its use follows. These simulation and estimation tasks are the two major requirements of the maneuver analysis procedure.

This study performs six separate evaluations. The first is a preliminary maneuver analysis with as close to perfect data as is available from the simulation. This evaluation assesses the maneuvers themselves, without any added uncertainty other than that inherent in the simulation and estimation, and builds a basic set of maneuvers for the other studies. Four additional evaluations investigate the individual effects of instrument precision, measurement bias, noise, and acquisition system sampling rate on the parameter estimation. Finally, precision, bias, and noise are combined to more realistically represent flight test data. Each evaluation includes both longitudinal and lateral-directional maneuvers. Since the changes in most performance measures due to ground effect are between ten and forty percent, a parameter estimate within ten percent of the simulated value is considered a useful estimate in this study. Ten percent accuracy also proves to be a realistic goal for the parameter estimation, although many estimates are considerably better - these more accurate estimates improve the likelihood that the ground effect will be "visible".

Tables 5 and 6 present the longitudinal and lateral-directional maneuvers considered in this study. Unless otherwise noted, each maneuver begins in straight, level, unaccelerated flight at twenty-five feet above the runway. The preliminary evaluation selects those maneuvers suitable for further evaluation, based on the evaluation criteria in Figure 2 without added uncertainty (bias, noise, or precision). One drawback of using pEst's maximum likelihood scheme is that aircraft excitation is absolutely essential. In light of this requirement, constant altitude flare maneuvers with little excitation provide poor estimates. Maneuvers with more excitation, and thus more height change, provide much better estimates, but this height variation precludes ground effect study at specific altitudes. Rather, the maneuvers in this study will permit measurement of the average ground effect in a range of heights

Table 5 Longitudinal Maneuver Matrix

#1a - 1° 1 second up elevator pulse
#1b - 3° 1 second up elevator pulse
#1c - 5° 1 second up elevator pulse
#1d - 7° 1 second up elevator pulse
#2a - 1° 2 second up-down elevator doublet
#2b - 3° 2 second up-down elevator doublet
#2c - 5° 2 second up-down elevator doublet
#2d - 7° 2 second up-down elevator doublet
#3a - 3° 4 second up-down elevator doublet
#3b - 5° 4 second up-down elevator doublet
#4a - 1° 8 second up-down elevator doublet
#4b - 3° 8 second up-down elevator doublet
#5a - 3° 1 second up elevator pulse, 1 second pause, 3° 1 second down elevator pulse
#5b - 5° 1 second up elevator pulse, 1 second pause, 5° 1 second down elevator pulse
#5c - 3° 1 second up elevator pulse, 2 second pause, 3° 1 second down elevator pulse
#5d - 5° 1 second up elevator pulse, 2 second pause, 5° 1 second down elevator pulse
#6a - 3° 2 second up elevator pulse, 2° glide path
#6b - 5° 2 second up elevator pulse, 2° glide path
#6c - 1° 2 second up elevator pulse, 2° glide path
#7a - 5° 1 second up elevator pulse, 2° glide path

Table 6 Lateral-Directional Maneuver Matrix

#1a - 1° 1 second right aileron pulse
#1b - 3° 1 second right aileron pulse
#1c - 5° 1 second right aileron pulse
#1d - 7° 1 second right aileron pulse
#1e - 3° 2 second right aileron pulse
#1f - 5° 2 second right aileron pulse
#2a - 1° 2 second right-left aileron doublet
#2b - 3° 2 second right-left aileron doublet
#2c - 5° 2 second right-left aileron doublet
#2d - 7° 2 second right-left aileron doublet
#2e - 3° 1 second right-left aileron doublet
#2f - 5° 1 second right-left aileron doublet
#2g - 3° 4 second right-left aileron doublet
#2h - 5° 4 second right-left aileron doublet
#3a - 1° 1 second right rudder pulse
#3b - 3° 1 second right rudder pulse
#3c - 5° 1 second right rudder pulse
#3d - 7° 1 second right rudder pulse
#3e - 3° 2 second right rudder pulse
#3f - 5° 2 second right rudder pulse
#4a - 1° 2 second right-left rudder doublet

Table 6 (Continued)

#4b - 3° 2 second right-left rudder doublet
#4c - 5° 2 second right-left rudder doublet
#4d - 7° 2 second right-left rudder doublet
#4e - 3° 1 second right-left rudder doublet
#4f - 5° 1 second right-left rudder doublet
#4g - 3° 4 second right-left rudder doublet
#4h - 5° 4 second right-left rudder doublet
#5a - 3° 1 second right aileron pulse, 3° 1 second left rudder pulse
#5b - 5° 1 second right aileron pulse, 5° 1 second left rudder pulse
#5c - 3° 1 second right aileron pulse, 1 second pause, 3° 1 second left rudder pulse
#5d - 5° 1 second right aileron pulse, 1 second pause, 5° 1 second left rudder pulse
#5e - 3° 1 second right aileron pulse, 2 second pause, 3° 1 second left rudder pulse
#5f - 5° 1 second right aileron pulse, 2 second pause, 5° 1 second left rudder pulse
#5g - 5° 1 second right aileron pulse, 5° 1 second right rudder pulse
#6a - 3° 2 second right aileron doublet, 3° 2 second left rudder doublet
#6b - 5° 2 second right aileron doublet, 5° 2 second left rudder doublet
#6c - 3° 2 second right-left aileron doublet, 1 second pause, 3° 2 second right-left rudder doublet

Table 6 (Continued)

#6d - 5° 2 second right-left aileron doublet, 1 second pause, 5° 2 second right-left rudder doublet
#6e - 3° 2 second right-left aileron doublet, 2 second pause, 3° 2 second right-left rudder doublet
#6f - 5° 2 second right-left aileron doublet, 2 second pause, 5° 2 second right-left rudder doublet

and the relative influence of ground effect on the longitudinal and lateral-directional parameters.

Most of the maneuvers in Tables 5 and 6 involve very small control inputs, which may be difficult for the test pilot to perform. A visual device in the cockpit marking the yoke and rudder pedal inputs required for appropriate aileron, elevator, and rudder deflections will be necessary for performing these maneuvers. A removable control brace or gate may also be helpful, but the safety of any device restricting control movements must be carefully evaluated before it is used in flight.

Not all measurement equipment is capable of the same precision; therefore, the second evaluation establishes desired levels of instrument precision. The precision analysis varies precision by rounding the time history data appropriately as they are passed through the formatting program, either LNFRMT.C or LDFRMT.C.

The simulated system sampling rate is altered by changing the interval between discrete time points in MATLAB's integration of the equations of motion. This analysis compares 10Hz and 50Hz sampling rates, in addition to the basic 25Hz rate.

In addition to varying precision, many instruments exhibit measurement bias. Bias is simulated by adding or subtracting an appropriate value to the time history data, again as the data go into the formatting routines.

The noise analysis considers four types of noise: a random normal distribution; a random uniform distribution; a 10Hz periodic input; and a 5Hz periodic input. A pseudo-random number generator in MATLAB provides the random distributions. Periodic noise is added by superimposing a sine wave of the appropriate frequency on the data within MATLAB. The simulation routine randomly phase-shifts these periodic inputs to ensure they are independent among the responses.

The final evaluation sums together levels of precision, bias, and noise that provide good estimates by themselves. Since physical systems exhibit all these characteristics to some degree, this final evaluation provides the most realistic simulation of a flight test maneuver measured with a data acquisition system, and the most realistic parameter estimation.

MANEUVER ANALYSIS RESULTS

PRELIMINARY MANEUVER ANALYSIS RESULTS

The first stage of the maneuver analysis is an idealized evaluation without any added uncertainty or bias. This preliminary evaluation studies the maneuvers themselves, and builds a basic set of maneuvers for the subsequent studies. The results of this evaluation are as close to perfect as is possible with the simulation; these results are available for comparison with later results and the responses are used to evaiuate the safety of each maneuver. The preliminary analysis considers the maneuvers from Tables 5 and 6 using the procedure outlined in Figure 2, without adding uncertainty or bias.

Longitudinal Results

The longitudinal maneuvers in Table 5 all provide estimates of at least four parameters within ten percent of the simulated values. Numerous maneuvers, in fact, allow more accurate estimates, within three to four percent, of seven or all eight of the lift and moment derivatives. None of the longitudinal maneuvers permit accurate estimates of the four drag derivatives. Appendix D includes the numerical estimation results, including Cramer-Rao bounds.

An acceptable test maneuver must keep the aircraft in ground effect; therefore, height is limited to forty feet, slightly less than the forty-six foot span-width. Of the twenty longitudinal maneuvers in Table 5, only twelve meet this criterion. The other eight maneuvers, namely 1b, 1c, 1d, 3a, 3b, 4a, and 4b, are accordingly ruled out. The height ranges for each maneuver are in the right-hand column of Table 7.

Table 7 Longitudinal Response Ranges

	u (ft/s)	w (ft/s)	q (deg/sec)	θ (deg)	h (ft)
#1a	168 - 170	-0.5 - 2.0	-1.0 - 1.5	-0.2 - 1.1	25 - 31
#1b	166 - 170	-0.75 - 6.5	-2.5 - 4.5	-0.5 - 3.5	25 - 44
#1c	164 - 170	-1.0 - 11.0	-4.0 - 7.0	-1.0 - 5.5	25 - 55
#1d	161 - 170	-2.0 - 15.0	-6.0 - 10.0	-0.5 - 5.0	25 - 67
#2a	169 - 171	-2.2 - 2.0	-2.2 - 1.5	-0.6 - 1.0	24 - 27
#2b	168 - 171	-7.0 - 6.0	-7.0 - 4.0	-2.0 - 3.0	23 - 30
#2c	167 - 171	-12.0 - 10.0	-11.0 - 7.0	-3.0 - 5.0	23 - 34
#2d	167 - 171	-15.0 - 15.0	-15.0 - 10.0	-4.0 - 7.0	21 - 37
#3a	166 - 171	-8.0 - 7.0	-7.0 - 4.0	-2.5 - 5.0	25 - 44
#3b	163 - 172	-13.0 - 12.0	-11.0 - 7.0	-4.0 - 9.0	22 - 56
#4a	166 - 170	-2.5 - 2.5	-2.5 - 1.5	-2.5 - 3.0	25 - 44
#4b	158 - 170	-7.0 - 7.0	-7.0 - 4.0	-7.0 - 8.0	25 - 80
#5a	168 - 171	-6.0 - 6.0	-4.0 - 4.5	-2.0 - 3.0	23 - 34
#5b	166 - 171	-10.0 - 10.0	-7.0 - 7.0	-3.0 - 5.0	22 - 40
#5c	167 - 171	-6.0 - 6.0	-4.5 - 4.5	-2.0 - 3.0	24 - 38
#5d	165 - 171	-10.0 - 10.0	-8.0 - 8.0	-3.5 - 5.5	25 - 46
#6a	162 - 170	5.5 - 14.0	-3.0 - 4.0	-1.0 - 5.0	13 - 25
#6b	157 - 170	5.0 - 18.0	-5.0 - 7.0	-2.0 - 9.0	14 - 43
#6c	167 - 170	5.8 - 8.5	-1.0 - 1.5	-0.5 - 2.0	-20 - 25
#7a	164 - 170	5.0 - 17.0	-4.0 - 7.0	-1.0 - 5.0	13 - 25

The next set of criteria ensure that the maneuver is safe. The following response limits, based on the author's flying experience, are established:

$$u : \pm 20 \text{ ft/sec}$$

$$w : \pm 10 \text{ ft/sec}$$

$$q : \pm 10 \text{ deg/sec}$$

$$\theta : \pm 5 \text{ deg}$$

$$h : 10 \text{ ft minimum} \qquad (27)$$

These limits are instantaneous limits - each maneuver must be evaluated individually to ensure small deviations over time do not result in an unsafe flight path. In addition, they are designed for a maneuver starting at twenty-five feet above the ground - if lower initial altitudes are desired, the limits must be adjusted.

Table 7 lists the response ranges for each maneuver. All maneuvers meet the minimum forward velocity criterion. In fact, very little velocity change occurs during most maneuvers. These small velocity perturbations most likely contribute to the poor drag estimates encountered. Maneuvers 1c, 1d, 2c, 2d, 3b, 6a, 6b, and 7a do not meet the limits on normal velocity. Three maneuvers, 2c, 2d, and 3b, exceed the pitch rate limits. Maneuver 6c, a one degree up-elevator pulse from a glide path, results in a minimum height of -20 feet, which the airplane would never reach in reality.

After the above concerns are considered, five maneuvers remain which meet the ground effect and safety criteria. They are: a one degree up elevator pulse from level flight (1a); a one degree up-down elevator doublet from level flight (2a); a three degree up-down elevator doublet from level flight (2b); a three degree up elevator pulse, followed by a one second pause and a three degree down pulse (5a); and a five degree up elevator pulse, followed by a one second pause and a five

degree down pulse (5b). Of these, the ones that provide the best parameter estimates are the most promising flight test techniques.

Figures 5 through 9 present the estimation results of the five maneuvers above. One parameter, C_{m0}, is approximately zero for the Beech B99. The estimates for this parameter are less than 0.001 for all five maneuvers, which is an order of magnitude below any other estimate. The estimates are therefore considered close to zero, and though they do not appear in the figures, are accurate estimates. None of the drag derivative estimates are close enough to the simulated values to appear within the range of the figures.

From Figure 5, all of the lift and moment derivative estimates are within four percent of their simulated values. The one degree doublet in Figure 6 provides estimates of five parameters within two percent, and two others within eight

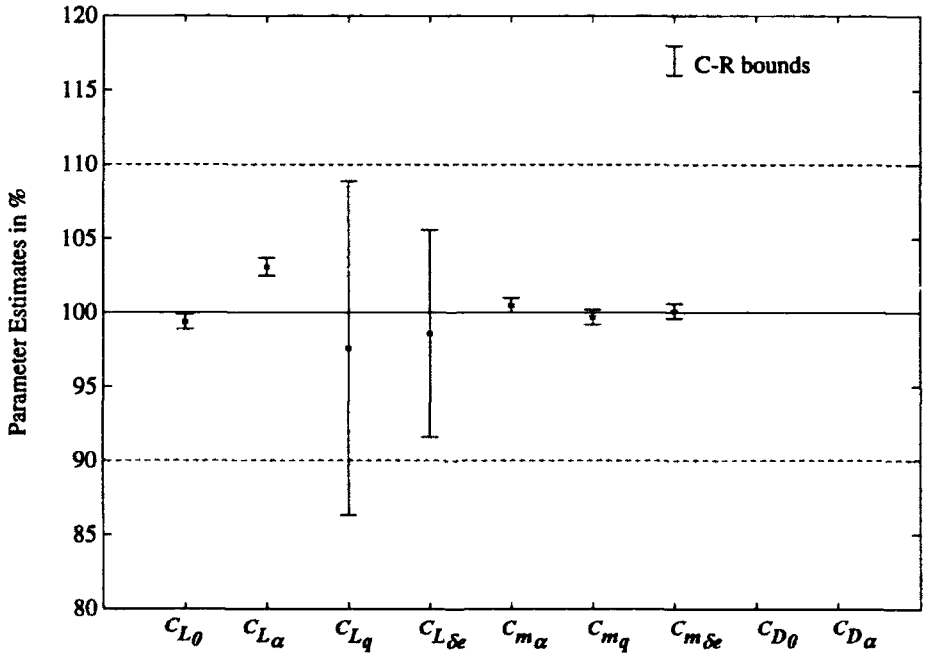

Figure 5 Parameter Estimates from a One Degree Elevator Pulse (Maneuver 1a)

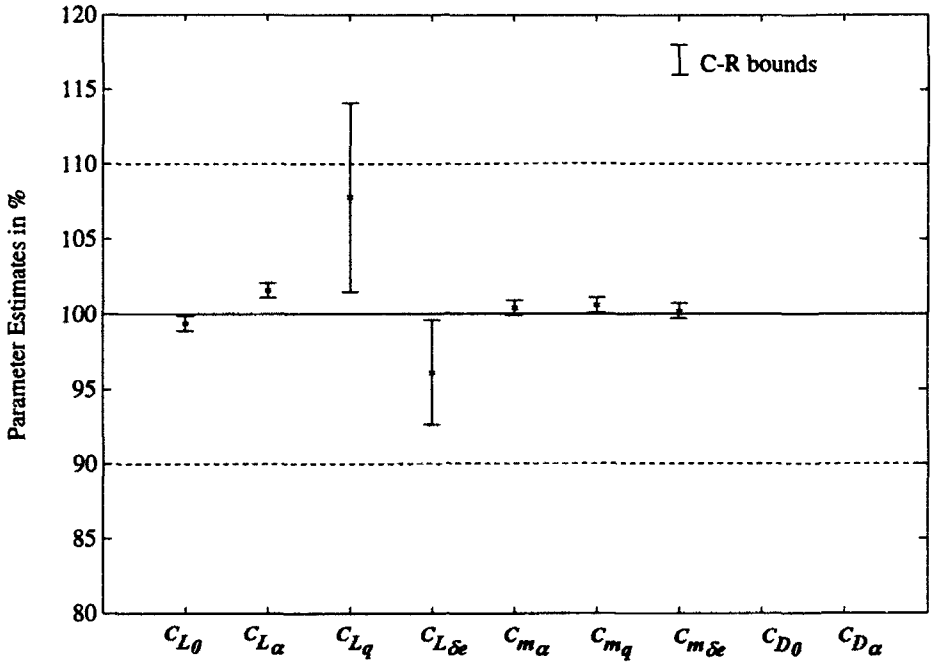

Figure 6 Parameter Estimates from a One Degree Elevator Doublet (Maneuver 2a)

percent. The three degree doublet in Figure 7 results in a slightly less accurate $C_{l_{\delta e}}$ estimate, but the other lift and moment estimates are acceptable. The reason for the less accurate control derivative is not clear. Maneuvers 5a and 5b, in Figures 8 and 9, provide accurate estimates of six and seven parameters, respectively. Again, all parameter estimates and Cramer-Rao bounds are in Appendix D.

The primary reason for the poor drag estimates is the absence of thrust terms in the longitudinal model. A thrust model is not included because thrust derivatives for a twin-engine aircraft were not found in available literature. This omission makes the model somewhat incomplete - for the simulation, thrust and drag are effectively equal throughout the maneuver, and very little velocity excitation, usually less than five feet per second, results. Adding an accurate thrust model into the simulation should provide better drag estimates, and would be a useful improvement.

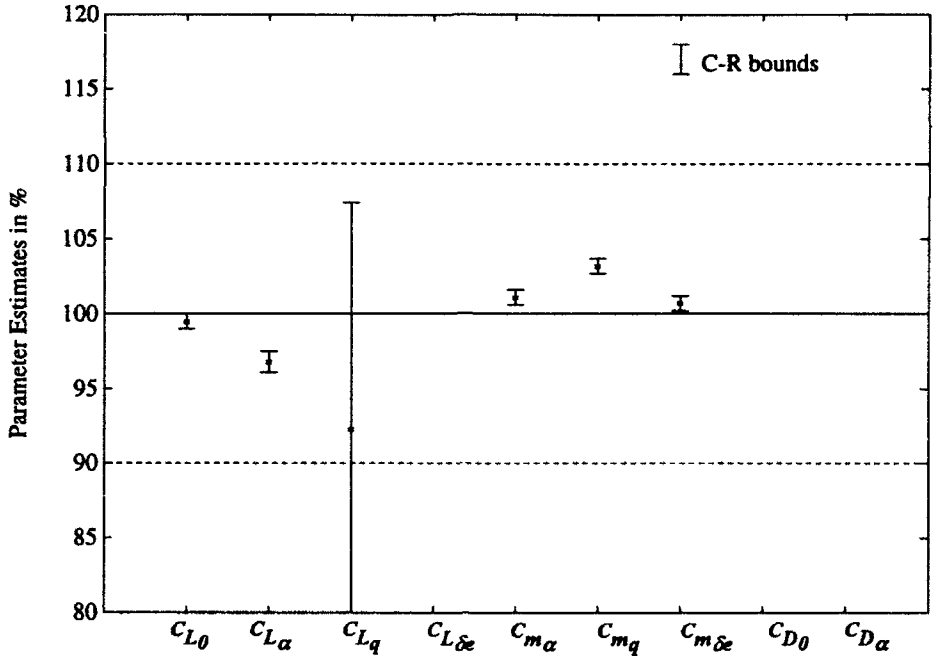

Figure 7 Parameter Estimates from a Three Degree Elevator Doublet (Maneuver 2b)

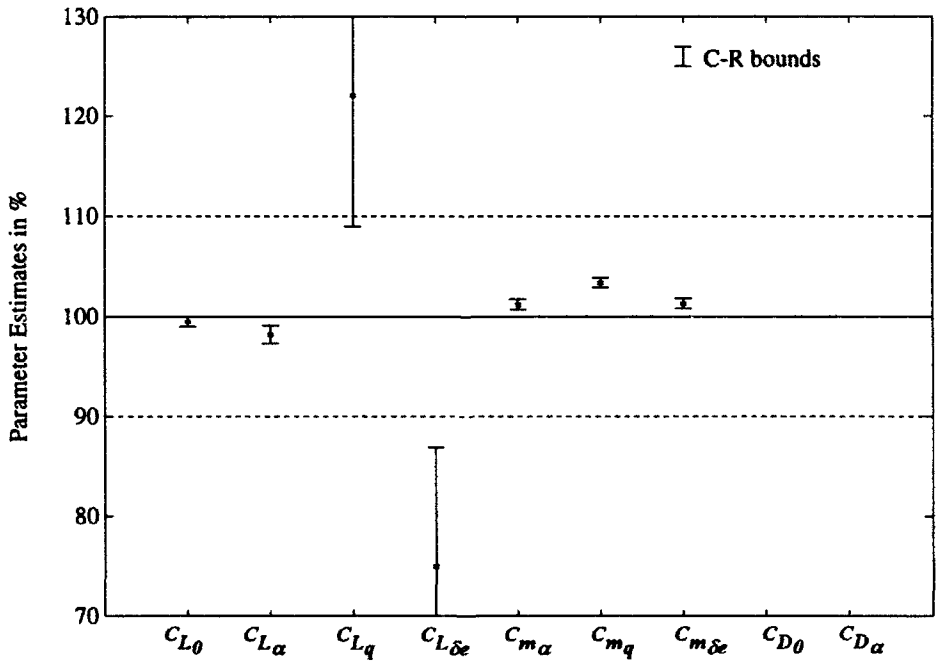

Figure 8 Parameter Estimates from a Three Degree Up Elevator Pulse, One Second Pause, Three Degree Down Pulse (Maneuver 5a)

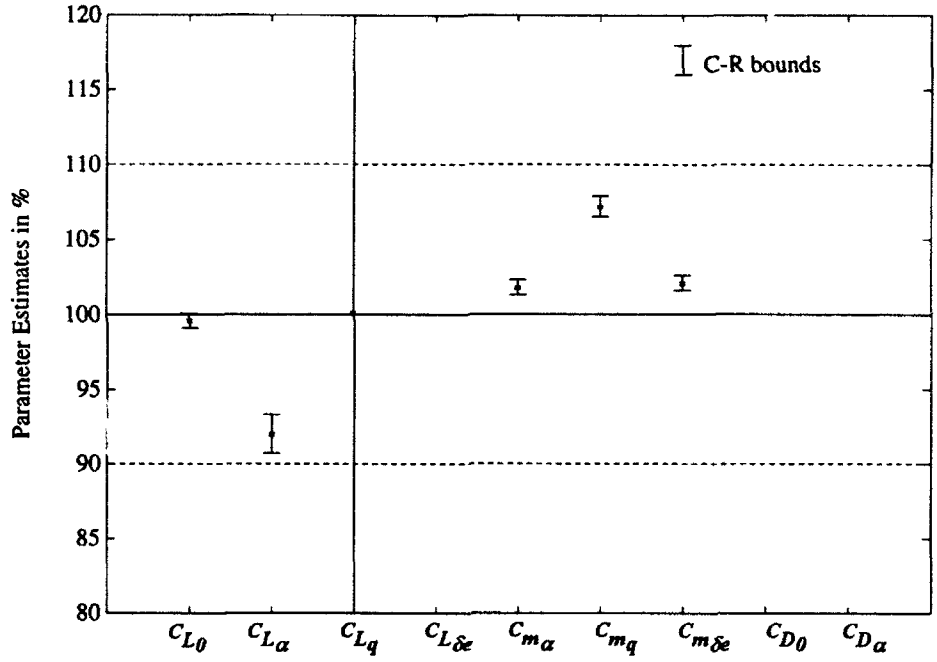

Figure 9 Parameter Estimates from a Five Degree Up Elevator Pulse, One Second Pause, Five Degree Down Pulse (Maneuver 5b)

Total lift and moment coefficients result from the following relations:

$$C_L = C_{L_0} + C_{L_\alpha}\Delta\alpha + C_{L_q}\Delta q + C_{L\delta_e}\Delta\delta_e \tag{28}$$

$$C_m = C_{m_0} + C_{m_\alpha}\Delta\alpha + C_{m_q}\Delta q + C_{m\delta_e}\Delta\delta_e \tag{29}$$

From these relations, multiplying the parameter estimates and associated maximum response perturbations provides each parameter's contribution to the total lift and moment coefficients. Each term in these totals, then, clearly indicates the relative influence of each derivative in the total, and thus the importance of accuracy in each parameter's estimate. Because each response has both positive and negative perturbations, and each parameter may be positive or negative, both the maximum perturbations and the estimates are represented as magnitudes. Therefore, the total derivatives noted below are estimates of the magnitudes only, and are meant merely to indicate relative influence rather than direction. Because all the terms are added,

the total value is the maximum possible. Tables 8 and 9 present these relative terms for the estimates in the preliminary analysis, as calculated in Appendix D.

Table 8 Lift Coefficient Relative Influences

Estimated terms (% of actual C_L magnitude)					Total (% of actual C_L)
Maneuver	C_{L_0}	$C_{L_\alpha}\cdot\Delta\alpha$	$C_{L_q}\cdot\Delta q$	$C_{L_{\delta_e}}\cdot\Delta\delta_e$	C_L
1a	76.6	8.3	13.9	0.6	**99.4**
2a	72.3	7.0	21.3	0.6	**101.2**
2b	45.8	12.6	36.6	0.7	**95.7**
5a	53.3	14.9	36.3	1.1	**105.6**
5b	41.8	18.3	36.3	0.5	**96.9**

Table 9 Pitching Moment Coefficient Relative Influences

Estimated terms (% of actual C_m magnitude)					Total (% of actual C_m)
Maneuver	C_{m_0}	$C_{m_\alpha}\cdot\Delta\alpha$	$C_{m_q}\cdot\Delta q$	$C_{m_{\delta_e}}\cdot\Delta\delta_e$	C_m
1a	0.1	4.1	92.2	3.4	**99.8**
2a	0.1	2.6	95.5	2.4	**100.6**
2b	0.1	2.5	98.2	2.3	**103.1**
5a	0.1	3.8	96.0	3.5	**103.3**
5b	0.1	4.1	98.9	3.7	**106.8**

From Table 8, C_{L_0} and C_{L_q} have the most significant influence on lift coefficient, and thus are the most important to estimate accurately. The C_{L_q}

estimates for the five selected maneuvers are generally less accurate and have higher uncertainty bounds than the estimates for C_{L_0} and C_{L_α}, and the maneuvers where this parameter has large influence result in less accurate estimates of the total lift magnitude. Thus, manuevers allowing more accurate C_{L_q} estimates, such as Maneuvers 1a, 2a, or 5b, may be preferred.

Likewise, from Table 9, C_{m_q} is clearly the dominant factor in the moment coefficient for these maneuvers. The estimates for C_{m_q}, however, are within five percent for all but Maneuver 5b, and result in accurate total moment magnitudes.

Lateral-Directional Results

Each of lateral-directional maneuvers from Table 6 allows accurate estimation of at least seven of the fifteen stability and control parameters of interest. As in the longitudinal case, a number of maneuvers result in estimates within three percent of the simulated values. Collectively, the maneuvers considered permit accurate estimates of all the lateral-directional parameters simulated. Appendix E includes the numerical estimates for these maneuvers and their Cramer-Rao bounds.

For lateral and directional maneuvers with small inputs, longitudinal motion is considered negligible; the height limits enforced in the longitudinal case are therefore unimportant in this case. Again, these limits are based on the author's flying experience, but are reasonably conservative, in his opinion. The instantaneous safety limits for lateral-directional responses are:

$$\begin{aligned} \phi &: \pm 10 \text{ deg} \\ \beta &: \pm 5 \text{ deg} \\ p &: \pm 10 \text{ deg/sec} \\ r &: \pm 10 \text{ deg/sec} \end{aligned} \tag{30}$$

These limits are instantaneous: response values below these limits may not be acceptable if they are prolonged. An example of this instance involves bank angle ϕ, during the five degree aileron pulse maneuver. During this maneuver, the aircraft remains at more than five degrees of bank for several seconds. This bank results in a heading change and some lateral displacement, possibly taking the aircraft beyond the lateral limits of the runway. With the aircraft beyond the runway edges, accidental ground contact is considerably less safe; therefore, the maneuver is unacceptable on safety grounds. In addition to the displacement problem, prolonged bank may invalidate the assumption that height loss is small in a lateral-directional maneuver. For similar reasons, several other maneuvers that meet the instantaneous criteria are deemed unacceptable.

Table 10 lists the response ranges for lateral-directional maneuvers. Maneuvers 1c, 1d, 1e, and 1f, all aileron pulses, are unacceptable because of prolonged bank, as well as excessive bank angle and roll rate in some cases. High roll rates rule out two aileron doublets, Maneuvers 2d and 2h. Maneuvers 3f and 4h, among the larger rudder maneuvers, both have high bank angles; the latter maneuver also exceeds roll rate and sideslip angle limits. Five aileron-rudder pulse maneuvers, 5b, 5d, 5e, 5f, and 5g, also result in prolonged bank and are unsafe. Thus, of the forty-one maneuvers considered, twenty-eight meet the safety criteria.

Of these twenty-eight, eleven are selected for the accuracy of their estimates. Consideration is given to the simplicity of each maneuver - combined aileron-rudder maneuvers, while providing some accurate parameter estimates, demand more from the test pilot in a general aviation aircraft. Accordingly, the final eleven include only two combined maneuvers. In an aircraft with a programmable flight control system, the combined maneuvers would make excellent choices, since they

Table 10 Lateral-Directional Response Ranges

	ϕ (deg)	β (deg)	p (deg/sec)	r (deg/sec)
#1a	0.0 - 1.7	-0.1 - 0.3	-0.3 - 1.8	-0.01 - 0.45
#1b	0.0 - 5.0	-0.3 - 0.8	-1.0 - 5.5	-0.05 - 1.4
#1c	0.0 - 8.0	-0.4 - 1.2	-2.0 - 9.0	-0.05 - 2.3
#1d	0.0 - 11.5	-0.7 - 1.7	-2.5 - 13.0	-0.1 - 3.2
#1e	0.0 - 10.5	-0.4 - 1.4	-1.5 - 6.0	-0.05 - 2.8
#1f	0.0 - 17.0	-0.7 - 2.3	-3.0 - 10.0	-0.1 - 4.5
#2a	-0.3 - 1.4	-0.2 - 0.2	-1.8 - 1.8	-0.22 - 0.27
#2b	-1.0 - 4.0	-0.6 - 0.6	-5.0 - 5.0	-0.7 - 0.8
#2c	-1.5 - 7.0	-1.0 - 0.9	-9.0 - 9.0	-1.1 - 1.4
#2d	-2.0 - 9.0	-1.5 - 1.3	-13.0 - 13.0	-1.5 - 1.8
#2e	-0.2 - 1.2	-0.13 - 0.13	-2.0 - 3.0	-0.15 - 0.2
#2f	-0.3 - 2.0	-0.22 - 0.22	-3.0 - 5.0	-0.22 - 0.3
#2g	-3.0 - 10.0	-1.7 - 1.3	-7.5 - 6.0	-2.0 - 2.5
#2h	-4.0 - 16.0	-3.0 - 2.2	-13.0 - 10.0	-3.0 - 4.0
#3a	-1.2 - 0.1	-0.4 - 0.5	-0.8 - 0.7	-0.6 - 0.4
#3b	-3.5 - 0.1	-1.2 - 1.5	-2.5 - 2.0	-1.7 - 1.2
#3c	-6.0 - 0.2	-2.0 - 2.5	-4.0 - 3.0	-3.0 - 2.0
#3d	-8.0 - 0.2	-3.0 - 3.5	-6.0 - 4.5	-4.0 - 3.0
#3e	-7.0 - 0.2	-2.0 - 2.5	-4.0 - 3.5	-2.8 - 2.0
#3f	-12.0 - 0.4	-3.5 - 4.2	-7.0 - 6.0	-4.5 - 3.2
#4a	-0.7 - 0.6	-0.6 - 0.4	-0.7 - 0.9	-0.6 - 0.8

Table 10 (Continued)

	ϕ (deg)	β (deg)	p (deg/sec)	r (deg/sec)
#4b	-2.2 - 1.8	-1.6 - 1.3	-2.0 - 2.5	-1.7 - 2.3
#4c	-3.5 - 3.0	-2.7 - 2.0	-3.5 - 4.5	-3.0 - 4.0
#4d	-5.0 - 4.0	-4.0 - 3.0	-5.0 - 6.0	-4.0 - 5.0
#4e	-0.5 - 0.4	-0.4 - 0.4	-0.6 - 0.6	-0.8 - 0.5
#4f	-0.8 - 0.7	-0.6 - 0.6	-1.0 - 1.0	-1.5 - 0.8
#4g	-6.0 - 5.0	-4.5 - 3.5	-5.0 - 7.0	-4.5 - 4.0
#4h	-10.0 - 8.0	-8.0 - 6.0	-8.0 - 12.0	-8.0 - 6.5
#5a	0.0 - 5.0	-1.5 - 2.2	-3.0 - 5.5	-1.2 - 2.5
#5b	0.0 - 8.5	-2.5 - 3.5	-6.0 - 9.0	-2.0 - 4.0
#5c	0.0 - 5.0	-1.0 - 1.7	-3.0 - 5.5	-0.8 - 2.0
#5d	0.0 - 8.5	-2.0 - 2.7	-4.0 - 9.0	-1.5 - 3.2
#5e	0.0 - 5.0	-0.8 - 1.2	-2.0 - 5.5	-0.5 - 1.5
#5f	0.0 - 8.0	-1.3 - 2.0	-3.0 - 9.0	-1.0 - 2.5
#5g	0.0 - 13.0	-1.5 - 2.0	-4.0 - 9.5	0.0 - 3.5
#6a	-2.5 - 4.0	-1.7 - 1.2	-5.5 - 5.5	-1.7 - 2.0
#6b	-4.0 - 7.0	-2.7 - 2.0	-9.0 - 9.0	-3.0 - 3.5
#6c	-2.0 - 4.0	-1.2 - 0.8	-5.5 - 5.5	-2.0 - 1.6
#6d	-3.0 - 7.0	-2.0 - 1.5	-9.0 - 9.0	-3.0 - 2.7
#6e	-2.0 - 4.0	-1.5 - 1.4	-5.5 - 5.5	-2.5 - 2.0
#6f	-4.0 - 7.0	-2.5 - 2.5	-9.0 - 9.0	-4.0 - 3.5

allow simultaneous estimates of both aileron and rudder parameters. Preference is also given to maneuvers with larger excitations when practical, as these are less affected by noise and bias. The eleven selected maneuvers are: a three degree aileron pulse (1b); one degree, three degree, and five degree aileron doublets (2a, 2b, and 2c); five degree and seven degree rudder pulses (3c and 3d); five degree and seven degree two second rudder doublets (4c and 4d); a three degree four second rudder doublet (4g); a three degree aileron pulse, followed by a one second pause and a three degree opposite rudder pulse (5c); and a five degree aileron doublet, followed by a five degree opposite rudder doublet (6b). As expected, evaluations indicate no significant difference in parameter estimates for inputs in opposite directions. For example, a left aileron pulse provides essentially the same results as does a right aileron pulse.

Figures 10 through 20 present the parameter results for the above maneuvers. One parameter, $C_{y_{\delta_a}}$, is simulated as zero, and does not appear in the figures. The estimates for this control derivative, however, are small enough that they are effectively zero for all the selected maneuvers. All four of the aileron maneuvers result in accurate estimates for the twelve pertinent parameters. For the rudder maneuvers, C_{y_p} and C_{y_r} estimates suffer, but the others are within ten percent. In particular, the three rudder control estimates are within two percent of their simulated values in each case. Both the combined aileron-rudder maneuvers provide excellent estimates of all fifteen parameters of interest.

Again, total force and moment coefficients exist; in this case they are side force, rolling moment, and yawing moment parameters. As in the longitudinal case, multiplying each parameter's value by the maximum perturbation in the corresponding response estimates each parameter's influence. Summing these

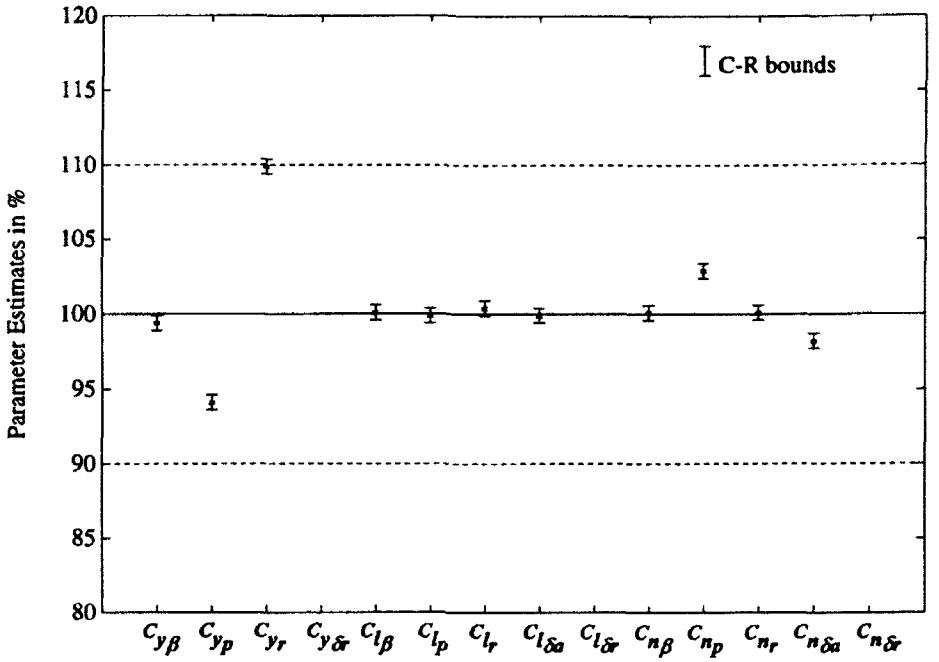

Figure 10 Parameter Estimates from a Three Degree Right Aileron Pulse (Maneuver 1b)

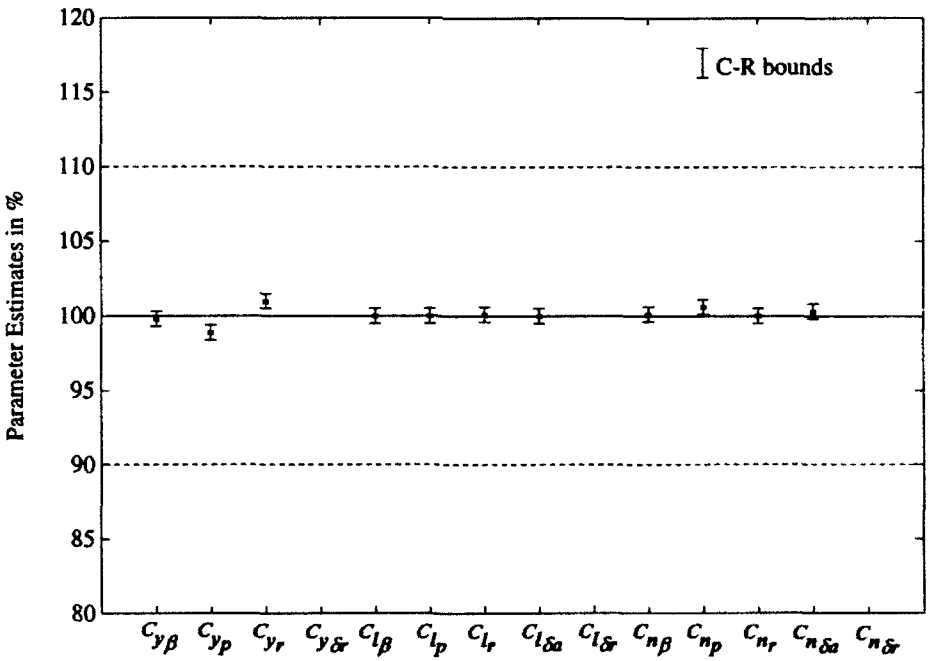

Figure 11 Parameter Estimates from a One Degree Aileron Doublet (Maneuver 2a)

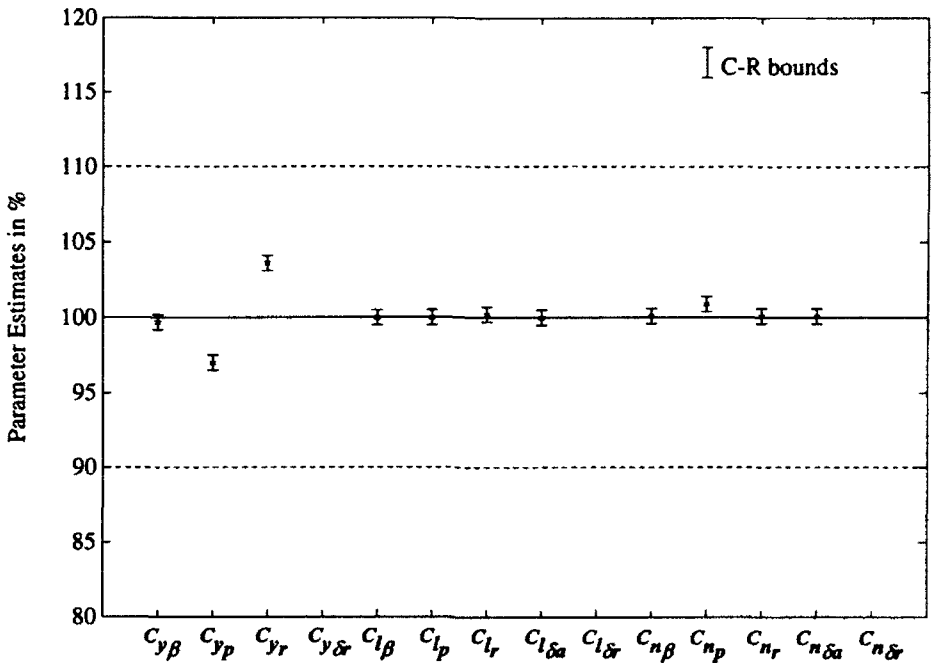

Figure 12 Parameter Estimates from a Three Degree Aileron Doublet (Maneuver 2b)

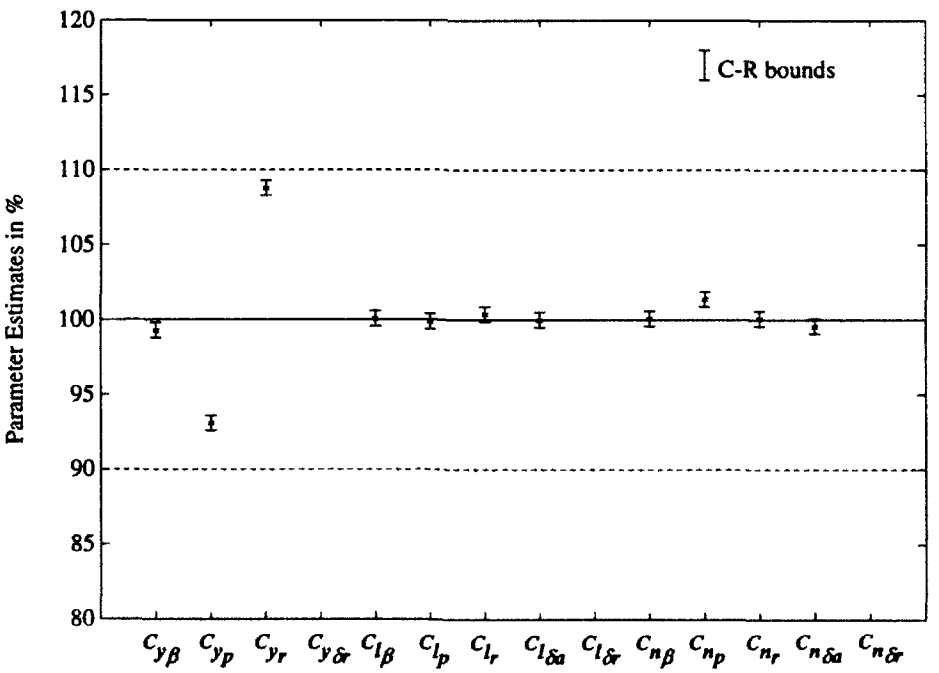

Figure 13 Parameter Estimates from a Five Degree Aileron Doublet (Maneuver 2c)

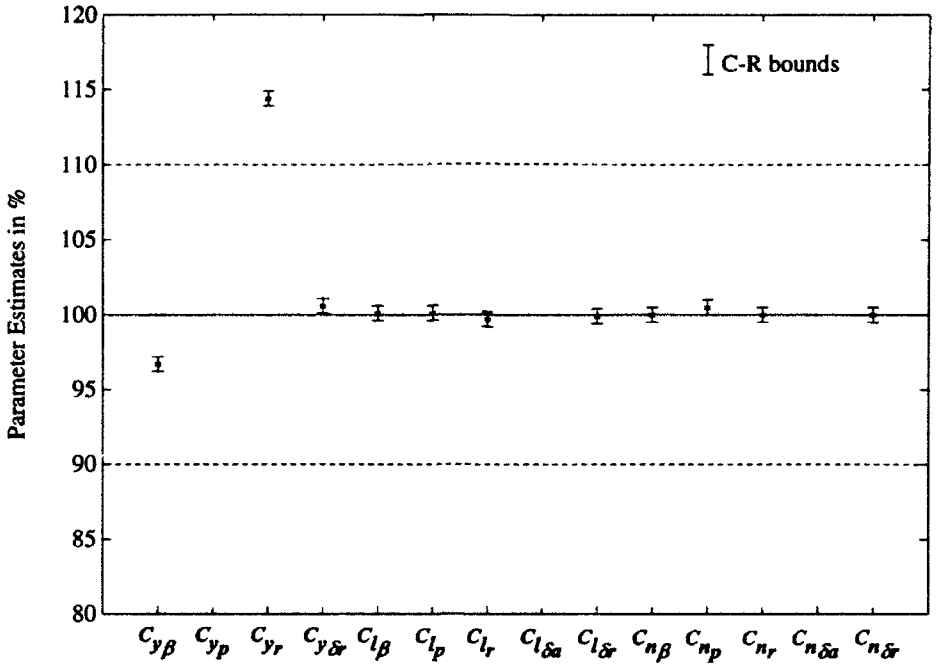

Figure 14 Parameter Estimates from a Five Degree Right Rudder Pulse (Maneuver 3c)

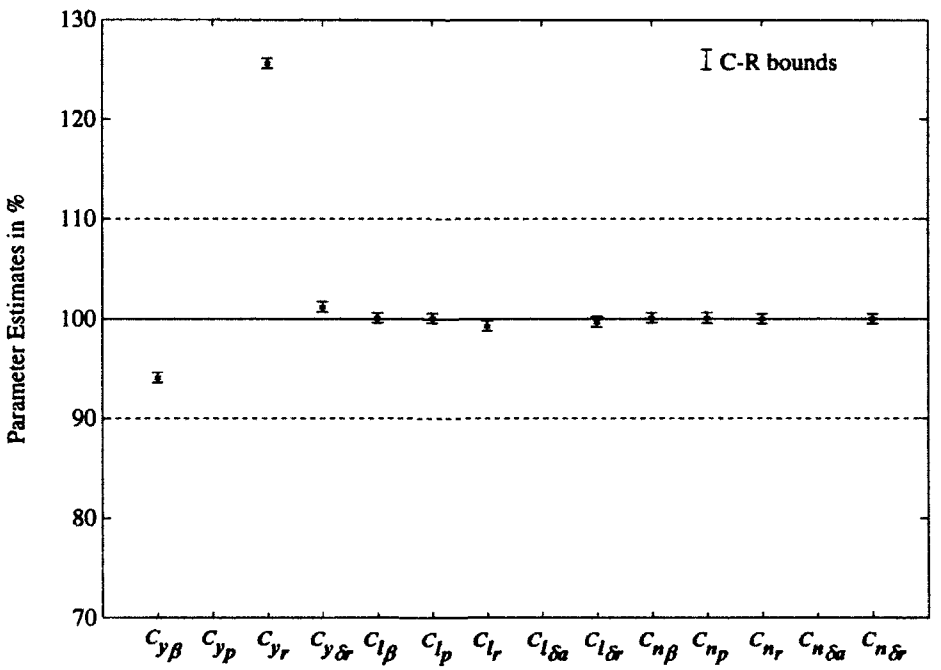

Figure 15 Parameter Estimates from a Seven Degree Right Rudder Pulse (Maneuver 3d)

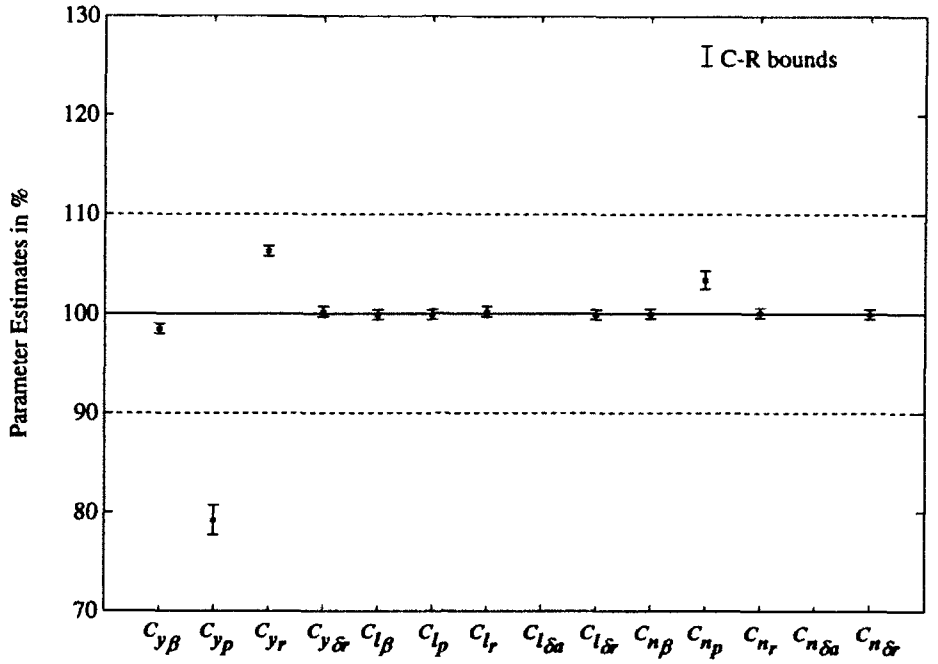

Figure 16 Parameter Estimates from a Five Degree, Two Second Rudder Doublet (Maneuver 4c)

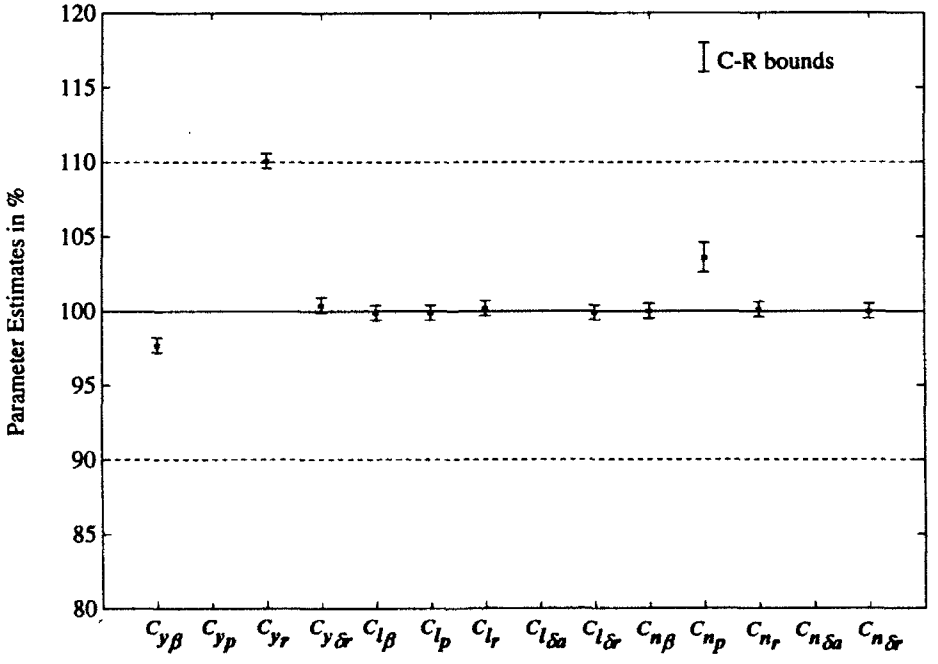

Figure 17 Parameter Estimates from a Seven Degree, Two Second Rudder Doublet (Maneuver 4d)

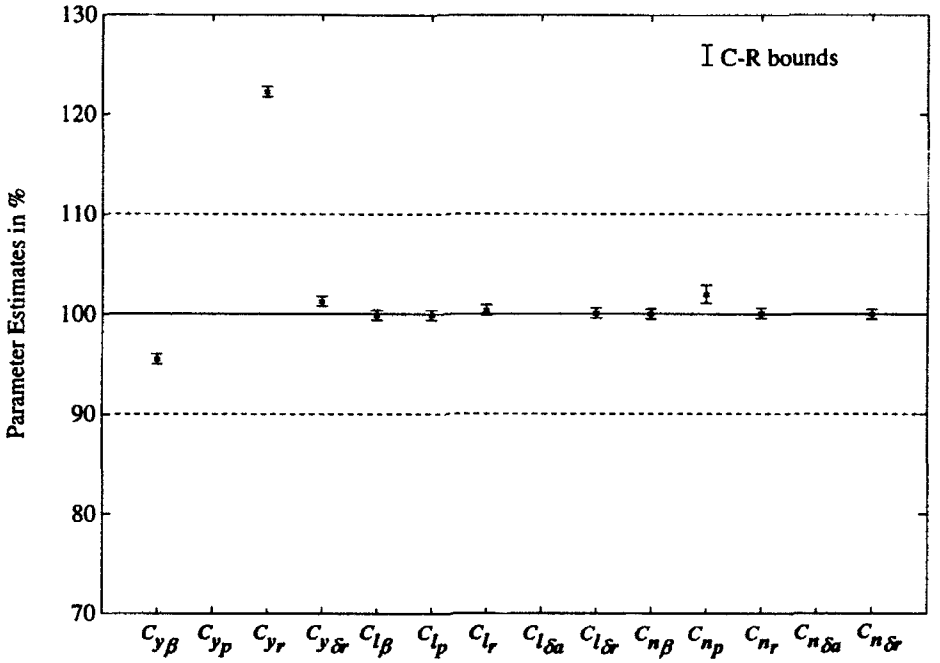

Figure 18 Parameter Estimates from a Three Degree, Four Second Rudder Doublet (Maneuver 4g)

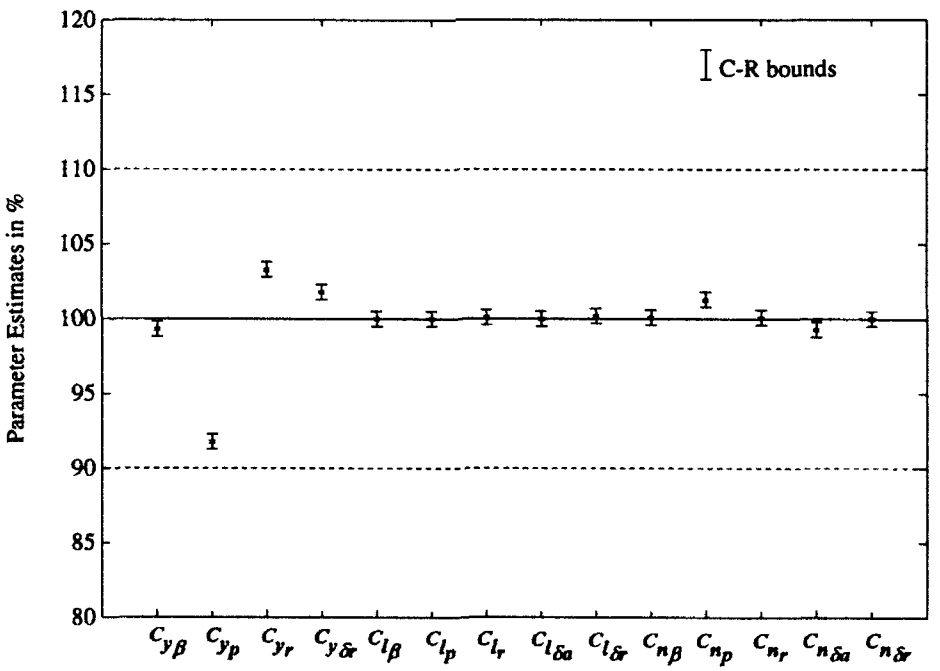

Figure 19 Parameter Estimates from a Three Degree Right Aileron Pulse, One Second Pause, Three Degree Left Rudder Pulse (Maneuver 5c)

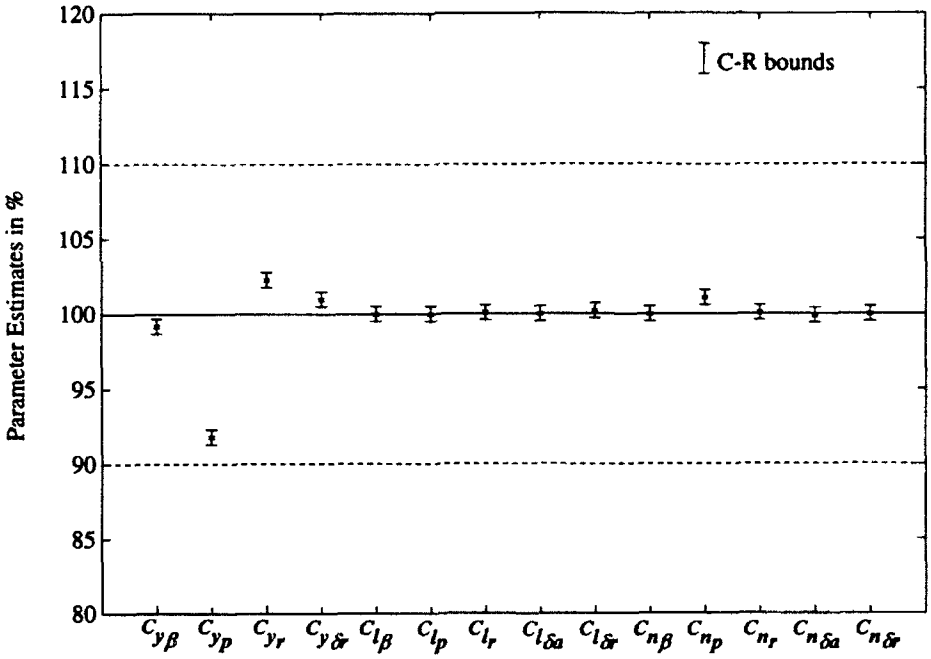

Figure 20 Parameter Estimates from a Five Degree Aileron Doublet, Five Degree Opposite Rudder Doublet (Maneuver 6b)

influences indicates the relative importance of each parameter on the total. Once more, the total values are conservative magnitudes, and are not meant to indicate direction. Tables 11, 12, and 13 present the relative influences in side force, rolling moment, and yawing moment, based on calculations in Appendix E.

The side force results in Table 11 indicate accurate total derivatives in most cases, and significant influence from β, p, r, and, for rudder maneuvers, δ_e derivatives. Several maneuvers, particularly 3d and 4d, result in C_{y_p} and C_{y_r} estimates outside ten percent - these estimates have detrimental effects on the totals.

All the rolling and yawing moment estimates are very accurate, and in each case in Tables 12 and 13 the total derivative estimate is within one percent of the actual. The derivative C_{l_p} is by far the most influential in rolling moment, as expected, and yawing moment depends largely on β, r, and δ_e parameters.

Table 11 Side Force Coefficient Relative Influences

Estimated terms (% of actual C_y magnitude)						Total (% of actual C_y)
Maneuver	$C_{y_\beta}\cdot\Delta\beta$	$C_{y_p}\cdot\Delta p$	$C_{y_r}\cdot\Delta r$	$C_{y_{\delta_a}}\cdot\delta_a$	$C_{y_{\delta_r}}\cdot\delta_r$	C_y
1b	21.6	50.1	27.6	0.2	--	**99.5**
2a	19.5	62.2	17.7	0.1	--	**99.5**
2b	20.5	59.4	18.8	0.2	--	**98.9**
2c	19.3	58.2	19.7	0.4	--	**97.6**
3c	33.9	10.8	31.8	--	17.2	**93.7**
3d	33.0	3.8	33.3	--	17.3	**87.4**
4c	32.5	15.6	34.4	--	15.0	**97.5**
4d	35.0	12.9	32.7	--	15.4	**96.0**
4g	40.1	8.5	34.1	--	6.9	**89.6**
5c	29.5	31.5	23.9	0.3	13.0	**98.2**
6b	28.4	31.2	25.1	0.2	13.0	**97.9**

Table 12 Rolling Moment Coefficient Relative Influences

Estimated terms (% of actual C_l magnitude)						Total (% of actual C_l)
Maneuver	$C_{l_\beta}\cdot\Delta\beta$	$C_{l_p}\cdot\Delta p$	$C_{l_r}\cdot\Delta r$	$C_{l_{\delta_a}}\cdot\delta_a$	$C_{l_{\delta_r}}\cdot\delta_r$	C_l
1b	3.0	80.7	2.5	13.7	--	**99.9**
2a	2.3	82.0	1.5	14.2	--	**100**
2b	2.5	80.8	1.6	15.1	--	**100**
2c	2.4	81.9	1.5	14.2	--	**100**
3c	12.7	78.5	7.0	--	1.7	**99.9**
3d	12.3	79.9	6.3	--	1.6	**100.1**
4c	12.1	78.0	8.3	--	1.5	**99.9**
4d	13.4	77.3	7.7	--	1.6	**100**
4g	13.3	79.9	6.2	--	0.6	**100**
5c	6.2	76.7	3.4	13.0	0.7	**100**
6b	6.0	76.5	3.6	13.2	0.7	**100**

Table 13 Yawing Moment Force Coefficient Relative Influences

Estimated terms (% of actual C_n magnitude)						Total (% of actual C_n)
Maneuver	$C_{n_\beta}\cdot\Delta\beta$	$C_{n_p}\cdot\Delta p$	$C_{n_r}\cdot\Delta r$	$C_{n_{\delta_a}}\cdot\delta_a$	$C_{n_{\delta_r}}\cdot\delta_r$	C_n
1b	23.2	6.9	69.3	0.9	--	**100.3**
2a	26.8	10.1	61.8	1.4	--	**100.1**
2b	27.2	9.6	61.9	1.4	--	**100.1**
2c	26.2	10.0	62.7	1.3	--	**100.2**
3c	22.8	1.5	46.7	--	29.0	**100**
3d	23.3	1.7	45.4	--	29.6	**100**
4c	21.0	1.5	53.0	--	24.6	**100.1**
4d	23.2	1.5	49.6	--	25.8	**100.1**
4g	31.3	2.1	53.4	--	13.3	**100.1**
5c	23.4	3.2	46.9	0.4	26.2	**100.1**
6b	22.0	3.1	48.7	0.4	25.9	**100.1**

INSTRUMENT PRECISION ANALYSIS

Desired levels of precision are established for the responses used in the parameter estimation. These precision levels define the measurement accuracy required for the instruments in the data acquisition system. Because the maneuvers considered for ground effect studies are generally more subtle than those used in other test programs, the precision requirements are unique to this problem.

This analysis simulates instrument precision by formatting response data appropriately before the data are used in pEst. Initial precision levels are selected and, based on the accuracy of the resulting estimates, adjusted to find the least precise level that allows acceptable accuracy. A brief summary on the feasibility of the recommended precision levels follows the lateral-directional analysis.

Longitudinal Results

Table 14 lists the precision levels considered for the longitudinal responses. Development of the initial precision level is detailed in Appendix F. Since both pitch angle and elevator deflection likely will be measured using similar devices, such as radial optical encoders, these quantities are given the same precision.

Figure 21 presents the estimates for longitudinal Maneuvers 1a and 2b using Precision Level 1. Cramer-Rao bounds are not plotted, but are included in Appendix B. From the figure, the parameter estimates suffer a great deal compared to the preliminary case: only C_{L_0} and C_{m_0} are reasonably accurate.

For Precision Level 2, pitch rate precision increases to 0.1 degrees per second. From Figure 22, this change results in much better estimates - seven are within four percent for Maneuver 1a, and six parameters are within eight percent for 2b. In both cases, the estimates of C_{m_0} are effectively zero, as expected.

Table 14 Longitudinal Precision Levels

Precision Level	a_x, a_n	u	q	θ, δ_e
Level 1	0.0001g	0.001 ft/sec	1 deg/sec	0.01 deg
Level 2	0.0001g	0.001 ft/sec	0.1 deg/sec	0.01 deg
Level 3	0.0001g	0.001 ft/sec	0.1 deg/sec	0.1 deg
Level 4	0.001g	0.01 ft/sec	0.1 deg/sec	0.01 deg
Level 5	0.001g	0.01 ft/sec	0.1 deg/sec	0.1 deg
Level 6	0.0001g	0.001 ft/sec	0.5 deg/sec	0.01 deg
Level 7	0.0001g	0.001 ft/sec	0.1 deg/sec	0.05 deg
Level 8	0.0001g	0.001 ft/sec	0.5 deg/sec	0.05 deg

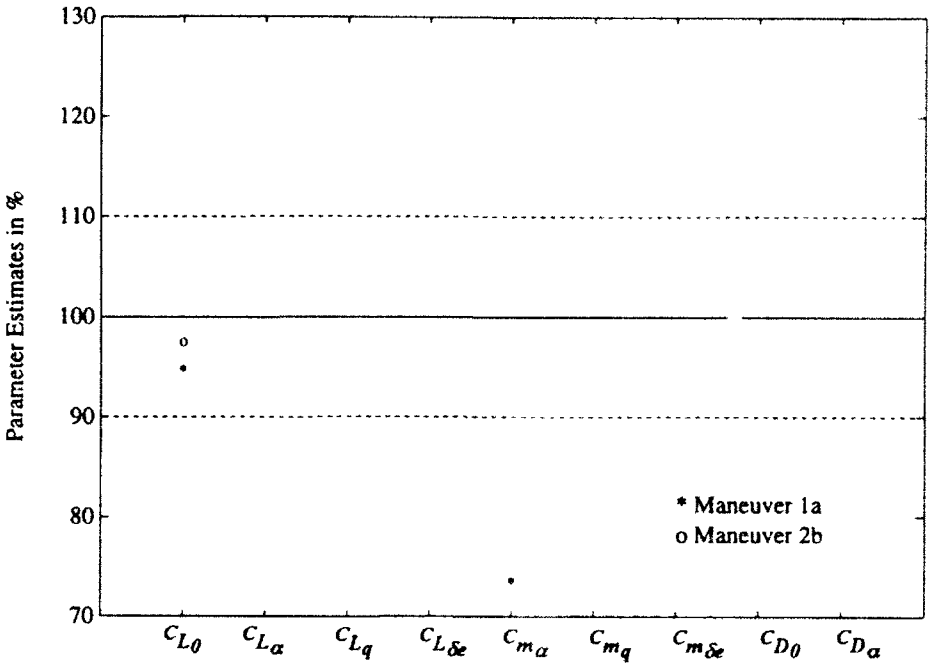

Figure 21 Longitudinal Results at Precision Level 1

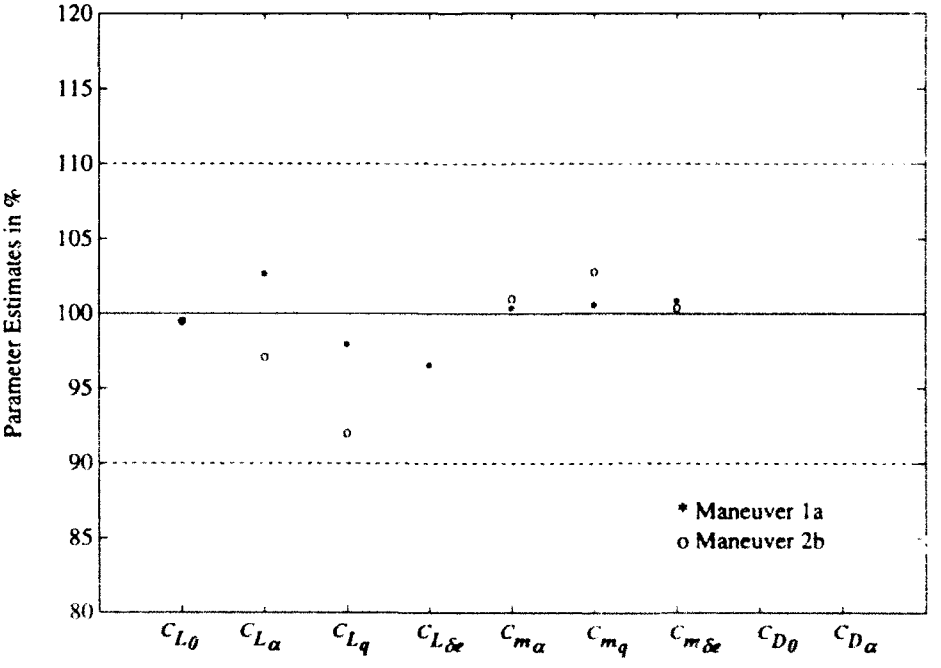

Figure 22 Longitudinal Results at Precision Level 2

From Level 2, the precision of angular measures decreases to 0.1 degrees. The estimates from the two maneuvers at Level 3 are in Figure 23, with seven and five accurate estimates, respectively. Again, moment coefficient estimates are close to zero. Thus, Precision Level 3 results are only slightly worse than Level 2 results.

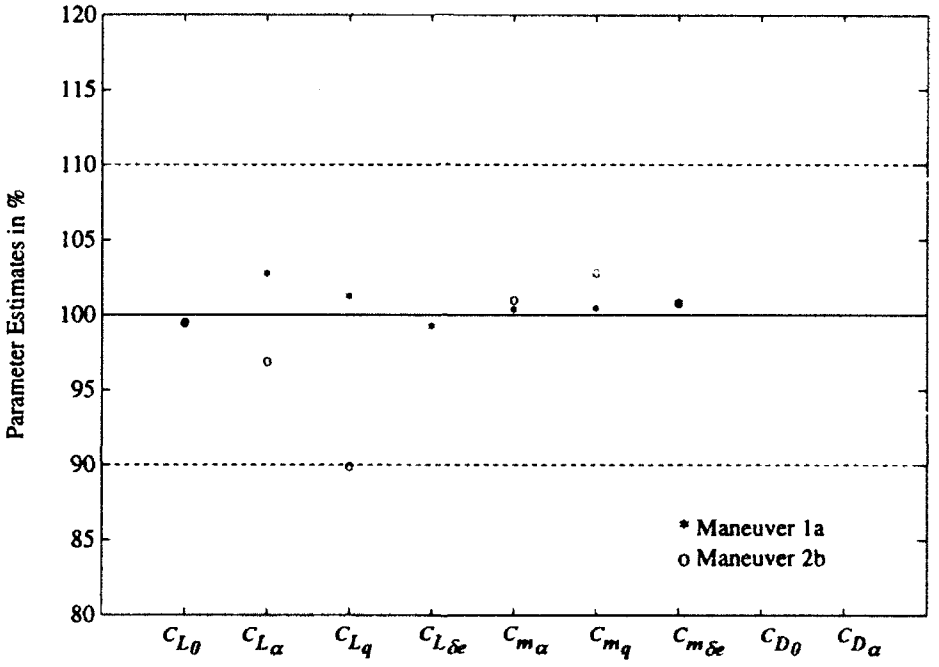

Figure 23 Longitudinal Results at Precision Level 3

Precision Level 4 reduces the precision of the accelerations and velocity to 0.001g and 0.01 feet per second, and that of angular measures returns to 0.01 degrees. These results, in Figure 24, are similar to those obtained with Level 3.

For Precision Level 5, angular measure precision returns to 0.1 degrees. The results for this case, in Figure 25, suffer only slightly from those at Level 4.

Since the rate gyro and angular measure precisions affect the estimates most profoundly, Precision Levels 6, 7, and 8 examine the requirements for the gyros and

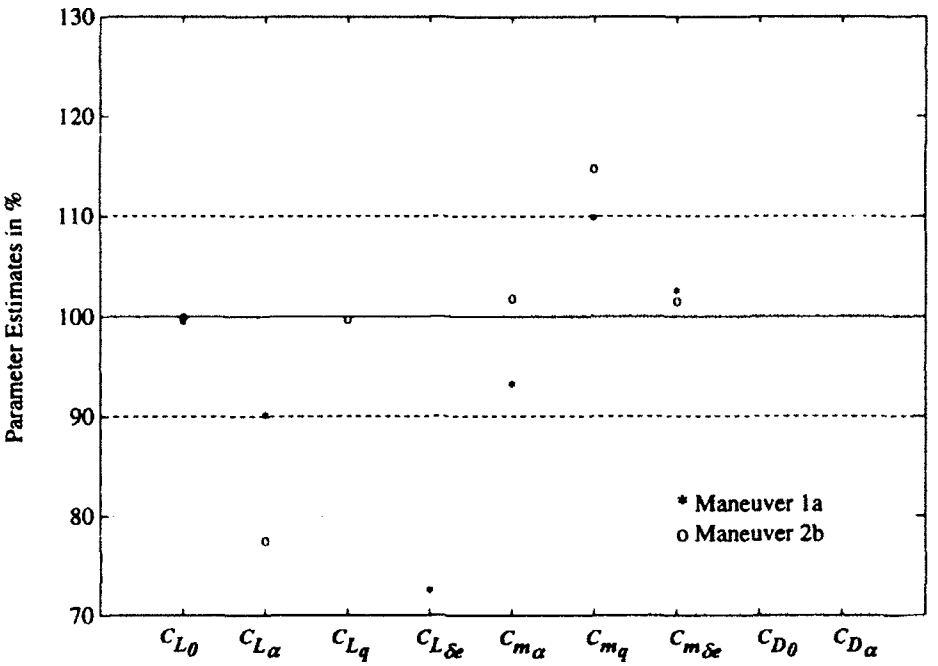

Figure 24 Longitudinal Results at Precision Level 4

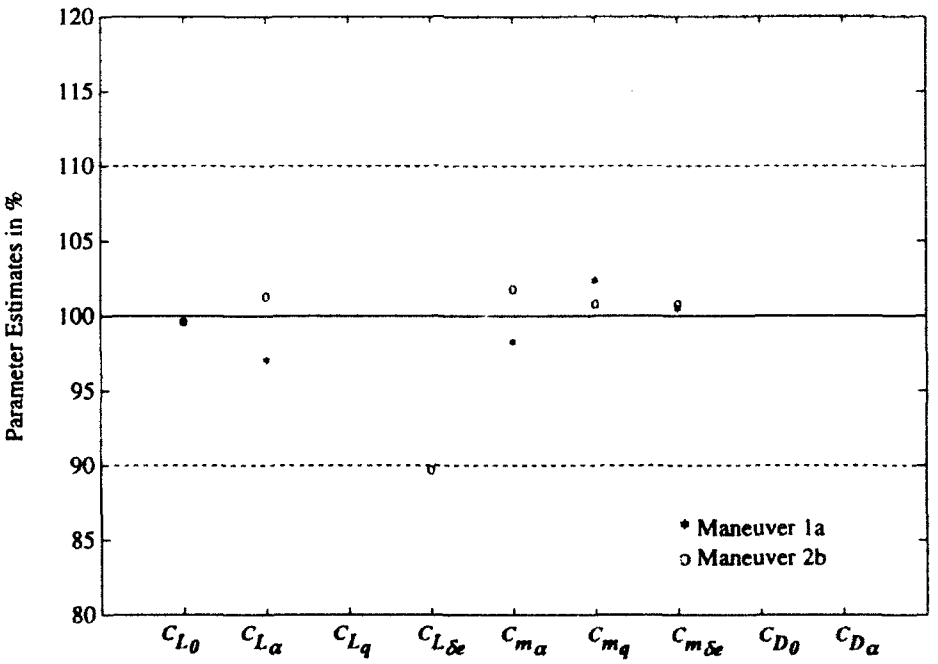

Figure 25 Longitudinal Results at Precision Level 5

angular deflections more closely. From Precision Level 2, which works well for both maneuvers, Precision Level 6 sets the rate gyro precision at 0.5 degrees per second. Figure 26 presents the estimates at Level 6, which suffer considerably, especially for the smaller Maneuver 1a. At Precision Level 7, angular measure precision decreases to 0.05 degrees. From Figure 27, this change results in less accurate estimates of C_{L_q} and $C_{L_{\delta_e}}$. With results in Figure 28, Level 8 combines the two adjustments, setting rate precision at 0.5 degrees per second and

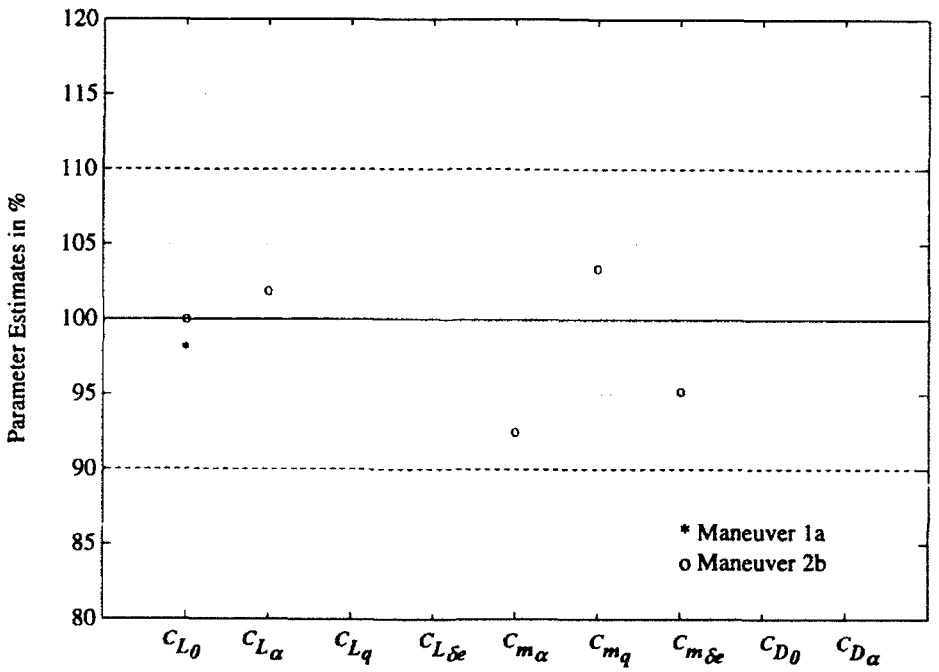

Figure 26 Longitudinal Results at Precision Level 6

angular precision at 0.05 degrees. While this level provides some good estimates for the larger Maneuver 2b, the estimates for Maneuver 1a are poor, as illustrated in Figure 28. Therefore, all three levels provide distinctly inferior results to Precision Level 2.

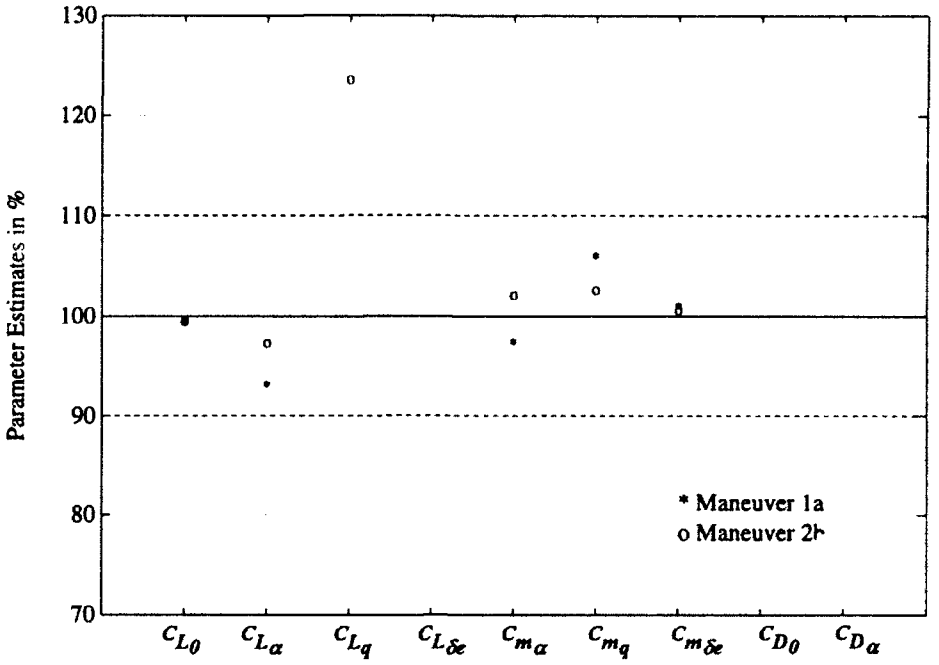

Figure 27 Longitudinal Results at Precision Level 7

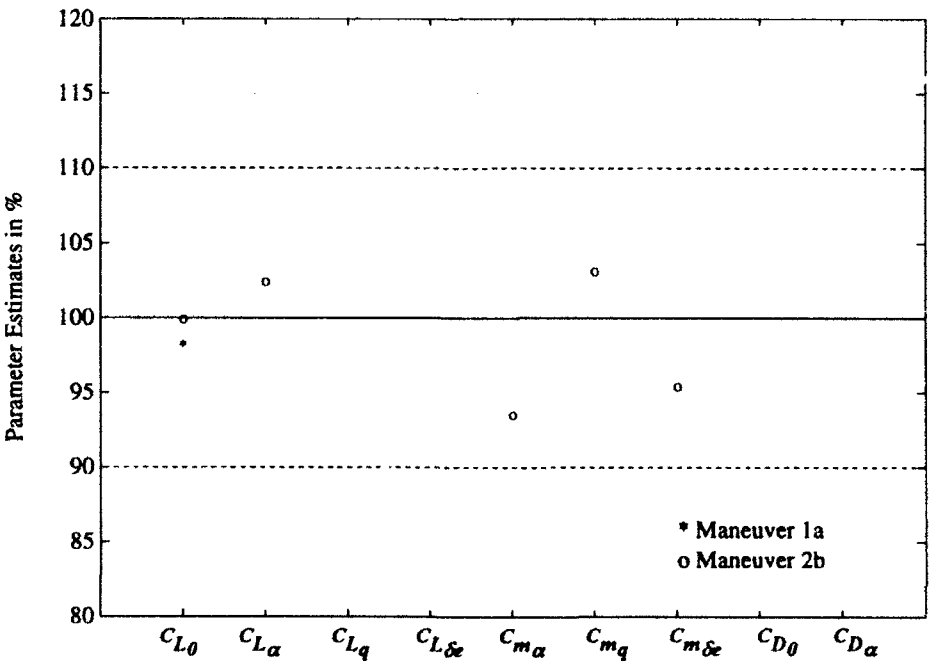

Figure 28 Longitudinal Results at Precision Level 8

In conclusion, estimates from data at Precision Level 2 are essentially identical to those in the preliminary study. Thus, Level 2 is the desired precision level for longitudinal study; precision above this level is unnecessary, and any precision below will result in fewer acceptable parameter estimates. Appendix D includes the results presented in Figures 21 through 28.

Lateral-Directional Results

Table 15 lists the precision levels used in the lateral-directional analysis; the analysis compares Maneuvers 1b, 2b, and 4d. Again, all angular measures, including aileron and rudder deflections, have the same precision. As illustrated in Figure 29, the initial level, Level 1, provides poor estimates for all three maneuvers.

Table 15 Lateral-Directional Precision Levels

Precision Level	p , r	ϕ , β , δ_a , δ_r
Level 1	1 deg/sec	0.01 deg
Level 2	0.1 deg/sec	0.01 deg
Level 9	0.1 deg/sec	0.001 deg
Level 10	0.5 deg/sec	0.001 deg
Level 11	0.1 deg/sec	0.005 deg
Level 12	0.5 deg/sec	0.005 deg

Level 2, the desired precision level from the longitudinal analysis, works well for the aileron maneuver, but parameter estimates from the rudder maneuver suffer. Even so, accurate estimates of all lateral-directional parameters is possible if both

aileron and rudder maneuvers are used. Figure 30 depicts the estimates from Maneuvers 2b and 4d using Precision Level 2.

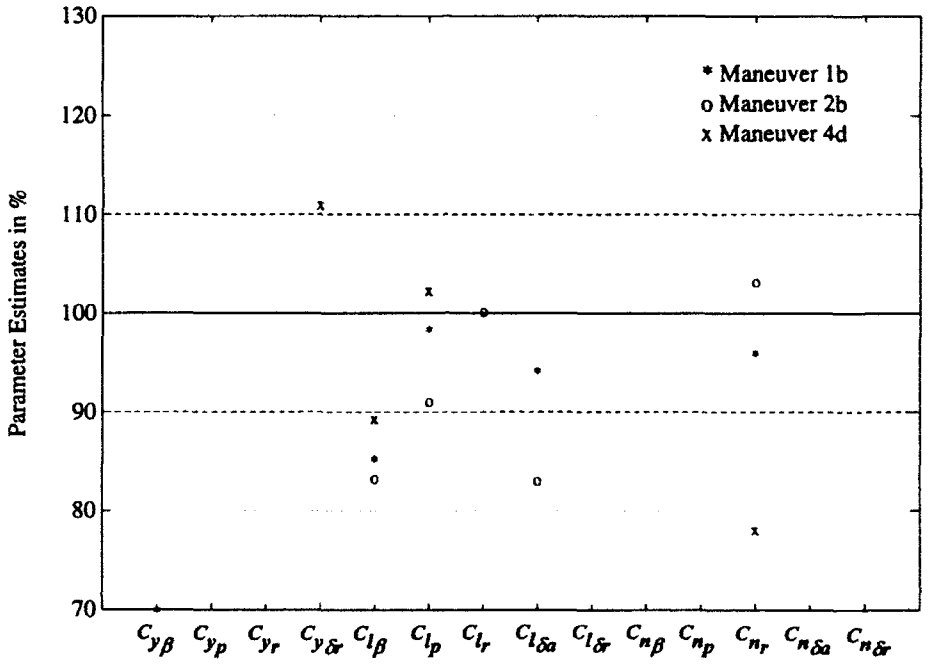

Figure 29 Lateral-Directional Results at Precision Level 1

An additional level, Precision Level 9, provides slightly better results than Level 2 for Maneuvers 2b and 4d because angular precision increases to 0.001 degrees. Figure 31 presents parameter estimates from Maneuvers 2b and 4d using Level 9.

As in the longitudinal case, the quality of the estimates is most sensitive to changes in the rate gyro and angular deflection precisions. Therefore, Precision Levels 10, 11, and 12 examine the precisions of these components more closely. From Level 9, rate gyro precision decreases to 0.5 degrees per second in Level 10.

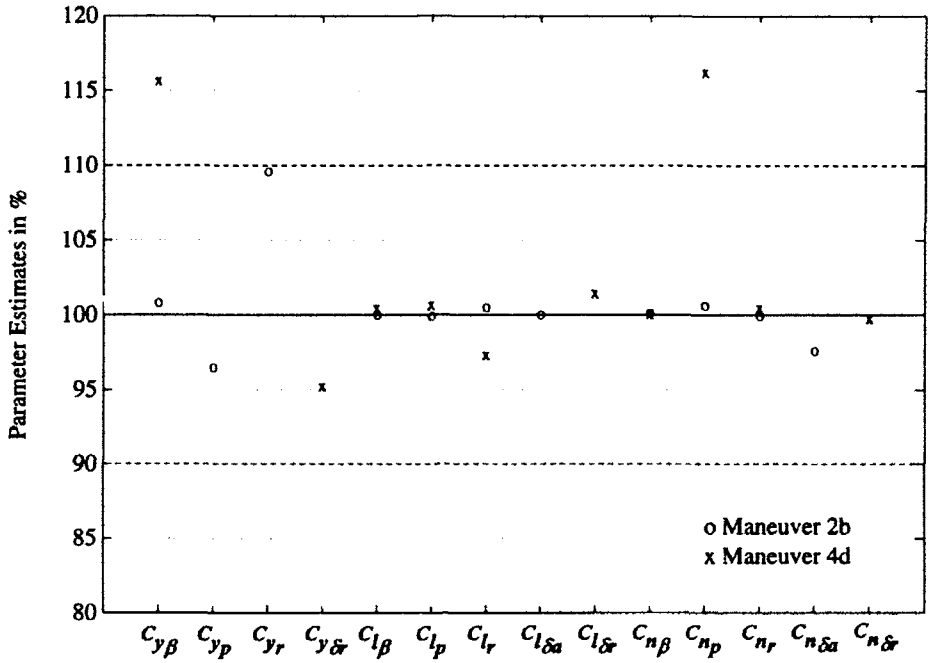

Figure 30 Lateral-Directional Results at Precision Level 2

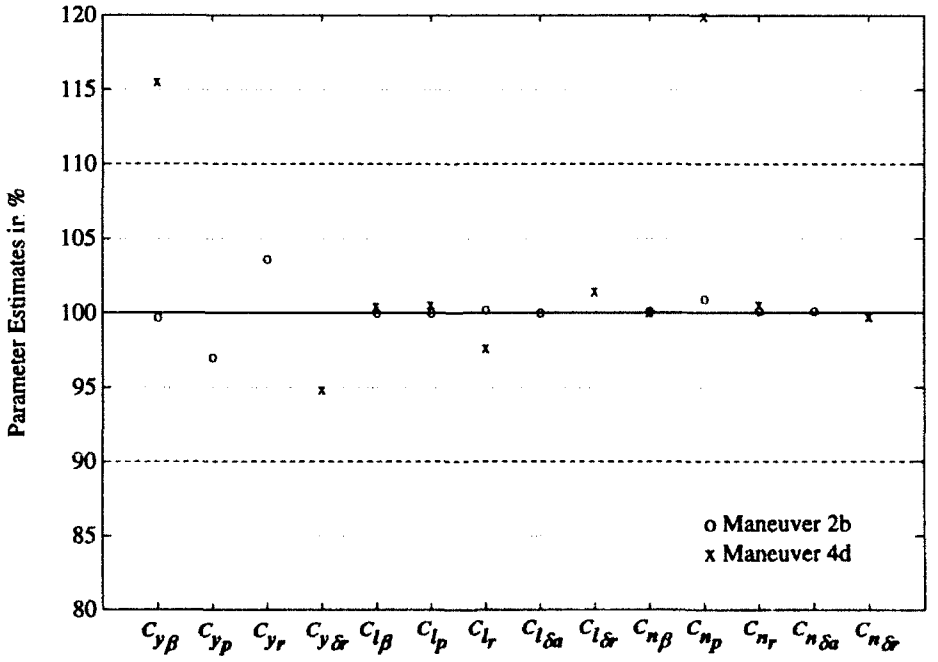

Figure 31 Lateral-Directional Results at Precision Level 9

With the less precise rate gyros, the results, presented in Figure 32, are similar to those at Level 1. Figure 33 contains the estimates at Precision Level 11, which has an angular deflection precision of 0.05 degrees. While these results do not suffer nearly as much as those at Level 10, two parameter estimates, C_{y_r} and C_{l_r}, now fall outside ten percent of their actual values. As expected, given the results at Precision Levels 10 and 11, Level 12 provides poor results, which are illustrated in Figure 34.

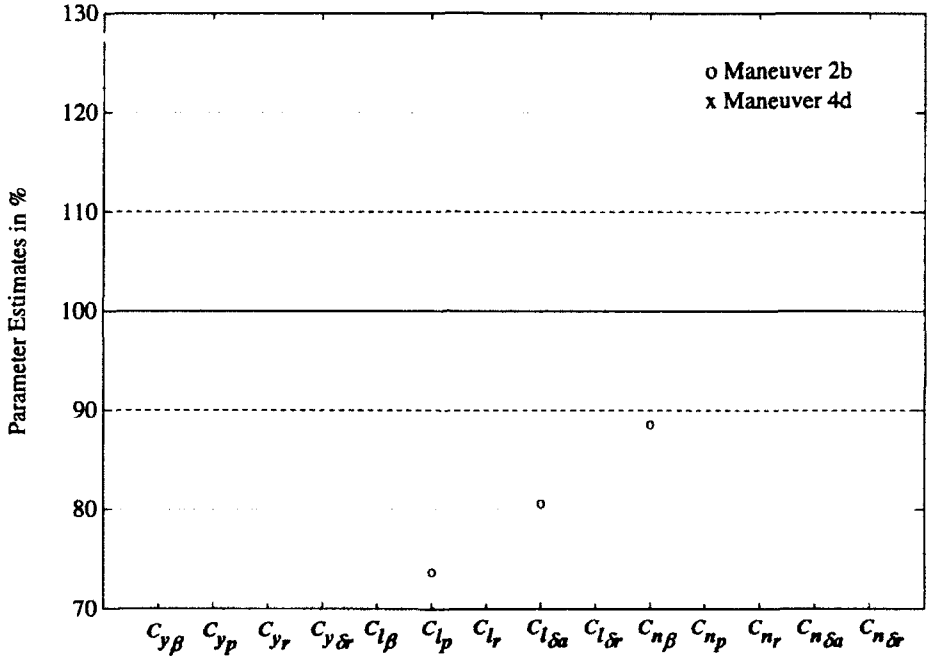

Figure 32 Lateral-Directional Results at Precision Level 10

In summary, because the lateral-directional maneuvers studied generally contain less excitation than the longitudinal maneuvers, the lateral - directional estimates are more sensitive to instrument precision, particularly in the p and r rate gyros. Precision Level 9 provides estimates comparable to those in the preliminary analysis, and all lateral-directional parameters may be identified if both

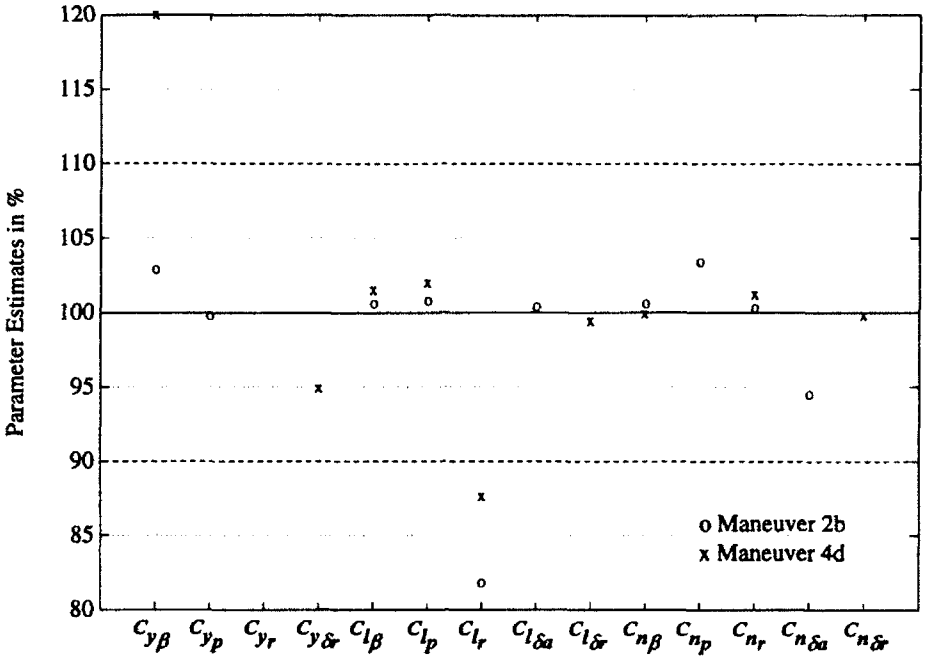

Figure 33 Lateral-Directional Results at Precision Level 11

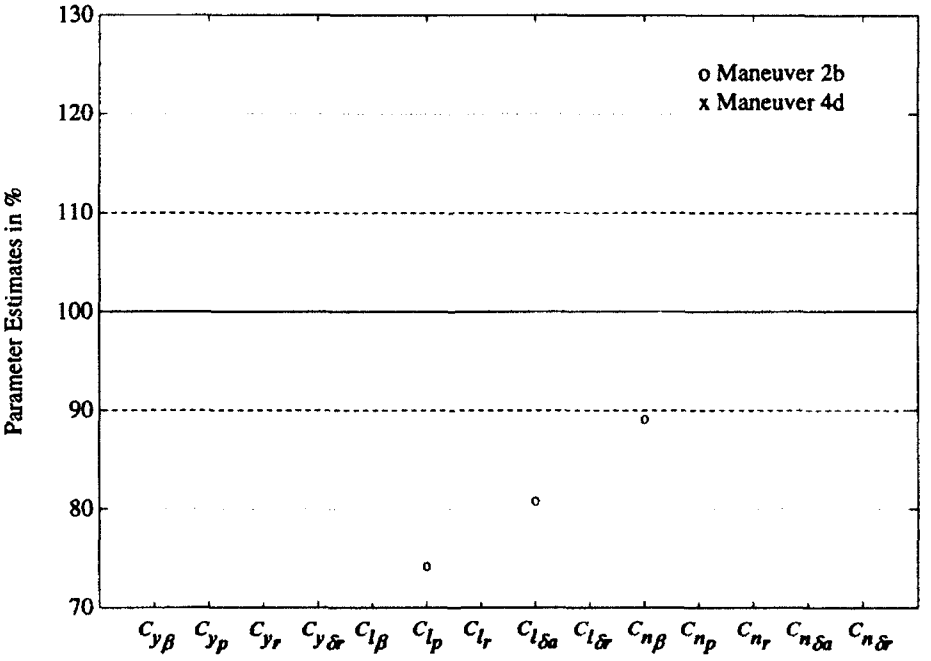

Figure 34 Lateral-Directional Results at Precision Level 12

aileron and rudder maneuvers are used. Levels 2 and 11 are also suitable if less accurate results are acceptable for a few parameters, such as C_{y_r} and C_{l_r}. In general, the lateral directional results are most affected by the sensitivity of the two rate gyros. In summary, Level 9 is recommended for lateral-directional response measurements. Appendix E lists the numerical results depicted in Figures 29 through 34.

Practical Considerations on the Precision Analysis

The preceeding analyses recommend Precision Level 2 for longitudinal maneuvers and Precision Level 9 for lateral-directional maneuvers because these levels allow results similar to those in the preliminary analysis. In a practical aircraft data acquisition system, however, available hardware limits the attainable precision. The initial precision levels considered in the analysis are similar to those reported in References 15 and 16, and are developed in Appendix F. Appendix F also includes technical data on representative accelerometers, rate gyros, and rotary encoders, which measure angular displacements.

The Systron-Donner Model 4310 accelerometer has a resolution of 0.001 percent of full range, and is available with ranges from ±0.5g to ±35g. With ± 2g ranges for axial and lateral accelerations and ± 10g ranges for normal acceleration, this accelerometer has a precision better than 0.0001g on all three axes. Thus, this accelerometer meets the precision recommended at Precision Level 2.

Both longitudinal and lateral-directional estimates are very sensitive to angular rate precision. Two Humphrey rate gyro models are considered - one with a ± 100 degree per second range to measure roll rate, and one with a ± 50 degree per second range for pitch and yaw rates. Both models are accurate within one percent

of their full scale limits. The precision analysis, however, indicates that a precision of about 0.1 degrees is essential about the roll, pitch, and yaw axes. While the models noted above do not meet this requirement, a similar piece of equipment with a ±10 degree range would achieve the necessary precision. Normal aircraft maneuvers will easily exceed this narrow range and saturate the gyro; therefore, such a rate gyro will only be useful for applications such as ground effect flight tests. This study does not specify a rate gyro with suitable range and accuracy characteristics.

The digital optical encoder measures angular displacements accurately and dependably. The longitudinal analysis recommends a precision of 0.01 degrees for angular displacements - 0.001 degrees is the desired precision for lateral-directional angular measure. The E2 optical encoder, built by U.S. Digital Corporation, is available with a number of resolutions, up to 540 cycles per revolution. Two-channel quadrature quadruples this maximum resolution to 2160 cycles per revolution, or 0.167 degrees. While this precision is probably sufficient for most parameter estimation applications, it not adequate for measuring the subtle excitations that are safe in ground effect. If this encoder is used for ground effect test work, its accuracy must be improved with gears, pulleys, or some other mechanical device. Otherwise, its precision is simply not high enough. The resolution of the Canon X-1 Laser Encoder, on the other hand, is better than 0.002 degrees. Based on this resolution, this encoder is suitable for longitudinal data recording without modification. It is, in fact, close to the desired precision for lateral-directional maneuvers.

All in all, accelerometers with precision adequate for ground effect parameter estimation are clearly identified and are readily available. A more

sensitive rate gryo, or one with a lower measurement range, is required for the desired accuracy about all three axes. Finally, some modification or addition to available optical encoders is likely necessary before angular measurements suitable for ground effect parameter estimation are achieved.

SAMPLING RATE ANALYSIS

The time increment for the preliminary, precision, bias, and noise analyses is 0.04 seconds, which simulates an acquisition system sampling rate of 25Hz. Two alternative sampling rates, 10Hz and 50Hz, are considered for longitudinal and lateral-directional maneuvers. Adjusting the time increments used in the MATLAB simulation to 0.1 seconds and 0.02 seconds simulates these sampling rates.

A generally accepted rule for selecting sampling rates suggests that signals with periodic responses should be sampled at a minimum of twice the highest frequency in the signal. In this case, there is no high-frequency noise in the data; therefore, the aircraft control inputs, excitations, and transient response modes are the relevant responses. If high-frequency noise is present, the sampling rate must be adjusted accordingly for accurate estimation.

Longitudinal Results

The longitudinal sampling analysis uses Maneuvers 2b and 5b at the additional sampling rates above. Figures 35 and 36 present the parameter estimates for all three sampling rates. With several estimates of each parameter appearing, Cramer-Rao bounds are removed for clarity, but they are tabulated with the results in Appendix D. These bounds become smaller as sampling rate increases, but not

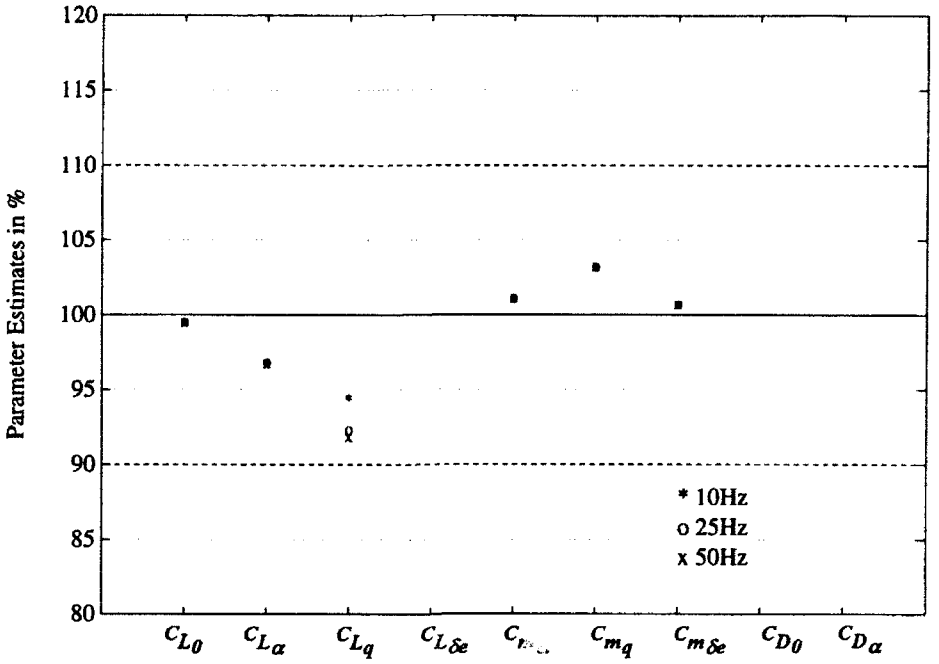

Figure 35 Longitudinal Sampling Analysis - Maneuver 2b

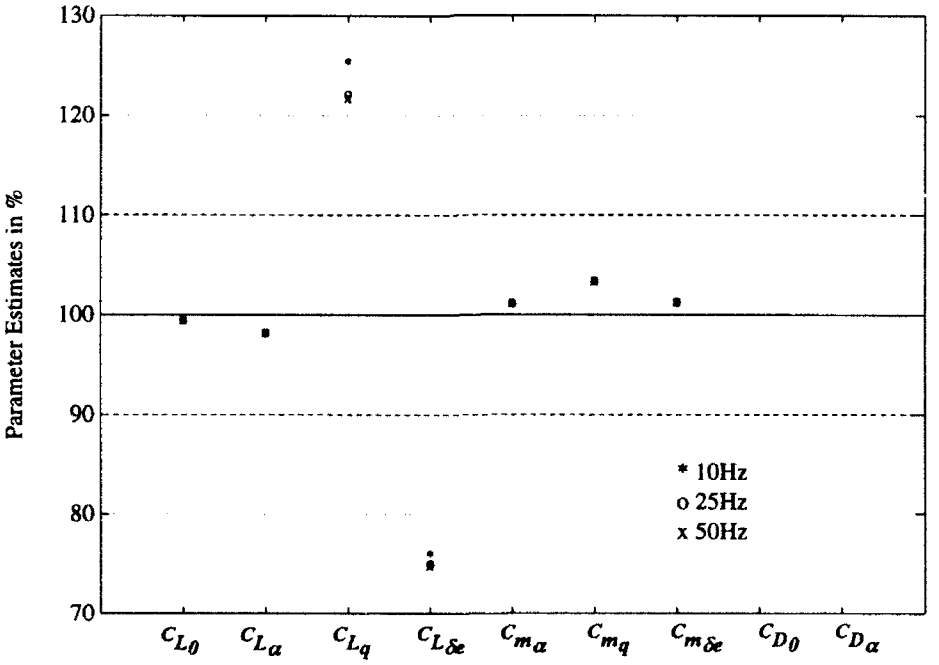

Figure 36 Longitudinal Sampling Analysis - Maneuver 5a

significantly so. From the figures, the estimates are virtually identical, and appear independent of the three rates studied.

The above result is expected, because the control inputs and transient response frequencies are well below 10Hz. The input periods are two seconds and three seconds, respectively. The frequencies of the Beech B99's longitudinal transient responses are 0.39Hz for the short-period mode, and 0.037Hz for the phugoid. These constants are determined using the eigenvalues of the longitudinal system in Equation (5).

Lateral-Directional Results

The lateral-directional sampling analysis uses Maneuvers 2c and 4d. The results appear in Figures 37 and 38 - as in the longitudinal case, estimates vary only insignificantly among the three sampling rates. Again, this result is expected, since both inputs occur at 0.5Hz, and the Dutch roll frequency (from the eigenvalues of Equation (14)) is 0.21Hz.

INSTRUMENT BIAS ANALYSIS

Measurement bias in acquisition system components is simulated by adding a constant value to the appropriate responses as data are formatted in LNFRMT.C or LDFRMT.C. Texas A&M University Flight Mechanics Laboratory reports[15,16] suggest representative levels of bias, which are used in the analysis. Table 16 summarizes the bias levels considered for both longitudinal and lateral-directional maneuvers. Although pEst assumes control input histories are bias-free, the software has the capability to estimate biases of the aircraft

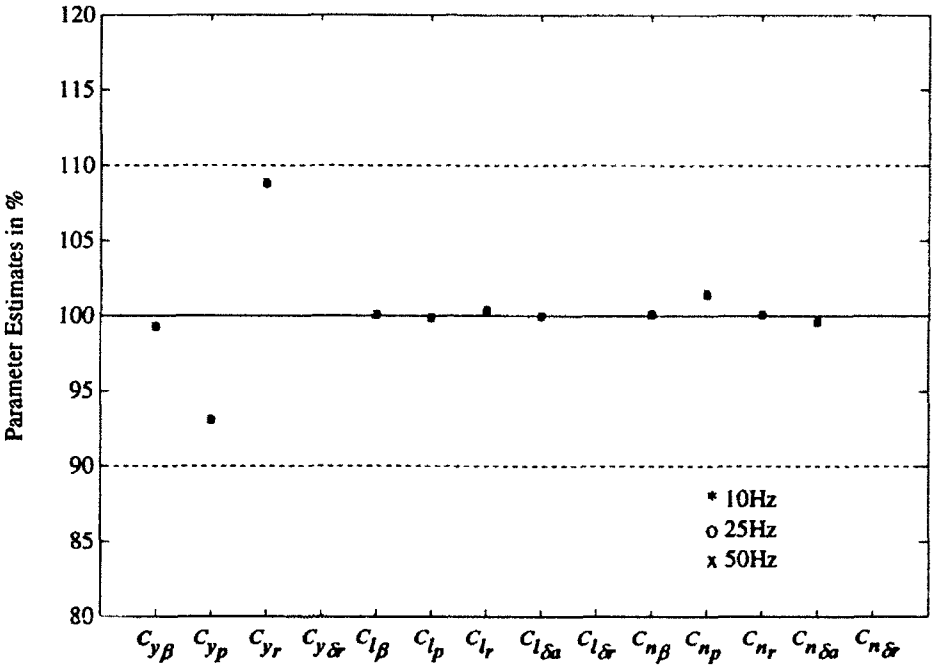

Figure 37 Lateral-Directional Sampling Analysis - Maneuver 2c

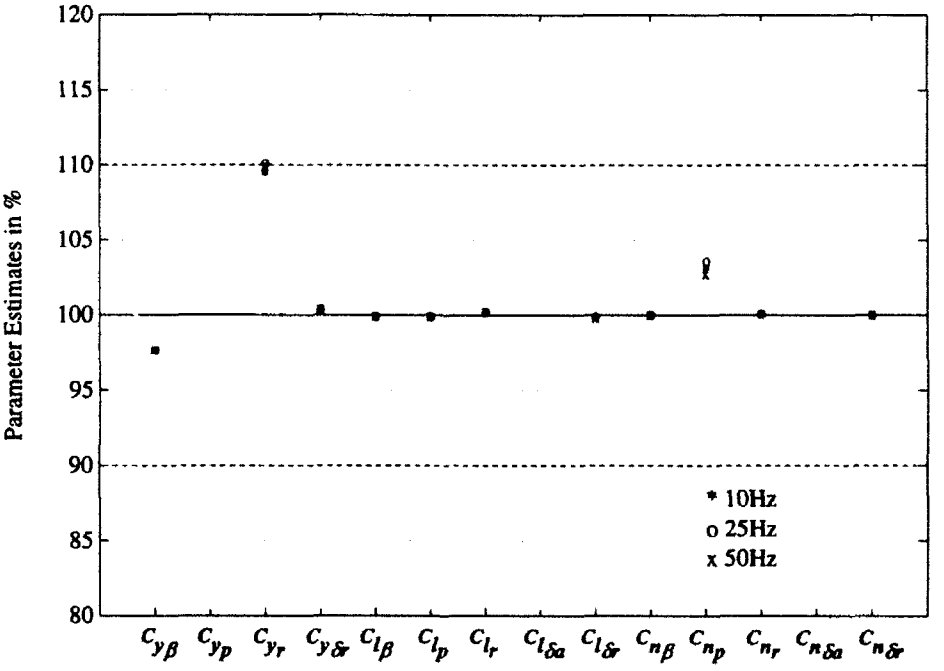

Figure 38 Lateral-Directional Sampling Analysis - Maneuver 4d

Table 16 Bias Analysis Levels

Bias Level	Accelerometers	Velocities	Rate Gyros	Angular Measure
Bias Level 1	0.2g	1 ft/sec	0.5 deg/sec	1 deg
Bias Level 2	0.1g	0.5 ft/sec	0.25 deg/sec	0.5 deg

responses. Accordingly, bias analysis is performed with the bias estimate terms activated as well as with these terms inactive.

Longitudinal Results

Longitudinal bias analysis is performed using Maneuvers 1a and 2b. Figures 39 and 40 include the parameter estimates for these maneuvers at Bias Level 1, with bias estimators on and off. With Maneuver 1a in Figure 39, the estimates suffer, but less so with the bias estimators on. When the bias estimators are off, only one parameter estimate, C_{L_0}, is within ten percent of the simulated value. For Maneuver 2b, in Figure 40, the distinction is not so clear. When bias estimators are on, three parameter estimates are within four percent of the ideal. When they are off, one additional estimate is within ten percent, but the estimates for the three parameters above are farther from the simulated values, and have larger Cramer-Rao bounds.

Figure 41 illustrates the results of further analysis using Maneuver 2b and Bias Level 2. For this lower level of bias, the estimates are clearly superior with biases off.

From these results, measurement bias hurts longitudinal parameter estimation, with or without pEst's bias estimators activated. For maneuvers with larger inputs (2b in this case) and lower bias levels, leaving the bias estimators off

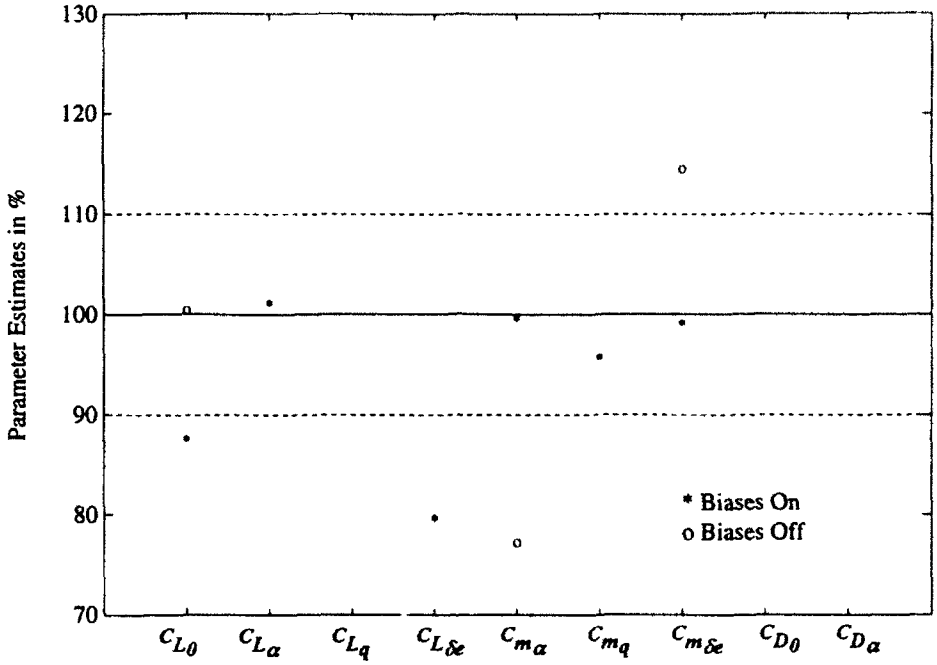

Figure 39 Longitudinal Bias Analysis, Bias Level 1, Maneuver 1a

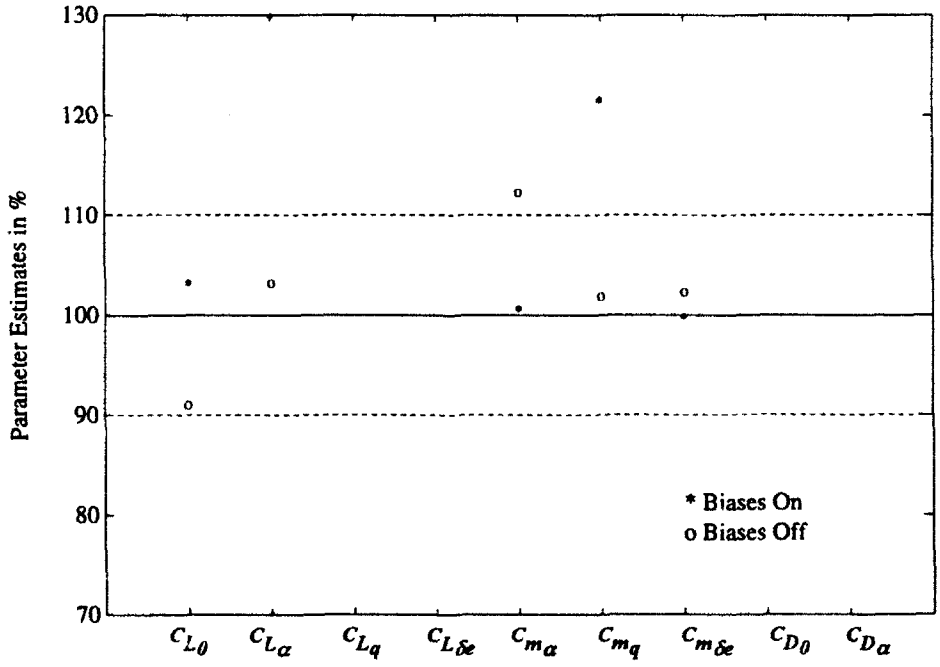

Figure 40 Longitudinal Bias Analysis, Bias Level 1, Maneuver 2b

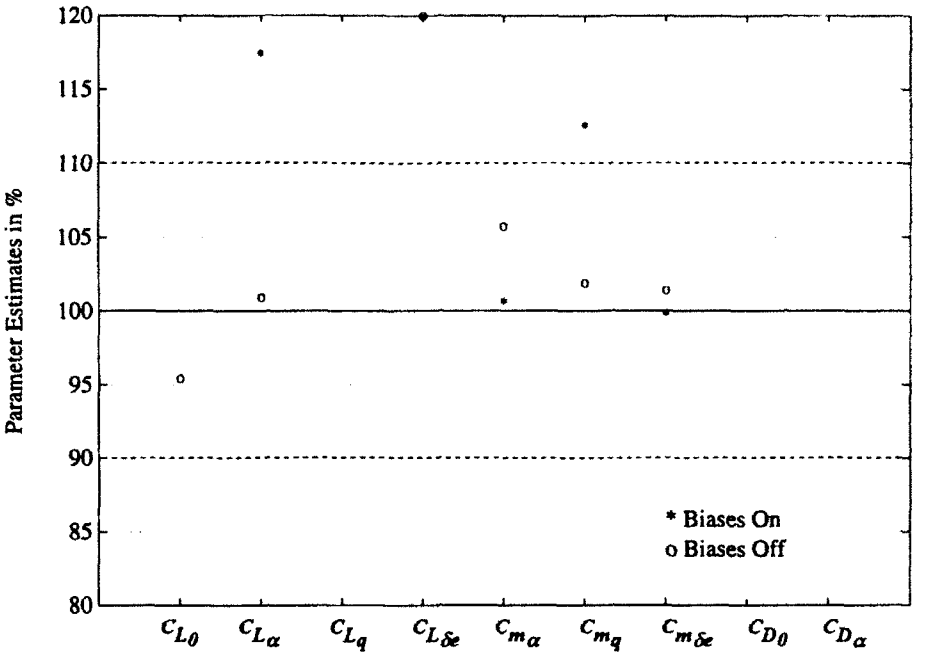

Figure 41 Longitudinal Bias Analysis, Bias Level 2, Maneuver 2b

appears to provide more accurate results. For more subtle maneuvers or higher bias levels, these estimators are best turned on. In any case, determining bias levels ahead of time and removing their effects from the data is the preferred option.

Lateral-Directional Results

The lateral-directional bias analysis uses an aileron doublet, Maneuver 2b, and a rudder doublet, Maneuver 4d. Figures 42 and 43 present the results of both maneuvers at Bias Level 1, with pEst's bias estimation terms both active and inactive. From these figures, active bias estimators improve the parameter estimates drastically. For both maneuvers, parameter estimates are slightly less accurate with bias in the data than in the preliminary analysis. Even so, both doublets provide nine

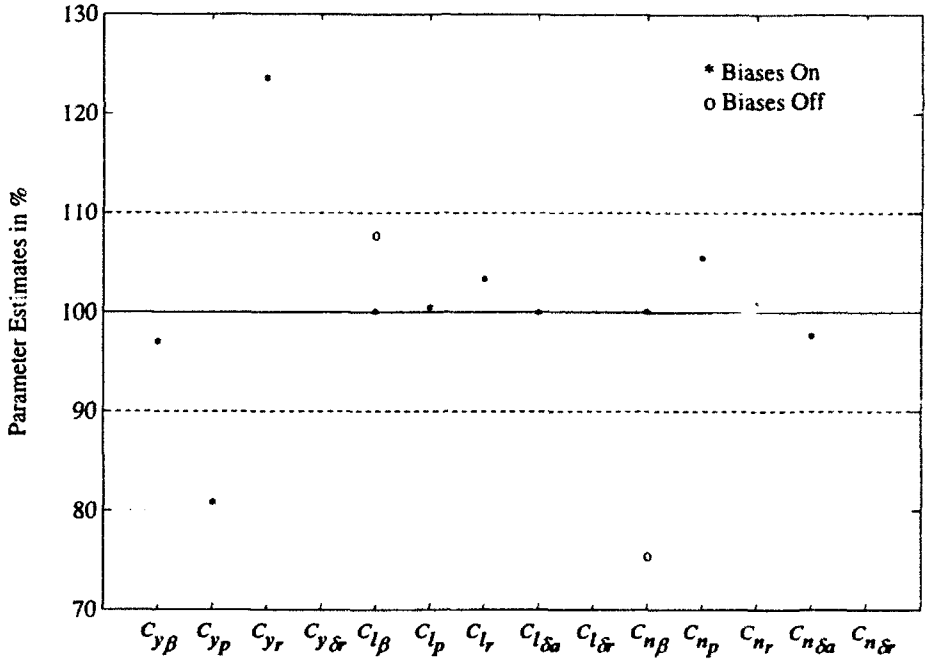

Figure 42 Lateral-Directional Bias Analysis, Bias Level 1, Maneuver 2b

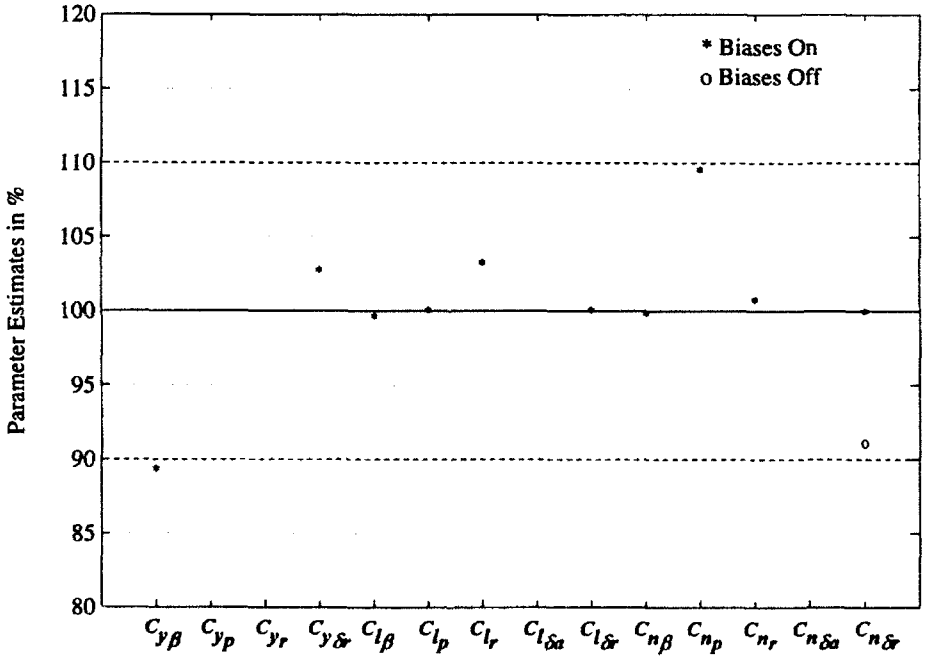

Figure 43 Lateral-Directional Bias Analysis, Bias Level 1, Maneuver 4d

estimates within ten percent. Maneuver 2b also provides a very small $C_{y_{\delta a}}$ estimate, close to the simulated value of zero.

Bias Level 2 is also applied to the responses of Maneuver 4d, with the bias estimators on. Figure 44 presents these parameter estimates. These results are similar to those at Level 1, but the estimates of C_{y_β} and C_{n_p} improve three to four percent. Thus, as in the longitudinal case, lateral-directional estimates suffer from bias in the maneuver responses, but for these maneuvers, leaving pEst's bias estimators on gives the best results, regardless of the bias level or maneuver excitation.

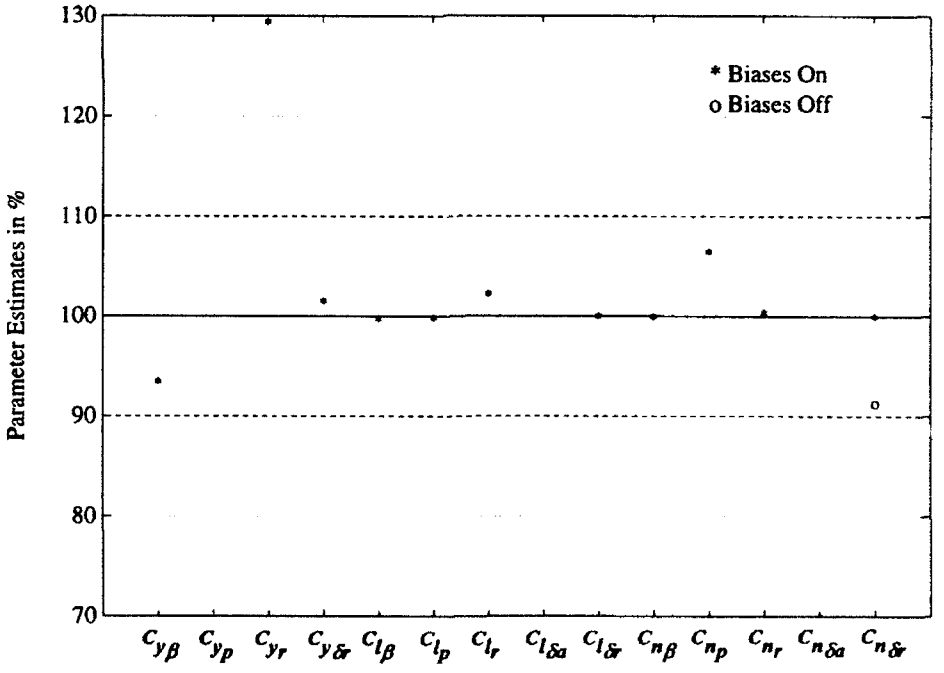

Figure 44 Lateral-Directional Bias Analysis, Bias Level 2, Maneuver 4d

NOISE ANALYSIS

In addition to containing bias, any data from an acquisition system contain noise. Noise has a wide variety of potential causes; this study considers two particular types of noise: random white noise simulating electronic noise or random occurrences such as wind gusts; and periodic noise simulating periodic electronic signals or vibrations in the aircraft structure or control surfaces.

For the first type, MATLAB's random number generator adds scaled, zero-mean, random distributions to the simulated response data. These distributions are either normal (Gaussian, bell-shaped) or uniform, and the applied scaling factor specifies the normal variance or the maximum level of the uniform noise. Since this noise is random, each set of parameter estimates is based on five sets of noisy data - Appendix D reports the averages and standard deviations of these sets. Statistically, a larger sample size would provide better estimates but, for this initial study, these results suffice to illustrate the effects of noise.

To simulate periodic noise, 5Hz and 10Hz sinusoids are also added to the response data. In reality, all vibrations do not synchronize in the responses, so these periodic data are randomly phase-shifted between zero and forty-five degrees to avoid being interpreted as dynamic responses.

As in the bias analysis, Flight Mechanics Laboratory reports[15,16] provide representative levels of noise. Noise in the control deflections is greater than that in other angular measures because of the possibility of vibrations in these surfaces.

Longitudinal Results

Noise levels used in the longitudinal analysis are in Table 17. Appendix G presents the development of these levels from those noted in the laboratory reports.

Table 17 Longitudinal Noise Levels

Noise Level	a_x , a_n	u	q	α , θ	δ_e
Level 1	0.05g	2 ft/sec	0.3 deg/sec	0.03 deg	0.1 deg
Level 2	0.025g	1 ft/sec	0.15 deg/sec	0.015 deg	0.05 deg
Level 3	0.005g	0.1609 ft/sec	0.18 deg/sec	0.0075 deg	0.025 deg

Longitudinal noise analysis uses Maneuvers 2a and 2b and all four noise distributions. Figures 45 and 46 present these results with random noise distributions. At Noise Level 1, Maneuver 2a provides only a few accurate estimates. Maneuver 2b, with its larger signal-to-noise ratio, provides better results: five parameters within ten percent, down from seven in the noise-free case.

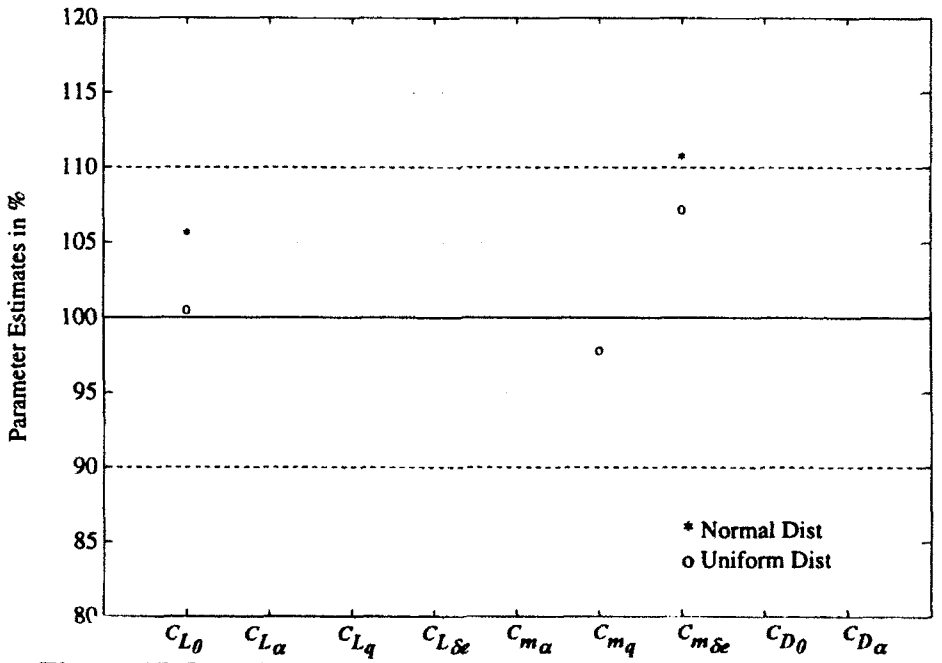

Figure 45 Longitudinal Noise Analysis - Noise Level 1, Random Distributions, Maneuver 2a

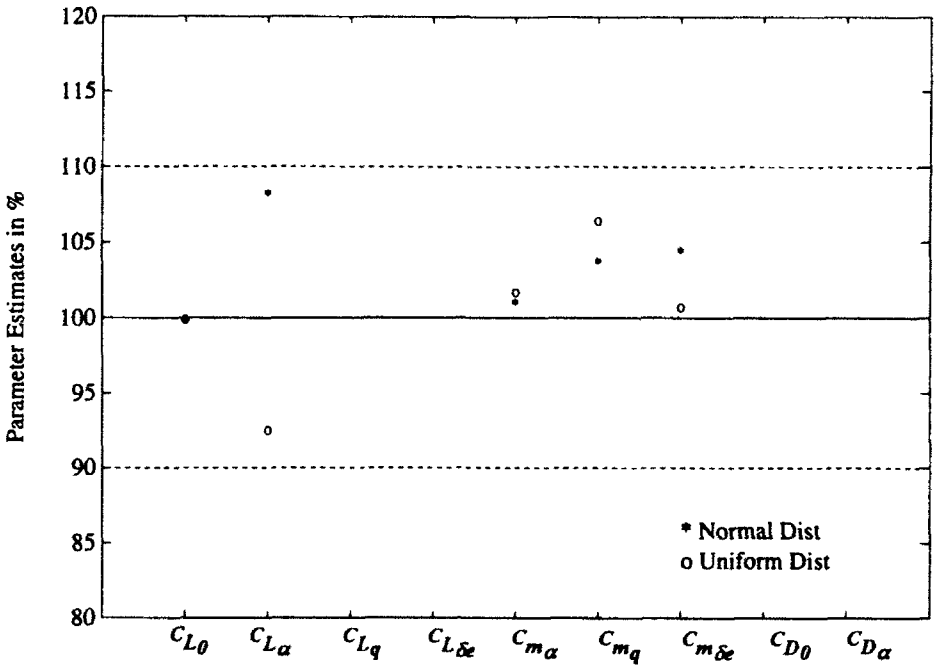

Figure 46 Longitudinal Noise Analysis - Noise Level 1, Random Distributions, Maneuver 2b

These averages, however, do not provide indications of the certainty of the estimates. At Noise Level 1, particularly with the wider normal distributions, the standard deviations are large, even though the averages are close to the noise-free estimates. Table 18 presents the averages and standard deviations at Noise Level 1.

In Figure 47, which presents the results of Maneuver 2b with periodic noise, parameter estimates vary only slightly from the noise-free estimates. For these cases, the Cramer-Rao bounds, presented in Appendix D, are considerably higher than in the noise-free case - this result is due to the higher cost associated with the noise, and does not indicate significantly less confidence in the estimates.

Noise Level 2, which is half the magnitude of Level 1, predictably provides better results. Results appear in Figures 48 and 49. For Maneuver 2a and uniform noise, seven parameter estimates are within ten percent, just as many as in the noise-

Table 18 Longitudinal Results - Noise Level 1

Average Estimates (% of actual value)	C_{L_0}	C_{L_α}	C_{L_q}	$C_{L_{\delta e}}$	C_{m_α}	C_{m_q}	$C_{m_{\delta e}}$
Man. 2a - Normal	105.7	417.4	966.4	672.8	283.8	15.7	110.8
Man. 2a - Uniform	**100.5**	**136.3**	**1196**	**266.3**	**148.5**	**97.8**	**107.2**
Man. 2b - Normal	99.9	108.3	295.5	209.8	101.1	103.8	104.5
Man. 2b - Uniform	**99.9**	**92.5**	**131.7**	**38.0**	**101.7**	**106.4**	**100.7**
Std Dev (% of parameter value)							
Man. 2a - Normal	8	290	1785	200	109	59	31
Man. 2a - Uniform	**1**	**79**	**790**	**256**	**57**	**37**	**5**
Man. 2b - Normal	55	60	242	181	55	57	57
Man. 2b - Uniform	**1**	**8**	**109**	**28**	**1**	**4**	**2**

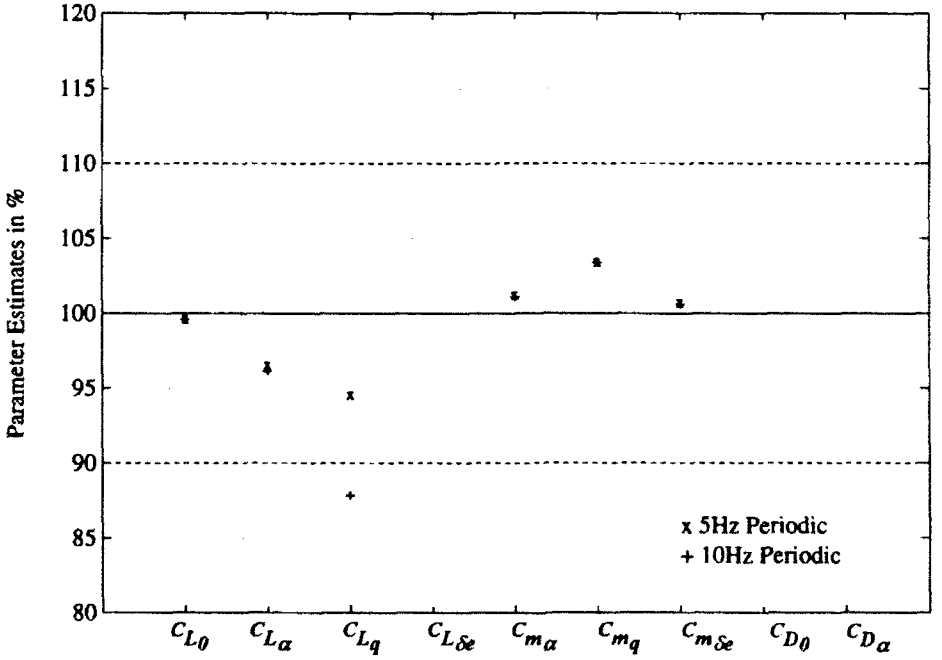

Figure 47 Longitudinal Noise Analysis - Noise Level 1, Periodic Distributions, Maneuver 2b

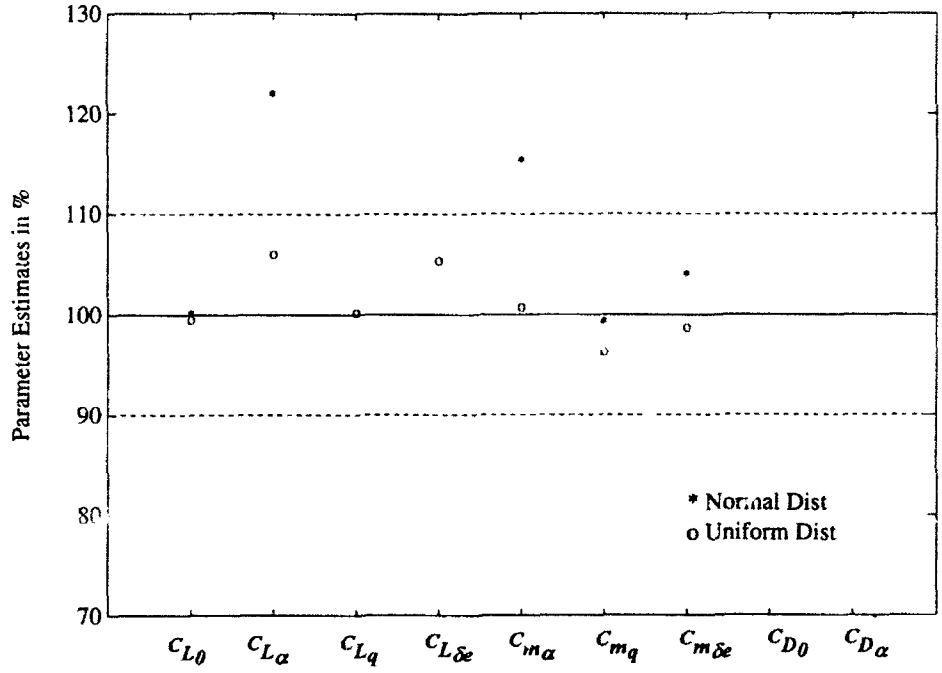

Figure 48 Longitudinal Noise Analysis - Noise Level 2, Random Distributions, Maneuver 2a

free case. Large standard deviations for two derivatives, C_{Lq} and $C_{L\delta e}$, result, but those for the other five are less than four percent of the estimated parameter values. Maneuver 2b provides similar results, as depicted in Figure 49.

Noise Level 3 uses the same noise levels, as a percentage of full-scale in each measurement, but adjusts the full-scale ranges as noted in Appendix F. These changes result in the individual noise levels in Table 17. From Figures 50 and 51, these cases yield results similar to those with Noise Level 2; numerous estimates are close to the simulated values, with reasonable standard deviations. Again, the narrower uniform distributions provide generally better estimates and tighter deviations. Periodic noise results at Level 3 are presented in Figure 52; these are similar to the periodic results at Level 1

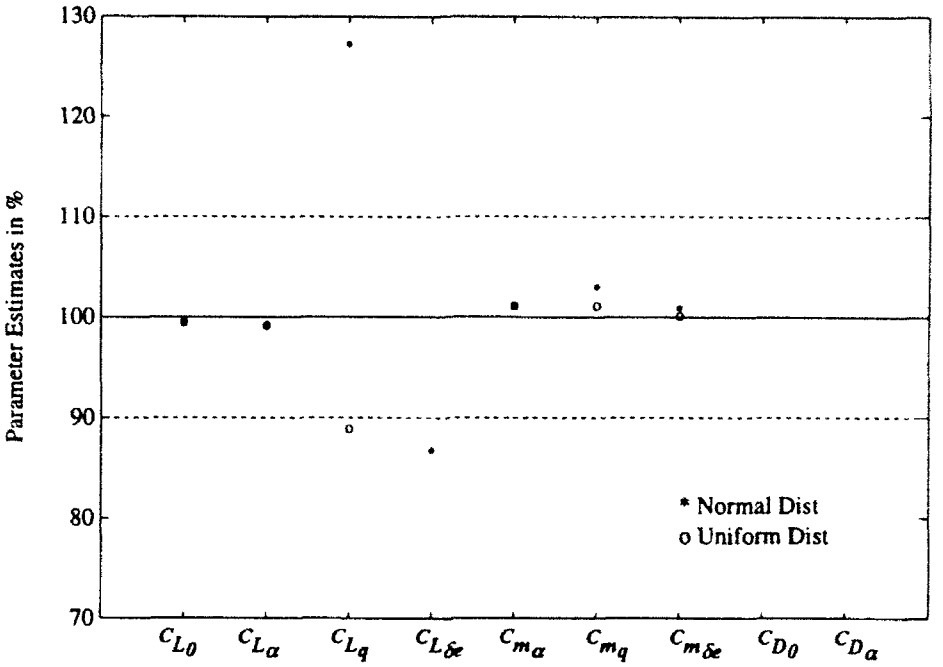

Figure 49 Longitudinal Noise Analysis - Noise Level 2, Random Distributions, Maneuver 2b

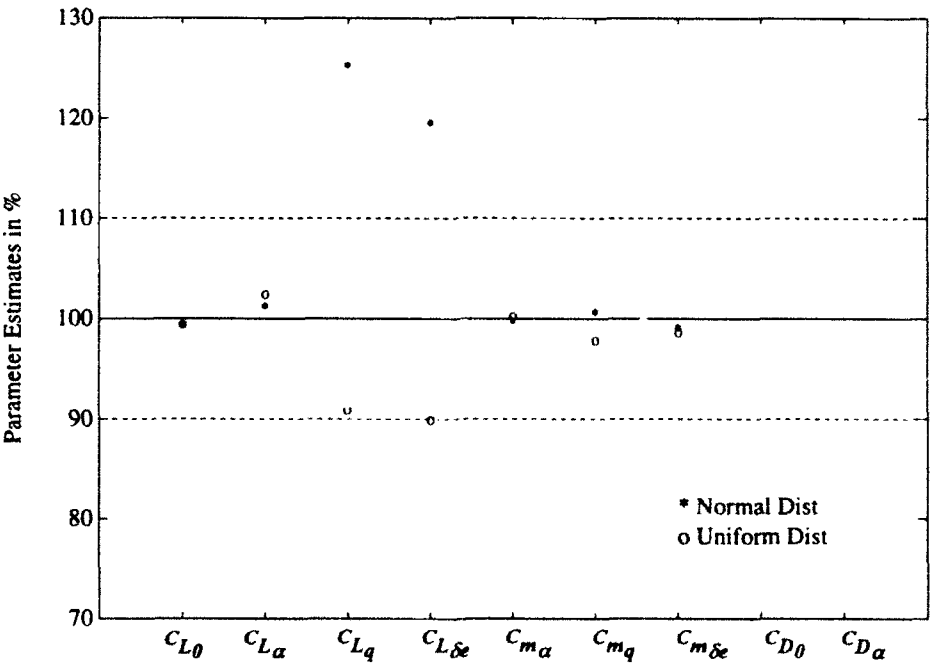

Figure 50 Longitudinal Noise Analysis - Noise Level 3, Random Distributions, Maneuver 2a

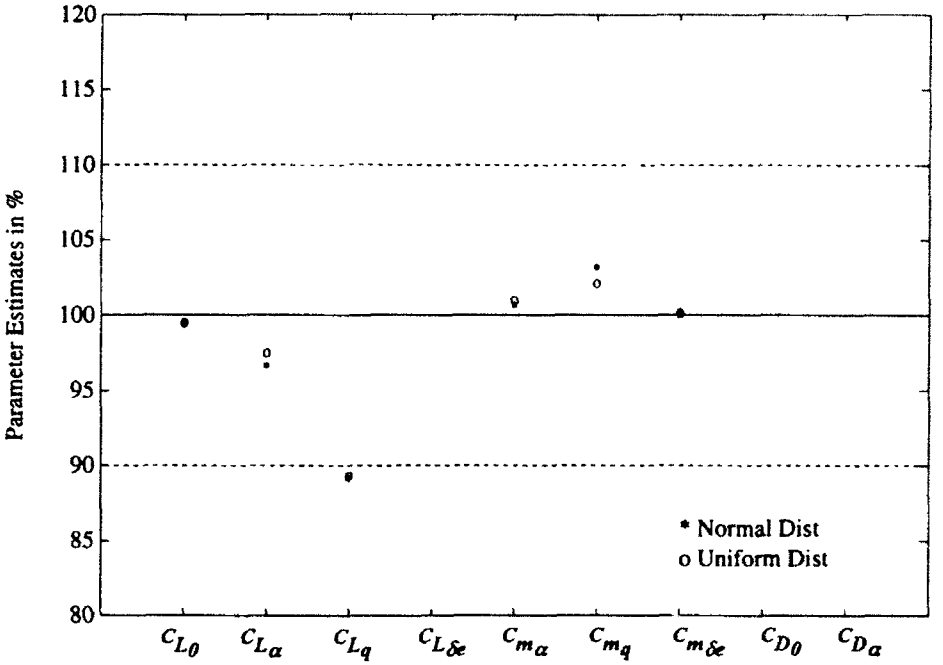

Figure 51 Longitudinal Noise Analysis - Noise Level 3, Random Distributions, Maneuver 2b

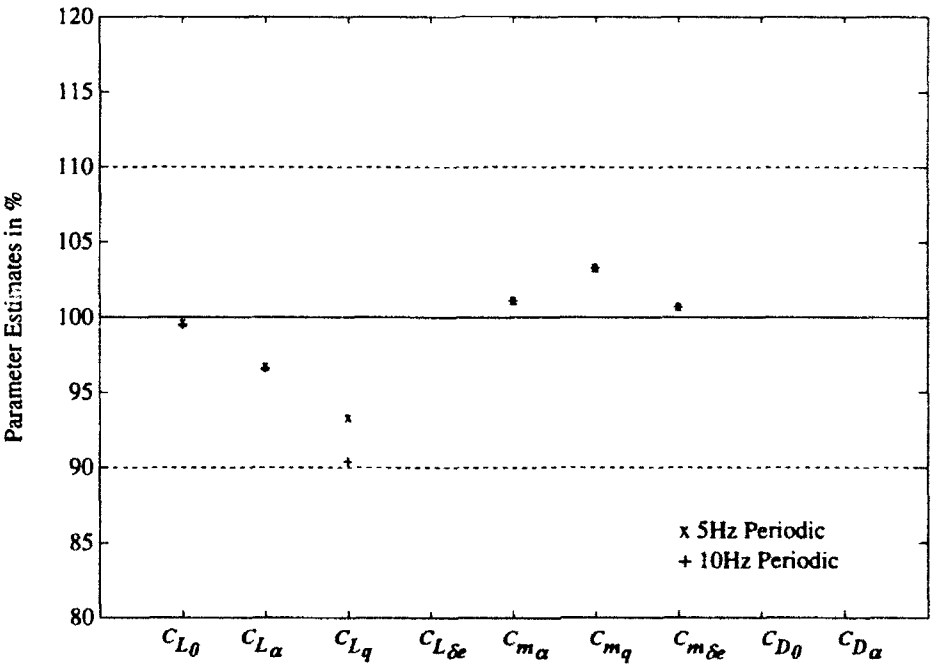

Figure 52 Longitudinal Noise Analysis - Noise Level 3, Periodic Distribution, Maneuver 2b

In conclusion, Noise Levels 2 and 3 are manageable for longitudinal parameter estimation without filtering. These levels allow accurate estimates of most parameters and reasonably small standard deviations among random cases. Predictably, maneuvers with more excitation suffer less from the effects of a given level of noise; therefore, maneuvers with more excitation should be chosen if significant noise is evident. Longitudinal estimates are most sensitive to noise in the angular measures, including pitch angle, angle of attack, and elevator deflection. Noise in the pitch rate data is also more significant than noise in the velocity measurements. Tables 19 and 20 present the maximum signal-to-noise ratios for the two maneuvers at each noise level, calculated using the ranges in Table 7. Signal-to-noise ratios that provide good results are not isolated, but identifying favorable ratios, if they exist, would be a useful ambition for future study. Periodic noise at a frequency less than half the sampling rate does not affect estimates appreciably, even with the higher Noise Level 1. Thus, if periodic noise is present, adjusting the system sampling rate accordingly reduces the effect of the noise considerably.

Table 19 Longitudinal Signal-to-Noise Ratios - Maneuver 2a

Noise Level	u	q	θ	δ_e
Level 1	86	7.3	33	10
Level 2	171	14.7	67	20
Level 3	1062	12.2	133	40

Table 20 Longitudinal Signal-to-Noise Ratios - Maneuver 2b

Noise Level	u	q	θ	δ_e
Level 1	86	23.3	100	30
Level 2	171	46.7	200	60
Level 3	1062	39	400	120

Lateral-Directional Results

For the lateral-directional case, the first three response noise levels are identical to those in the longitudinal analysis. Figures 53 and 54 present the estimates from Maneuvers 2c and 4d, respectively, at Noise Level 1. In Figure 53, accurate estimates for C_{l_β}, C_{l_p}, $C_{l_{\delta_a}}$, and C_{n_β} result, and the standard deviations of these estimates are reasonable. This level of noise affects the rudder maneuver to a greater extent because of its smaller excitations; the parameter estimates, even with averages within ten percent of the simulated value, have wide standard deviations. Appendix E lists the standard deviations for each estimate at each noise level.

Noise Level 2 provides somewhat better results, as illustrated in Figures 55 and 56. From Figure 55 and Appendix E, the aileron maneuver allows a number of good estimates with small standard deviations. Again, however, Maneuver 4d suffers from the noise; a number of the averages are close, but the standard deviations of these estimates are large. Only the estimates of C_{n_β} and $C_{n_{\delta_a}}$ are close to their simulated values and have standard deviations less than ten percent.

At Noise Level 3, the results are similar, but slightly less accurate than those at Level 2, due to more noise in the p and r rate gyros. The estimates, presented in

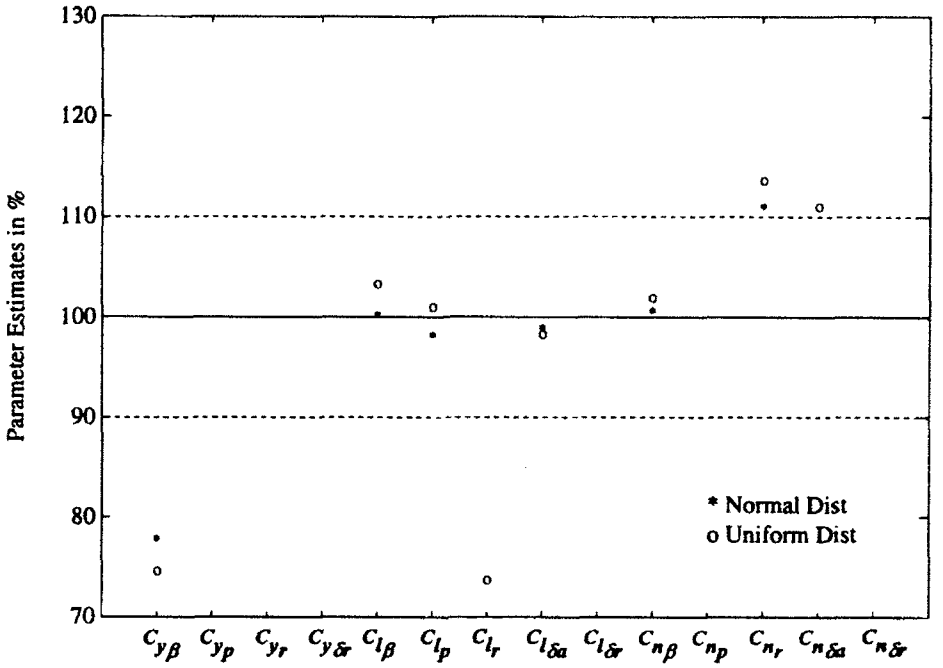

Figure 53 Lateral-Directional Noise Analysis - Noise Level 1, Random Distributions, Maneuver 2c

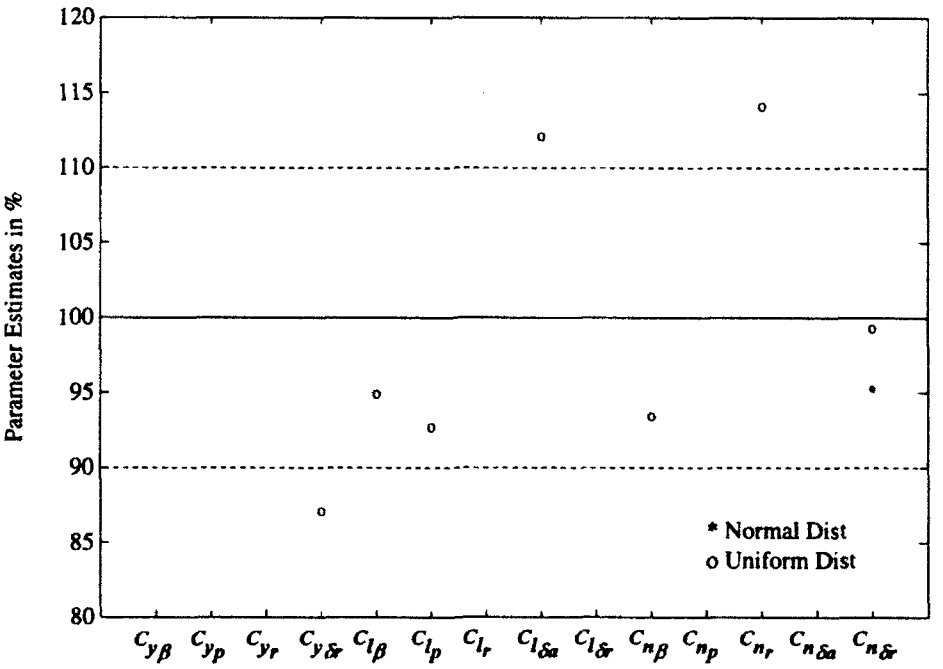

Figure 54 Lateral-Directional Noise Analysis - Noise Level 1, Random Distributions, Maneuver 4d

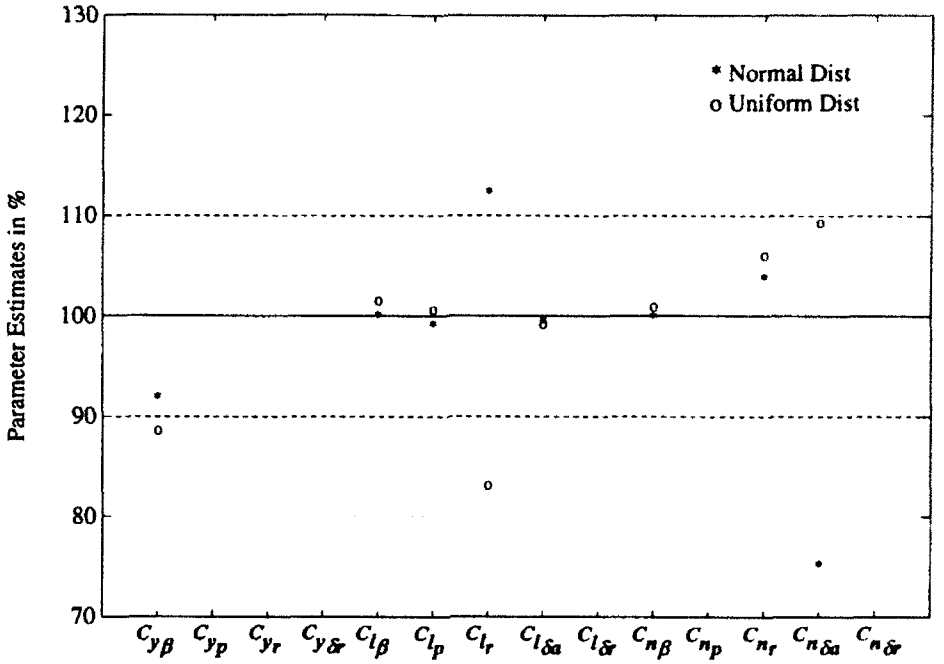

Figure 55 Lateral-Directional Noise Analysis - Noise Level 2, Random Distributions, Maneuver 2c

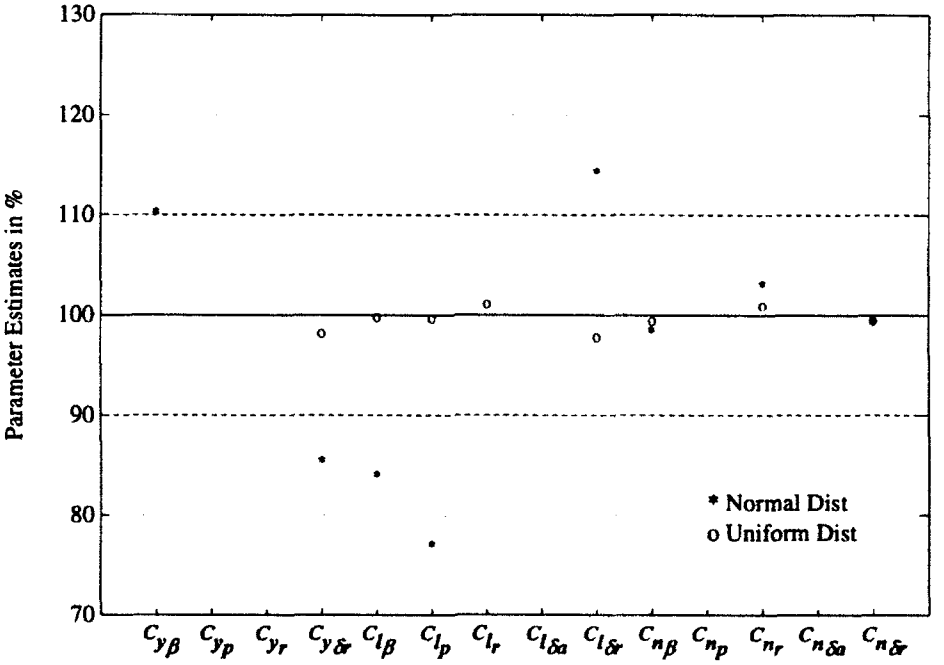

Figure 56 Lateral-Directional Noise Analysis - Noise Level 2, Random Distributions, Maneuver 4d

Figures 57 and 58 and Appendix E, show several good estimates for the aileron doublet, but scattered results and high standard deviations for the rudder doublet.

In addition, Figures 59 and 60 present parameter estimates with 5Hz and 10Hz periodic noise at Noise Level 3, for the aileron and rudder doublets. Like the random distributions, periodic noise affects the lateral-directional estimation more than it does the longitudinal. For the aileron doublet in Figure 59, six derivatives are within ten percent, but the estimates of C_{y_r}, C_{l_r}, C_{n_p}, and $C_{n_{\delta a}}$ suffer. With periodic noise, the rudder maneuver no longer provides useful estimates of C_{y_r}, C_{l_r}, and C_{n_p}, but the rudder control estimates are accurate. Thus, periodic noise adversely affects certain lateral-directional parameter estimates - some filtering may be helpful if the noise characteristics are known and appropriate filters are available.

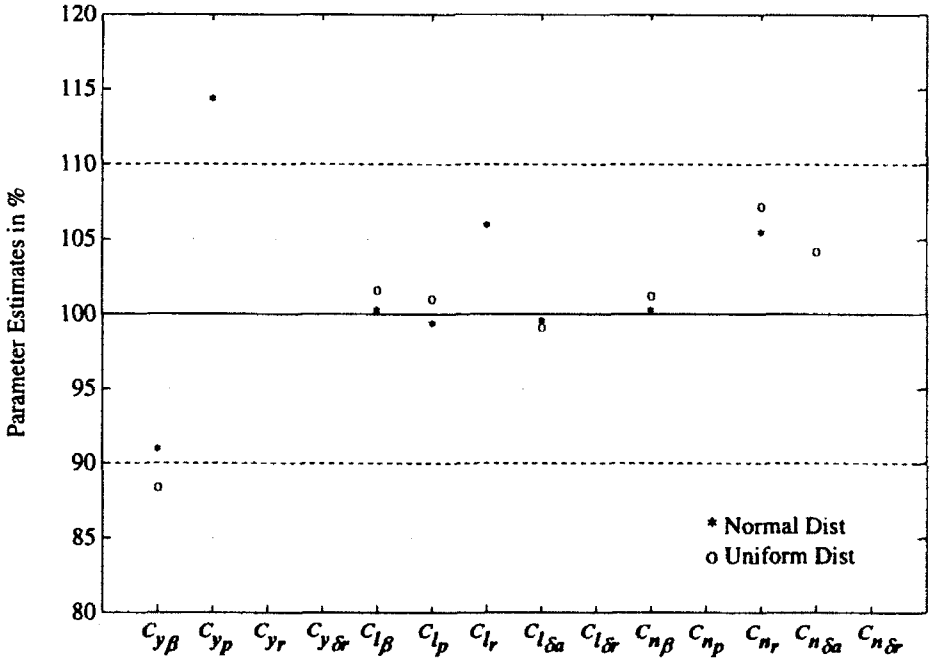

Figure 57 Lateral-Directional Noise Analysis - Noise Level 3, Random Distributions, Maneuver 2c

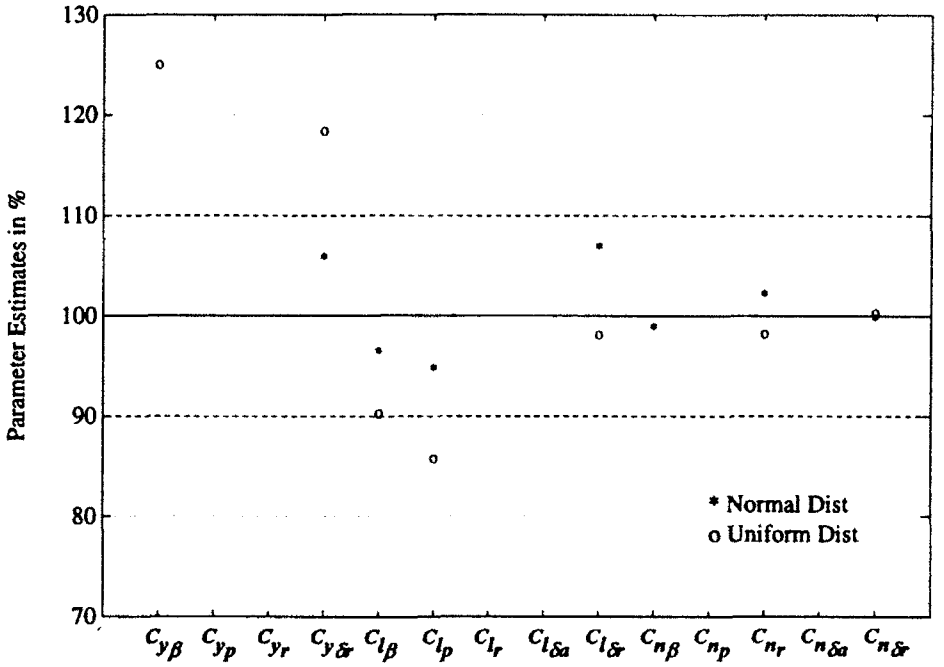

Figure 58 Lateral-Directional Noise Analysis - Noise Level 3, Random Distributions, Maneuver 4d

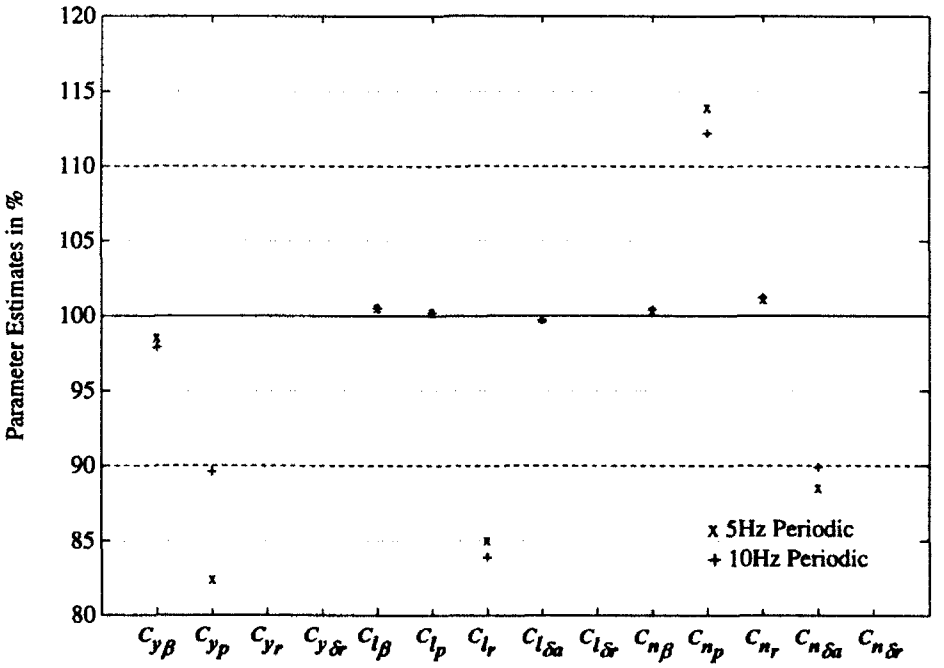

Figure 59 Lateral-Directional Noise Analysis - Noise Level 3, Periodic Distributions, Maneuver 2c

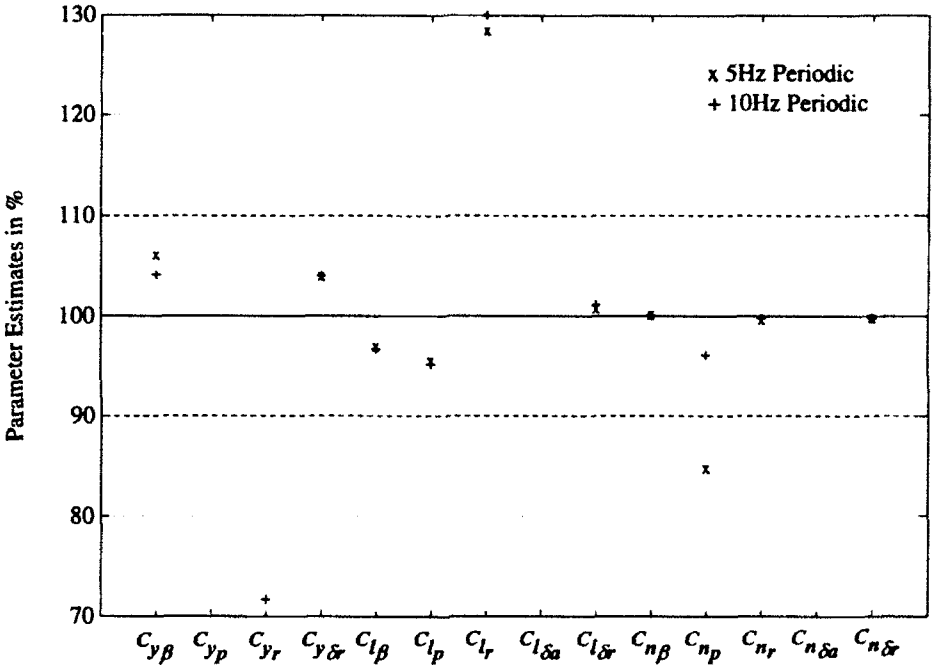

Figure 60 Lateral-Directional Noise Analysis - Noise Level 3, Periodic Distributions, Maneuver 4d

Because lateral-directional estimates are less tolerant of noise in the data, this study considers an additional level of noise, Noise Level 4, which is half the magnitude of Level 2. Thus, the noise levels for Level 4 are:

$$a_y : 0.0125\text{g}$$

$$p\,,\, r : 0.075 \text{ deg/sec}$$

$$\beta\,,\, \phi \;:\; 0.0075 \text{ deg}$$

$$\delta_a\,,\, \delta_r : 0.025 \text{ deg} \qquad (31)$$

For the aileron doublet, Noise Level 4 is a clear improvement over Level 2: useful estimates result for $C_{y\beta}$, $C_{l\beta}$, C_{l_p} , $C_{l_{\delta a}}$, $C_{n\beta}$, and C_{l_p} with both normal and uniform distributions. Figure 61 illustrates these results. In addition, for the other six parameters, five estimates are within twenty percent, and the standard deviations are considerably smaller than with Level 2 or 3. The rudder doublet results,

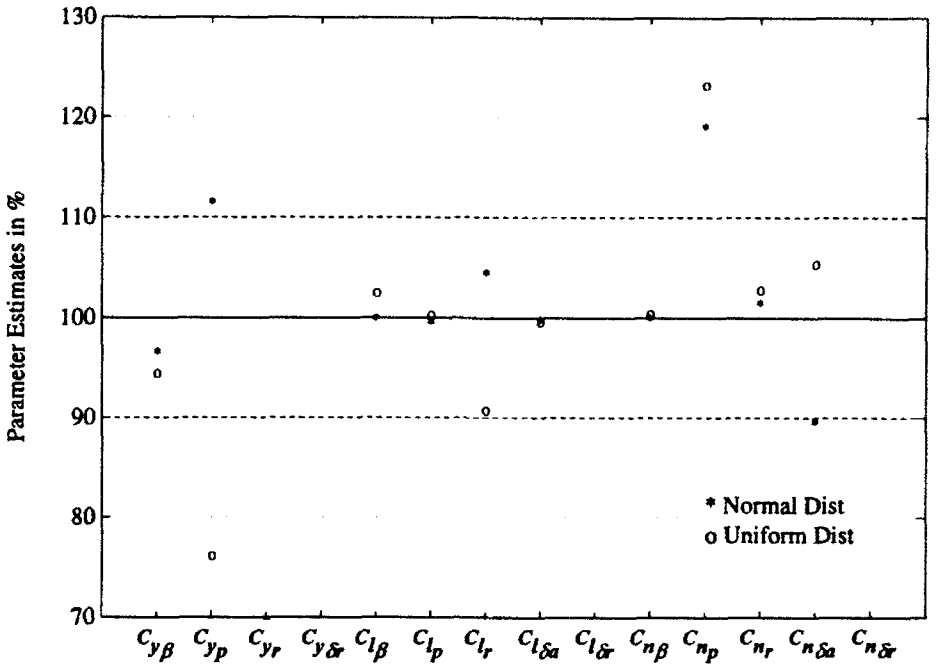

Figure 61 Lateral-Directional Noise Analysis - Noise Level 4, Random Distributions, Maneuver 2c

depicted in Figure 62, also show improvement. Five of the six parameters above have good estimates, and all of the rudder control derivatives are useful. Thus, while a lower noise level is desired, Level 4 does provide useful estimates for a number of derivatives.

The lateral-directional noise analysis indicates that noise affects this estimation more than it did the longitudinal. A lower noise level, Level 4, is introduced , and provides useful estimates with both aileron and rudder maneuvers. Tables 21 and 22 present the maximum signal-to-noise ratios for the two maneuvers considered in this analysis. Again, critical ratios for the various components are not established, but further study to identify these would be useful. Some parameters, particularly C_y terms, C_{l_r} , and C_{n_p} , are especially sensitive to noise, even periodic low-frequency noise. Aileron maneuvers are less affected by noisy data, mainly

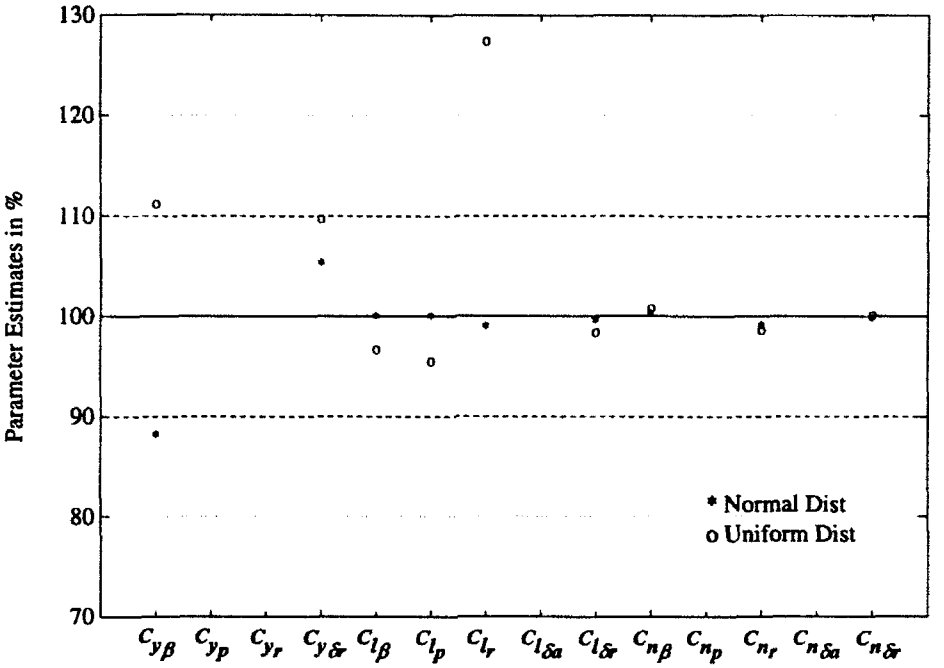

Figure 62 Lateral-Directional Noise Analysis - Noise Level 4, Random Distributions, Maneuver 4d

because of their larger excitations. Lateral-directional estimation is particularly sensitive to noise in both the p and r rate gyros. If accurate estimates of these parameters are important and noise is not significantly less than that considered here, judicious use of filtering or other data processing methods may prove helpful.

Table 21 Lateral-Directional Signal-to-Noise Ratios - Maneuver 2c

Noise Level	p	r	β	ϕ	δ_a
Level 1	30	4.7	33.3	233.3	50
Level 2	60	9.3	66.7	466.7	100
Level 3	50	7.8	133.3	933.3	200
Level 4	120	18.7	133.3	933.3	200

Table 22 Lateral-Directional Signal-to-Noise Ratios - Maneuver 4d

Noise Level	p	r	β	ϕ	δ_r
Level 1	20	16.7	133.3	166.7	70
Level 2	40	33.3	266.7	333.3	140
Level 3	33.3	27.8	533.3	666.7	280
Level 4	80	66.7	533.3	666.7	280

COMBINED EFFECTS

The final analysis, and that which most realistically simulates real flight test data, considers the combined effects of instrument precision, instrument bias, and measurement noise. For both longitudinal and lateral-directional cases, levels of precision, bias, and noise that work well by themselves are combined, and analyzed in pEst. Average parameter estimates provide approximations of the estimates that may be expected in flight data.

Longitudinal Results

The longitudinal combined analysis uses Maneuvers 2a and 2b, at Precision Level 2, Bias Level 2, and Noise Level 3. Bias estimators are left inactive, and the noise distribution is uniform.

Figure 63 presents the estimates for Maneuver 2a, and depicts their standard deviations in percent of the simulated parameter value. The estimates of C_{L_0}, C_{L_α}, C_{m_q}, and $C_{m_{\delta_e}}$ are within ten percent - two of these have standard deviations of less than five percent.

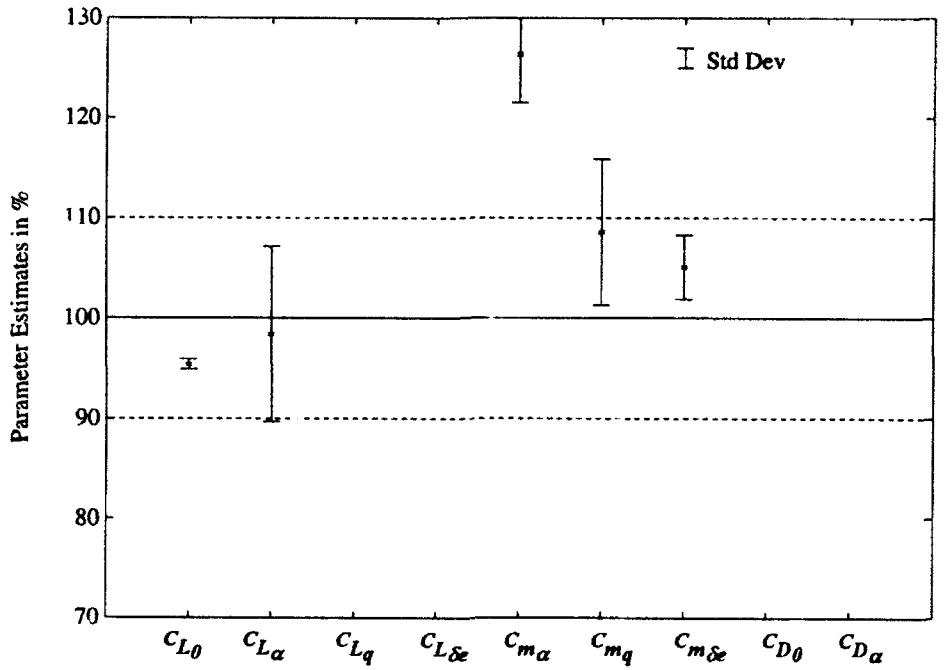

Figure 63 Longitudinal Combined Analysis - Precision Level 2, Bias Level 2, Noise Level 3, Maneuver 2a

The results for Maneuver 2b appear in Figure 64. In this case, six estimate averages are within ten percent, and five of these have standard deviations less than two percent. The estimate of C_{L_q} is inaccurate, as is that of C_{m0}. The $C_{L_{\delta e}}$ estimate is actually better in this case than in the preliminary analysis, but the standard deviation is high, so confidence in the estimate is low. Five other estimates, those of C_{L0}, C_{L_α}, C_{m_α}, C_{m_q}, and $C_{m_{\delta e}}$, are quite acceptable, however, and make this maneuver useful even with noise and bias corrupting the data. The results in this case correspond closely with those for this maneuver in the bias analysis, so the dominant uncertainty in the data is probably bias.

From this overall analysis, longitudinal maneuvers that are acceptable in ground effect can provide accurate parameter estimates, provided that precision, bias, and noise are close to the recommended levels. As in the individual uncertainty

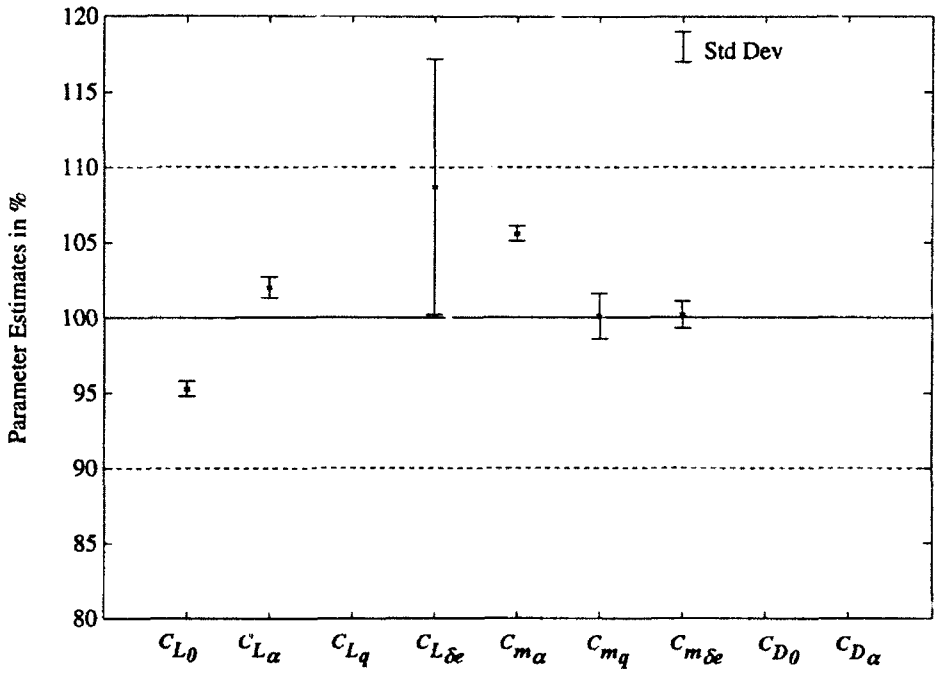

Figure 64 Longitudinal Combined Analysis - Precision Level 2, Bias Level 2, Noise Level 3, Maneuver 2b

analyses, maneuvers with larger excitations generally provide more accurate estimates.

Estimates of the relative influences of the longitudinal derivatives are in Table 23. For both maneuvers, the poor C_{L_q} estimates result in poor total lift estimates. From the preliminary analysis, this parameter has some influence on total lift, but not nearly the effect of C_{L_0}. In these examples, however, poor C_{L_q} estimates dominate the total lift estimates. Also from the preceeding analyses, bias has a much more detrimental effect on C_{L_q} than does noise; therefore, excessive bias in the data causes the poor estimates of this parameter and of the total lift coefficient. As expected, the larger Maneuver 2b does provide a somewhat better result. Since the combined C_{m_q} estimates are reasonably accurate, good estimates of total moment coefficient result, particularly for Maneuver 2b.

Table 23 Longitudinal Combined Relative Influences

Estimated terms (% of actual C_L magnitude)					Total (% of actual C_L)
Maneuver	C_{L_0}	$C_{L_\alpha}\cdot\Delta\alpha$	$C_{L_q}\cdot\Delta q$	$C_{L_{\delta_e}}\cdot\Delta\delta_e$	C_L
2a	69.4	6.8	219.6	1.2	**297.0**
2b	43.8	13.3	114.9	2.5	**173.5**
	Estimated terms (% of actual C_m magnitude)				Total (% of actual C_m)
Maneuver	C_{m_0}	$C_{m_\alpha}\cdot\Delta\alpha$	$C_{m_q}\cdot\Delta q$	$C_{m_{\delta_e}}\cdot\Delta\delta_e$	C_m
2a	1.5	3.3	103.2	2.5	**110.5**
2b	0.4	2.6	95.3	2.3	**100.6**

Lateral-Directional Results

Lateral-directional combined analysis considers Maneuvers 2c and 4d at Precision Level 2, Bias Level 2, and uniform Noise Level 3. For these lateral-directional maneuvers, bias estimators are active.

Maneuver 2c provides six average estimates within ten percent, as depicted in Figure 65. Five of these estimates have standard deviations of less than seven percent, and are therefore useful. In addition, the $C_{y_{\delta a}}$ estimate is less than one one-thousandth, which is reasonably close to zero, its actual value. The estimates for six other parameters are poor - if these parameters are of interest, the uncertainty in the data must be reduced or an additional maneuver analyzed.

Maneuver 4d provides fewer good results, as is typical for a noisy rudder maneuver. Figure 66 presents these estimates and standard deviations. Only four parameters, C_{l_β}, C_{n_β}, C_{n_r}, and $C_{n_{\dot{\beta}}}$, have good estimates and standard deviations

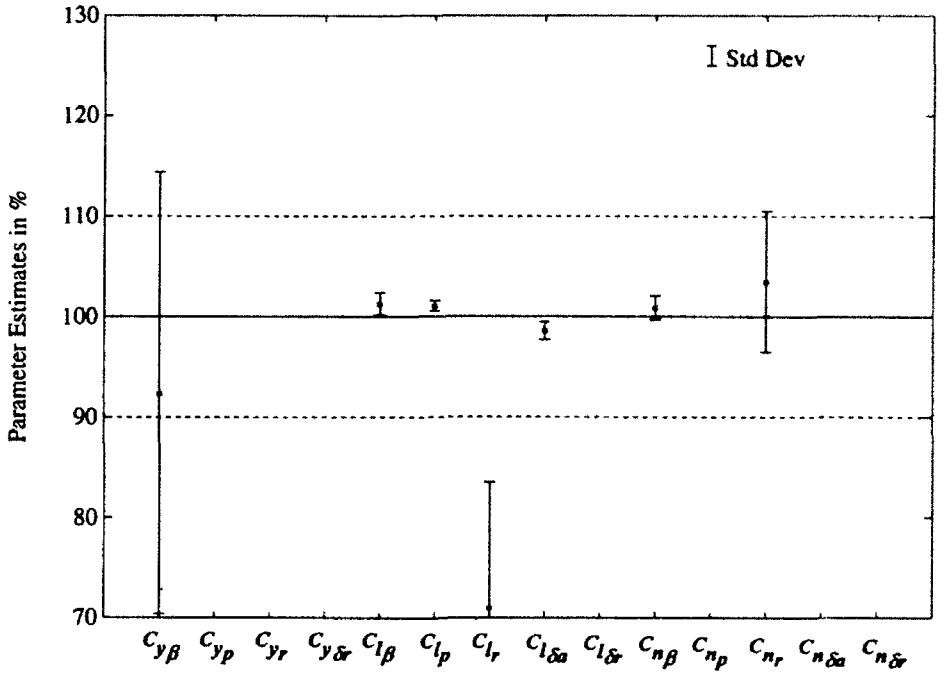

Figure 65 Lateral-Directional Combined Analysis - Precision Level 2, Bias Level 2, Noise Level 3, Maneuver 2c

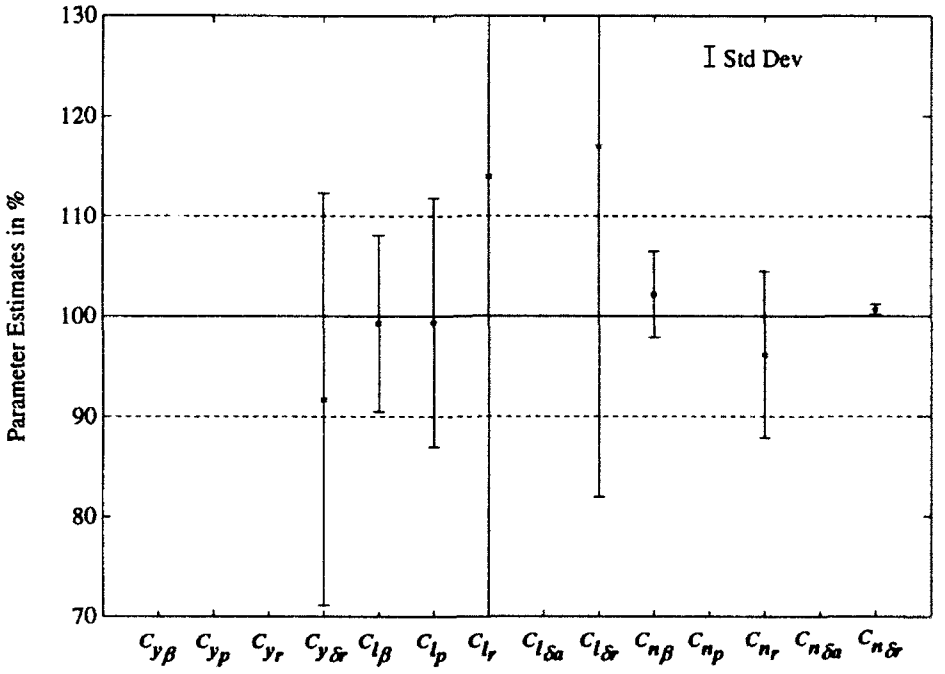

Figure 66 Lateral-Directional Combined Analysis - Precision Level 2, Bias Level 2, Noise Level 3, Maneuver 4d

below ten percent. Again, if other parameter estimates are desired, additional tests or processing are necessary.

All in all, lateral-directional parameter estimation requires a wider selection of test maneuvers or more precise data acquisition than does longitudinal analysis, if more than a select few derivatives are of interest. Both the maneuvers considered in the combined analysis provide good estimates of C_{l_β}, C_{l_p}, C_{n_β}, and C_{n_r}. In addition, the aileron doublet allows a good $C_{l_{\delta a}}$ estimate, and the rudder maneuver gives a good estimate of $C_{n_{\delta r}}$. Neither maneuver provides good estimates of the C_y terms with combined uncertainty. The results in this case correspond best with those in the noise analysis; therefore, noise appears to be the dominant source of uncertainty and error in these cases. Although some parameter estimates are poor, this analysis illustrates that estimating some lateral-directional parameters is feasible in ground effect, even with noise, bias, and moderate instrument precision.

Table 24 summarizes the relative influence estimates for the lateral-directional derivatives. Excessive C_{y_r} estimates are detrimental to both total side force estimates, but the poor estimates of C_{y_p} only affect the total significantly for the rudder maneuver. The estimates of total rolling and yawing moment coefficients are much more accurate, because estimates of the most influential parameters are reasonably good. Although some parameter estimates are not within ten percent of their actual values, these parameters generally have less influence on the totals. Thus, accurate estimates of the most important roll and yaw parameters are realistic, but accurate side force derivative estimates likely will require lower rate gyro noise levels.

Table 24 Lateral-Directional Combined Relative Influences

Estimated terms (% of actual C_y magnitude)						Total (% of actual C_y)
Maneuver	$C_{y_\beta}\cdot\Delta\beta$	$C_{y_p}\cdot\Delta p$	$C_{y_r}\cdot\Delta r$	$C_{y_{\delta_a}}\cdot\delta_a$	$C_{y_{\delta_r}}\cdot\delta_r$	C_y
2c	9.1	2.3	174.5	3.9	--	**189.8**
4d	4.7	239.0	183.0	0.0	14.0	**440.7**
Estimated terms (% of actual C_l magnitude)						Total (% of actual C_l)
Maneuver	$C_{l_\beta}\cdot\Delta\beta$	$C_{l_p}\cdot\Delta p$	$C_{l_r}\cdot\Delta r$	$C_{l_{\delta_a}}\cdot\delta_a$	$C_{l_{\delta_r}}\cdot\delta_r$	C_l
2c	2.2	76.5	6.4	12.9	--	**98.0**
4d	13.3	76.8	8.8	0.0	1.8	**100.7**
Estimated terms (% of actual C_n magnitude)						Total (% of actual C_n)
Maneuver	$C_{n_\beta}\cdot\Delta\beta$	$C_{n_p}\cdot\Delta p$	$C_{n_r}\cdot\Delta r$	$C_{n_{\delta_a}}\cdot\delta_a$	$C_{n_{\delta_r}}\cdot\delta_r$	C_n
2c	6.0	3.8	94.6	0.1	--	**104.5**
4d	23.7	2.7	47.6	--	26.0	**100.0**

CONCLUSIONS AND RECOMMENDATIONS

Ground effect remains a phenomenon that is not completely understood, although it is germane for a number of aerospace applications. Previous studies regarding ground effect provide few consistent quantitative conclusions, and, in fact, do not even agree on appropriate test methods. One conclusion, however, is repeated throughout the literature: a flight test data base for ground effect study is sorely needed.

Flight testing in ground effect is problematic at best, and dangerous at worst. Useful flight tests depend on excitation of the aircraft response - ground proximity requirements and safety considerations severely constrain this excitation during ground effect testing. Numerical parameter estimation routines, such as pEst, and data acquisition systems make precise analysis of smaller maneuvers possible.

In this thesis, the ground effect test maneuver analysis is an iterative application of the following procedure: (1) estimate parameters with the program pEst, using simulated maneuver responses, (2) evaluate the safety and ground proximity requirements based on these responses, and (3) study the effects of instrument precision, system sampling rate, instrument bias, and noise on the estimation. This procedure isolates maneuvers suitable for ground effect flight testing. The safety and ground proximity requirements are based on the assumption that ground effect is measurable in the aircraft's response, but the change is not so great that it makes an otherwise safe maneuver unsafe. This assumption remains unverified (Rec. 1). In this study, pEst uses default response weights in minimizing the cost function - optimizing these weights may improve the estimation (Rec. 2).

Without uncertainty added to the data, the estimation results are quite promising. The study identifies five longitudinal and eleven lateral-directional maneuvers that provide good parameter estimates, keep the aircraft in ground effect, and do not result in excitations that are unsafe. The longitudinal maneuvers allow estimates of eight lift and moment derivatives within ten percent of their simulated values; because no thrust model is included in the longitudinal equations of motion, no drag term estimates are within fifty percent (Rec 3). The lateral-directional estimation achieves accurate estimates for all fifteen derivatives of interest - in many cases these estimates are within three percent. Useful lateral-directional maneuvers include aileron, rudder, and combined aileron-rudder maneuvers.

The precision analysis establishes levels of instrument precision appropriate for accurate parameter estimation. Longitudinal components should meet Precision Level 2 standards - Table 9 includes the specific precision levels considered. For lateral-directional estimates, more precision is required, and Level 9 is more appropriate. Accelerometers with acceptable resolution exist, but adequate rate gyros and angular measure equipment are not identified. Finer levels of precision would better define whether suitable acquisition system components are available (Rec. 4).

The sampling analysis indicates that, for noise-free data, the sampling rate has little effect on the parameter estimation, as long as the frequency is at least twice that of any control input or periodic transient response. One shortcoming of this study is that noisy data is not included in the sampling analysis (Rec. 5).

Based on this study, both longitudinal and lateral-directional estimates suffer if instrument bias is present. Bias estimation capability is included in pEst; however, for longitudinal maneuvers with low levels of bias and higher levels of excitement,

estimates improve with these bias estimators left off. For higher bias levels or more subtle maneuvers, active estimators allow better parameter estimates. This effort does not identify the dividing threshold between these two cases, but does include examples of each (Rec. 6). For lateral-directional maneuvers with bias, the bias estimators are best left on, regardless of the bias level or excitation. For both modes of motion, accurate parameters are obtained, even with biased data. In general, bias is more harmful to the longitudinal estimation than the lateral-directional.

Noise in the data tends to affect lateral-directional estimates more adversely than it does longitudinal. Random noise at Levels 2 and 3, which are specified in Table 12, allows useful longitudinal parameter estimates without filtering, though some estimates are poor. Predictably, maneuvers with higher excitation are less affected at a given level of noise. For longitudinal estimation, periodic noise that is less than half the sampling frequency has no significant effect on the estimates. Lateral-directional estimates suffer considerably at Levels 2 and 3; a lower level, Noise Level 4, allows good estimates for aileron maneuvers, and acceptable results for rudder maneuvers. Periodic noise affects lateral-directional estimation more than it does longitudinal, but does not prevent at least some useful estimates. In short, noise harms the estimation, particularly in the lateral-directional case, but useful estimates are still possible. The levels of noise considered are similar to those experienced in tests at the Texas A&M Flight Mechanics Laboratory. Acceptable signal-to-noise ratios for the two cases are not isolated (Rec. 7).

The final analysis combines the effects of Precision Level 2, Bias Level 2, and Noise Level 3. Both longitudinal and lateral-directional maneuvers provide several useful parameter estimates, even with these combined uncertainties. Since actual flight test data will likely combine all three of these factors, success in this

analysis indicates that flight measurement of stability and control derivatives in ground effect is practical.

Recommendations for further study, in a rough order of priority, are summarized below:

Recommendation 1 - Before test maneuvers may be flown in immediate proximity to the ground, the validity of the assumption that ground effect does not make maneuvers unsafe must be considered and verified.

Recommendation 2 - The effects of adjusting the response weights in the cost function should be studied, and these weights should be optimized, if possible.

Recommendation 3 - A more complete longitudinal system incorporating a thrust model should be developed and implemented in an attempt to determine drag derivatives.

Recommendation 4 - Finer levels of precision should be considered to define acquisition system requirements, and specific hardware, particularly rate gyros and angular measuring equipment, must be identified.

Recommendation 5 - The effect of sampling rate on data with noise should be studied, to determine whether higher sampling rates reduce the effect of noise.

Recommendation 6 - Further bias analysis should be performed on longitudinal maneuvers, to identify a decision criterion for leaving the bias estimators in pEst off or activating them.

Recommendation 7 - An attempt should be made to identify acceptable signal-to-noise ratios for both longitudinal and lateral-directional maneuvers.

REFERENCES

[1] East, L. F., "The Measurement of Ground Effect Using A Fixed Ground Board," R.A.E. Reports and Memoranda No. 3689, Bedford, U.K. , Jul. 1970.

[2] Recant, I. G., "Wind Tunnel Investigation of Ground Effect on Wings with Flaps," NACA T.N. No. 705, May 1939.

[3] Chambliss, E. B. and Millikan, D., "An Investigation of the Landing Characteristics of the NASA-MSC August 1969 Baseline Orbiter Configuration in Ground Effect," NASA-CR-120023, Oct. 1972.

[4] Coe, P. L. Jr. and Thomas, J. L., "Theoretical and Experimental Investigation of Ground Induced Effects for a Low Aspect Ratio Highly Swept Arrow Wing Configuration," NASA TP-1508, Sept. 1979.

[5]Stewart, V. R. and Kemmerly, G. T., "Effects of Ground Proximity On a Low Aspect Ratio Propulsive Wing/Canard Configuration," Proceedings, 1987 NASA Ames Research Center Ground-Effects Workshop, Feb. 1987, pp. 415-444.

[6]Rolls, L. S. and Koenig, D. G., "Flight-Measured Ground Effect On a Low-Aspect-Ratio Ogee Wing Including a Comparison with Wind-Tunnel Results," NASA TN-D-3431, June 1966.

[7] Schweikhard, W., "A Method for In-Flight Measurement of Ground Effect on Fixed-Wing Aircraft," *Journal of Aircraft*, Vol. 4, Mar.-Apr. 1967, pp. 101-104.

[8] O'Leary, C. O., "Flight Measurements of Ground Effect on the Lift and Pitching Moment of a Large Transport Aircraft (Comet 3B) and Comparison with Wind Tunnel and Other Data," R. A. E. Reports and Memoranda No. 3611, Bedford, U.K., Jun. 1968.

[9] Ljung, L., *System Identification: Theory for the User*, Prentice-Hall, Englewood Cliffs, N.J., 1987, pp. 1-8.

[10] *PRO-MATLAB User's Guide*, Math Works, Inc., South Natick, MA, 1985.

[11] Murray, J.E. and Maine, R.E., "pEst Version 2.1 User's Manual," NASA TM-88280, Sept. 1987.

[12] Maine, R.E. and Iliff, K. W., "Application of Parameter Estimation to Aircraft Stability and Control: The Output-Error Approach," NASA RP-1168, Jun. 1986.

[13] Nelson, R. C., *Flight Stability and Automatic Control*, McGraw-Hill, New York, N.Y., 1989.

[14] Maine, R.E., "Manual for *GetData* Version 3.1," NASA TM-88288, Oct.1987.

[15] Connell, M. A. and Sonntag, J. G., "Validation and Demonstration of the Rate Gyro / Accelerometer Package," Student Report, Texas A&M University Flight Dynamics Laboratory, Aug. 1990.

[16] Biskup, B. and Lewis, J. F., "Final Report - Commander 700 Control Surface Deflection Angle Measurement," Student Report, Texas A&M University Flight Dynamics Laboratory, Aug. 1990.

APPENDICES

APPENDIX A - BEECH B99 AIRCRAFT MODEL PARAMETERS AND pEst DEFAULT SETTINGS

BEECH B99 AIRCRAFT MODEL PARAMETERS*

Final Approach Flight Condition:

Altitude: Sea Level	Air Density: 0.002378 sl/ft^3
Speed: 170 ft/sec	Center of Gravity: 0.16 % chord

Geometric and Inertia Terms for Final Approach Configuration:

Wing Area: 280 ft^2	Wing Span: 46 ft
Wing Mean Geometric Chord: 6.5 ft	Weight: 11000 lbs
I_{xx}: 15189 sl ft^2	I_{yy}: 20250 sl ft^2
I_{zz}: 34141 sl ft^2	I_{xz}: 4371 sl ft^2

Stability and Control Parameters:

C_{L0} = 1.15	$C_{y\beta}$ = -0.59 /rad
C_{Lu} = 0.027	C_{yp} = -0.21 /rad
C_{Lq} = 8.1 /rad	C_{yr} = 0.39 /rad
$C_{L\alpha}$ = 6.24 /rad	$C_{y\delta a}$ = 0.0 /rad
$C_{L\delta e}$ = 0.58 /rad	$C_{y\delta r}$ = 0.144 /rad
C_{m0} = 0.0	$C_{l\beta}$ = -0.13 /rad
C_{mu} = 0.0	C_{lp} = -0.5 /rad
C_{mq} = -34.0 /rad	C_{lr} = 0.06 /rad

C_{m_α} = -2.08 /rad	$C_{l_{\delta a}}$ = 0.156 /rad
$C_{m_{\delta e}}$ = -1.9 /rad	$C_{l_{\delta r}}$ = 0.0087 /rad
C_{D_0} = 0.162	C_{n_β} = 0.12 /rad
C_{D_u} = 0.0	C_{n_p} = -0.005 /rad
C_{D_q} = 0.0 /rad	C_{n_r} = -0.204 /rad
C_{D_α} = 0.933 /rad	$C_{n_{\delta a}}$ = -0.0012 /rad
$C_{D_{\delta e}}$ = 0.0 /rad	$C_{n_{\delta r}}$ = -0.0763 /rad

*Aircraft information from: Roskam, J., *Airplane Flight Dynamics and Automatic Flight Control, Part I,* Roskam Aviation, Ottawa, Ks., 1979, pp. 598-601.

pEst DEFAULT SETTINGS USED:

Response Weights:

v : 3.0	β : 12.0
α : 3.0	p : 0.7
q : 8.0	r : 17.0
θ : 5.0	ϕ : 3.0

Convergence Bound = 0.0001 (if the percentage change in the cost function between iterations is less than this value, iteration stops and is considered converged)

APPENDIX B - AIRCRAFT SIMULATION PROGRAM FILES

Appendix B is included on a 3.5 inch diskette provided in a pocket on the back cover. Additional copies of this diskette are available from the author and from Dr. Donald Ward, in the Department of Aerospace Engineering, Texas A&M University (845-1732). Dr. Ward also has a master copy of the appendices on paper, suitable for photocopying.

Appendix B includes computer program files written in C language and MATLAB command format. They are included in text format in the file APPENDB.DOC (18 pages).

APPENDIX C - PARAMETER ESTIMATION SETUP FILES

Appendix C is included on a 3.5 inch diskette provided in a pocket on the back cover. Additional copies of this diskette are available from the author and from Dr. Donald Ward, in the Department of Aerospace Engineering, Texas A&M University (845-1732). Dr. Ward also has a master copy of the appendices on paper, suitable for photocopying.

Appendix C includes files for formatting time history data and configuring pEst. These are files written in C language and pEst command syntax. They are in text format in the file APPENDC.DOC (4 pages).

APPENDIX D - LONGITUDINAL ESTIMATION RESULTS

Appendix D is included on a 3.5 inch diskette provided in a pocket on the back cover. Additional copies of this diskette are available from the author and from Dr. Donald Ward, in the Department of Aerospace Engineering, Texas A&M University (845-1732). Dr. Ward also has a master copy of the appendices on paper, suitable for photocopying.

Appendix D includes the files below (7 files, 29 pages total), which present the results of the longitudinal analysis, formatted for the Microsoft Excel spreadsheet program (LOTUS 1-2-3 may be used as an alternative). The files are ready for input into the spreadsheet, and may be printed as text from within the spreadsheet. Headings with specifics on the data (such as maneuver numbers, precision levels, bias levels, etc.) are included. The total derivatives file includes a summary of the relative influence of each parameter on the total force and moment derivatives.

APPND1.XLS - Preliminary Maneuver Analysis Results
APPND2.XLS - Precision and Sampling Rate Analysis Results
APPND3.XLS - Bias Analysis Results
APPND4.XLS - Noise Analysis Results
APPND5.XLS - Noise Analysis Results
APPND6.XLS - Combined Analysis Results
APPND7.XLS - Total Derivatives

APPENDIX E - LATERAL-DIRECTIONAL ESTIMATION RESULTS

Appendix E is included on a 3.5 inch diskette provided in a pocket on the back cover. Additional copies of this diskette are available from the author and from Dr. Donald Ward, in the Department of Aerospace Engineering, Texas A&M University (845-1732). Dr. Ward also has a master copy of the appendices on paper, suitable for photocopying.

Appendix E includes the files below (10 files, 62 pages total), presenting the results of the lateral-directional analysis in spreadsheet format. They are similar to the longitudinal files mentioned above.

APPNE1 - Preliminary Maneuver Analysis Results
APPNE2 - Preliminary Maneuver Analysis Results
APPNE3 - Precision and Sampling Rate Analysis Results
APPNE4 - Bias Analysis Results
APPNE5 - Noise Analysis Results
APPNE6 - Noise Analysis Results
APPNE7 - Noise Analysis Results
APPNE8 - Noise Analysis Results
APPNE9 - Combined Analysis Results
APPNE10 - Total Derivatives

APPENDIX F - PRECISION LEVEL DEVELOPMENT

ACCELEROMETER PRECISION:

Representative Level = 0.001% full scale* - Let full scale = ± 2g

Then, precision = ± 0.00002g = ± 00064 ft/s^2

From this, let Precision Level 1 = ± 0.0001g

Velocities are determined by integrating these accelerations - assume time is known exactly - then let

Precision Level 1 = ± 0.001 ft/sec

RATE GYRO PRECISION:

Representative Level = 1% full scale* - Let full scale = ± 100 deg/sec

Then, precision = ± 1 deg/sec

From this, let Precision Level 1 = ± 1 deg/sec

ANGULAR MEASUREMENT PRECISION (including control deflections)

Representative Level = 0.01% full scale* - Let full scale = ± 30 deg

Then, precision = 0.003 deg

From this, let Precision Level 1 = ± 0.01 deg

*Representative Levels of precision are from the A&M Flight Mechanics Laboratory Reports, References 15 and 16 (see next page).

REPRESENTATIVE DATA FOR POTENTIAL ACQUISITION SYSTEM COMPONENTS

A check mark (√) indicates a range / resolution combination that meets the precision levels recommended in the Precision Analysis, Section 3.

ACCELEROMETERS:

Systron-Donner Model 4310
Range: ± 0.5g to ± 35g
Resolution: < 0.001% Full Range

X-, Y-accelerometers:
With a ± 2g range, Precision < 2g x 0.00001 < 0.00002g √

Z-accelerometer:
With a ± 10g range, Precision < 10g x 0.00001 < 0.0001g √

Data from Reference 15, Appendix I.

RATE GYROS:

Humphrey RG28-0142-1
Range: ± 100 deg/sec
Accuracy: ± 1% Full Scale at low inputs within the range

Humphrey RG03-0602-1
Range: ± 50 deg/sec
Accuracy: ± 0.01 output ratio at low inputs within the range

Pitch rate gyro:
With a ± 50 deg/sec range, Precision = 50 deg/sec x 0.01 = 0.5 deg/sec

With a ± 10 deg/sec range, Precision = 0.1 deg/sec √

Roll rate gyro:
With a ± 100 deg/sec range, Precision = 1 deg/sec

With a ± 10 deg/sec range, Precision = 0.1 deg/sec √

Yaw rate gyro:
With a ± 50 deg/sec range, Precision = 0.5 deg/sec

With a ± 10 deg/sec range, Precision = 0.1 deg/sec √

Data from Reference 15, Appendix I.

ANGULAR MEASUREMENTS:

U.S. Digital E2 Optical Shaft Encoder
Range: Undefined
Resolution: up to 540 cycles/rev (quadruples with 2-channel quadrature)

Precision = 360 deg/rev ÷ (540 cycles/rev x 4) = 0.1667 deg

With three 3:1 gears, Precision = 0.1667 deg ÷ 27 = 0.0062 deg √

Canon X-1 Laser Rotary Encoder
Range: Undefined
Resolution: 225,000 pulses/rev

Precision = 360 deg/rev ÷ (225,000 pulses/rev) = 0.0016 deg √

Data from *Electronic Engineers Master Catalog 91-92, Volume B*, Hearst Business Communications, Inc., Garden City, NY, 1991.

APPENDIX G - NOISE LEVEL DEVELOPMENT

ACCELEROMETER NOISE:

Representative Level = 0.5% full scale* - Let full scale = ± 2g

Then, noise = ± 0.05g = ± 1.61 ft/s^2

From this, let Noise Level 1 = ± 0.05g; Noise Level 2 = ± 0.025g

For Noise Level 3, let full scale for z acceleration be +4g to -2g, and x and y accelerations be ± 1g.

Then, Noise Level 3 = ± 0.005g for the z-axis, and ± 0.02g for x and y-axes.

Velocities are determined by integrating these accelerations - assume time is known exactly - then let

Noise Level 1 = ± 2 ft/sec
Noise Level 2 = ± 1 ft/sec
Noise Level 3 = ± 0.1609 ft/sec

RATE GYRO NOISE:

Representative Level = 0.30% full scale* - Let full scale = ± 100 deg/sec

Then, noise = ± 0.3 deg/sec

From this, let Noise Level 1 = ± 0.3 deg/sec, Noise Level 2 = ± 0.15 deg/sec

For Noise Level 3, let full scale = ± 60 deg/sec
Then, noise = 0.18 deg/sec

ANGULAR MEASUREMENT NOISE (excluding control deflections)

Representative Level = 0.1% full scale* - Let full scale = ± 30 deg

Then, noise = 0.03 deg

From this, let Noise Level 1 = ± 0.03 deg, Noise Level 2 = 0.015 deg

For Noise Level 3, let full scale = ± 15 deg

Then, noise = ±0.0075 deg

CONTROL DEFLECTION NOISE:

Representative Level = 0.5% full scale* - Let full scale = ± 30 deg

Then, noise = ± 0.1 deg

From this, let Noise Level 1 = ± 0.1 deg, Noise Level 2 = 0.05 deg

For Noise Level 3, let full scale = ± 15 deg

Then, noise = ± 0.025 deg

*Representative Levels of noise are from the A&M Flight Mechanics Laboratory Reports, References 15 and 16.

VITA

James Matthew Clark was born September 20, 1967 in Wooster, Ohio. In May 1986, after living in several locations across the U.S., he graduated from Page High School in Greensboro, North Carolina, which he still considers home.

The following July, Jim accepted an appointment to the U.S. Air Force Academy in Colorado Springs, Colorado, as a member of the Class of 1990. He was a Distinguished Graduate of the Academy, receiving a Bachelor of Science degree in Aeronautical Engineering and a commission as a second lieutenant in the U.S. Air Force on May 30,1990.

Jim's first assignment as an officer was to Williams Air Force Base, Arizona for Undergraduate Pilot Training. He was awarded his pilot's wings at Williams in September 1991.

Following flight school, he was assigned to the Air Force Institute of Technology (AFIT) and began study for a Master of Science in Aerospace Engineering at Texas A&M University in January 1992.

Currently ranked a first lieutenant, Jim serves on active duty in the Air Force's Air Combat Command as a bomber pilot.

His permanent address is 3606 Redfield Dr., Greensboro, NC 27410.